NINEVAH UNIVERSITY

COLLEGE OF ELECTRONICS ENGINEERING

COMMUNICATION ENGINEERING DEPARTMENT

An Investigation into Planar Array Pattern Optimization

By

Abdulrazaq Abdulhaq Khmees-Al Sumaidaie

M.Sc. Thesis

In

Communication Engineering

Supervised by

Prof. Dr. Jafar Ramadhan Mohammed

2021 A.D.   **1442 A.H.**

An Investigation into Planar Array Pattern Optimization

Thesis Submitted

By

Abdulrazaq Abdulhaq Khmees-Al Sumaidaie

To

The Council of the College of Electronic Engineering

Ninevah University

As a Partial Fulfillment of the Requirements

For the Degree of Master of Science

In

Communication Engineering

Supervised by

Prof. Dr. Jafar Ramadhan Mohammed

2021 A.D.   **1442 A.H.**

بِسْمِ اللَّهِ الرَّحْمَنِ الرَّحِيمِ

نَرْفَعُ دَرَجَاتٍ مَنْ نَشَاءُ وَفَوْقَ كُلِّ ذِي عِلْمٍ عَلِيمٌ

صَدَقَ اللهُ العَظِيمُ

Supervisor�så Certification

I certify that the dissertation entitled (**An Investigation into Planar Array Pattern Optimization**) was prepared by **Abdulrazaq Abdulhaq Khmees u**nder my supervision at the Department of Communication Engineering, University of Ninevah, as a partial requirement for the Master of Science Degree in Communication Engineering.

Signature:

Name: Prof. Dr. Jafar Ramadhan Mohammed

Department of Communication Engineering

Date: /   /2021

Linguistic Advisor Certification

I certify that the linguistic evaluation of this thesis entitled **" An Investigation into Planar Array Pattern Optimization "** was carried out by me and it is accepted linguistically and in expression.

Signature:

Name:

Date: /   /2021

Post-Graduate Committee Certification

According to the recommendations presented by the supervisor of this dissertation and the linguistic reviewer, I nominate this dissertation to be forwarded to discussion.

Signature:

Name: Assistant Prof. Dr. Younis M. Abbosh

Department Head Certification

I certify that this dissertation was carried out in the Department of Communication Engineering. I nominate it to be forwarded to discussion.

Signature:

Name: Assistant Prof Dr. Younis M. Abbosh

Date: /   /2021

Committee Certification

We the examining committee, certify that we have read this dissertation entitled (**An Investigation into Planar Array Pattern Optimization**) and have examined the postgraduate student (**Abdulrazaq Abdulhaq Khmees**) in its contents and that in our opinion; it meets the standards of a dissertation for the degree of Master of Science in Communication Engineering.

Signature: Signature:

Name: Name:

Head of committee   Member

Date: /   /2021   **Date: /   /2021**

Signature: Signature:

Name: Name:

Member   Member and Supervisor

Date: /   /2021   **Date: /   /2021**

The college council, in its   ………… meeting on   /   /2021, has decided to award the degree of Master of Science in Communication Engineering to the candidate.

Signature: Signature:

Name: Name:

Dean of the College   Council registrar

Date: /   /2021   **Date: /   /2021**

ACKNOWLEDGEMENTS

"Praise be to ALLAH, Worlds, who says in the Holy Quran"

﴿رَبِّ أَوْزِعْنِي أَنْ أَشْكُرَ نِعْمَتَكَ ٱلَّتِي أَنْعَمْتَ عَلَيَّ وَعَلَىٰ وَٰلِدَيَّ وَأَنْ أَعْمَلَ صَٰلِحًا تَرْضَٰهُ﴾

I

Abstract

This thesis presents an investigation into the methods of synthesizing the planar antenna arrays under some desired constraints on their radiation patterns. In order to obtain optimum performance in terms of directivity, minimum sidelobe levels, null control, and simplest array complexity, an optimization algorithm is used to optimize the array design parameters. The genetic algorithm which is the most powerful and effective optimization method was used to optimize the considered arrays and accordingly obtain the desired radiation patterns.

In this research study, many planar array configurations such as rectangular two-dimensional shape, and two perpendicular linear arrays in the shape of a cross array were considered. For the rectangular planar arrays, their complexities were simplified by proposing an intelligent strategy to divide their array elements into two separate groups. The array elements in the first group are made adjusted in terms of amplitude and/or phase while the other elements are assumed to be fixed. In other words, the planar elements are divided into two contiguous, smaller sub-planar arrays symmetrical around the array center. The excitations of the elements in terms of amplitudes and/or phases of the outer sub-planar array are chosen to be adaptable during the optimization process to form the required constraints on the array pattern, while the excitations of the inner sub-planar array elements which have less impact on the radiation pattern are made constants and out of the optimization process. In this way, all the desired constraints can be obtained by concentrating the optimization process into only the most active elements which are smaller than the total number of elements to obtain a performance that is very similar to that of the conventional fully optimized planar array. The proposed array has many advantages compared to that of the conventional arrays as follows:

the number of the variable elements was significantly reduced; consequently, the convergence speed of the optimizer was greatly shortened. All the desired features were obtained with a simple array configuration without a need for complex arrays. Also, the manufacturing cost has been significantly reduced.

On the other hand, the good performance of the conventional heavy square planar array can be obtained by designing an equivalent array that consists of two crossed linear arrays with a far less number of the array elements. The best performances of the crossed arrays were obtained by designing their array element excitations according to either well-known deterministic methods or global optimization methods. Generally, it is found that the used optimization method is able to provide an array pattern that best matches to that of the conventional heavy square array with a far less number of the array elements.

TABLE OF CONTENTS

Subject	Page
Acknowledgments	I
Abstract	II
Table of Contents	IV
List of Figures	VIII
List of Tables	XIII
List of Abbreviations	XIV
List of Symbols	XV

LIST OF FIGURES

LIST OF TABLES

(4.1)	Performance measures of the proposed designs with 17 elements and the conventional square array with 25 elements	85
(4.2)	Performance measures of the proposed designs with 121 elements and the conventional square array with 961 elements.	95

LIST OF ABBREVIATIONS

Abbreviation	Name
5G	Fifth Generation
AF	Array Factor
ASLL	Average Side Lobe Level
BFGS	Broyden‑Fletcher‑Goldfarb‑Shanno
CE	Cross-Entropy
DBF	Digital Beamforming
DE	Differential Evolution
DFP	Davidson‑Fletcher‑Powell
FA	Firefly Algorithm
FNBW	Fist Null Beam Width
GA	Genetic Algorithm
HPBW	Half Power Beam Width
MIMO	Multiple-Input and Multiple-Output
MMW	Millimeter Wave
MPM	Matrix Pencil Method
NMDS	Nelder‑Mead downhill simplex
PSO	Practical Swarm Optimization
QPM	Quadratic Programming Method
SA	Simulated Annealing
SLL	Sidelobe Level

LIST OF SYMBOLS

Symbol	Name
a_{mn}	Amplitude excitation of the elements.
D_x	The directivity of the broadside linear array, x-axis.
D_y	The directivity of the broadside linear array, y-axis.
$D_\circ$	Directivity (dimensionless).
d_x	The spacings of element in x -axis.
d_y	The spacings of element in y -axis.
k	The wavenumber.
L	outer square rings that need to be optimized.
P_{rad}	Total radiated power (watt).
S_{11}	S-parameter (Reflection coefficient)
U_0	An isotropic source radiation intensity (Watt/unit solid angle).
U_{max}	Maximum radiation intensity (Watt/unit solid angle).
β_x	The progressive phase shifts in x -directions.
β_y	The progressive phase shifts in y -directions.
ε_r	Relative Permittivity
λ	The wavelength in free space.
λ_g	Guided wavelength
μ	Permeability
ρ_{nm}	phase excitation of the elements.

CHAPTER ONE

INTRODUCTION AND LITERATURE SURVEY

This chapter includes the introduction, literature survey, problem statement, objectives and the aims of the thesis. It also contains the whole organization of the thesis.

1.1. Introduction

The future of communication systems is expected to be more complex due to increased demands for new applications. Recently, they have undergone unparalleled rapid growth in which they cannot work effectively. The important part of the communication system that is responsible for effective transmission of the data in either transmit or receive modes is the antenna or antenna arrays. In fact, some of the features and performances of wireless communication are directly relying on the antenna designs that need the vision and the contributions of the designers and researchers to be developed.

Minimization or maximization of the antenna array characteristics such as sidelobe level, directivity, beamwidth, and null control has been always the aims of antenna array synthesis designers. It is necessary for the antenna engineers to have the latest tools to design antennas that meet the desired requirements. Optimization algorithms were widely used either to synthesize an antenna from the basic characteristics of radiation or simply to develop additional designs of the antennas. Generally, an effective optimization algorithm such as Practical Swarm Optimization (PSO)[1], Ant Colony optimization algorithm [2], Differential Evolution (DE)

algorithm [3], Cross-Entropy (CE) method [4], Convex Optimization [5], and Firefly Algorithm (FA) [6]…etc., can be used to design such antenna arrays. The elements of the antenna arrays can be arranged in simple linear or planar, such as rectangular, crossed, circular configurations. In all of these configurations, there are only three main variable parameters that can be optimized to get the desired radiation features. These design parameters include the amplitude element excitations, phase element excitations, and the separation distances between the array elements. We need to find the optimum values of the amplitudes, phases, and distances of the array elements to get the corresponding desired radiation characteristics.

The optimization of all array elements is referred to as fully optimized arrays. In such types of arrays, the current excitations in terms of amplitudes or phases of all the array elements are adjusting iteratively during the optimization process to achieve the desired radiation pattern. Thus, the fully optimized planar arrays are usually difficult to be practically implemented and time-consuming; therefore, simpler methods are highly advised. Therefore, a lot of work has been dedicated to optimize and quickly search for an optimal solution as accurate as possible. To solve this problem, a well-known optimization scheme based on genetic algorithms (GA) has been adopted. The genetic algorithm can be classified as robust, and stochastic in nature in searching the solutions. It models the design process according to natural selection and evolution. The principle and the fundamental concepts of the Genetic Algorithms (GAs) were introduced by Holland [7], which were represented in detail in 1989 by Goldberg [8].

To get a good design, the goal should be given in terms of how to obtain the desired radiation pattern with a minimum number of the optimized array elements. Reducing the number of optimized elements which is the main objective of this work is extremely important to simplify the feeding network of the antenna array. In this thesis, mainly the amplitudes and/or phases of the array elements are optimized to obtain the desired radiation pattern according to the pre-specified constraints.

1.2. Literature Survey

For several years, optimization techniques have been commonly used in the antenna synthesis community. It is also used for reducing the optimized number of the array elements that satisfy the desired performance. the purpose of this section is to give full information about the state of the art of optimization algorithms that currently being used in antenna designs [9].

In 1996, Randy Haupt used the GA to find the quantized phase weights that minimize the array sidelobe pattern in the scanning region [10].

In 1999, Francisco J. Ares-Pena et al, presented: three examples one included linear and planar arrays and two for linear arrays. To solve three critical problems dealt with antenna array pattern synthesis, by combining GA's and simulated annealing (SA) for array thinning, a hybrid approach is introduced, which solves the problem of removing unnecessary elements from a planar array [11].

In 2004 Sayidmarie and Mohammed designed a uniform linear array

with asymmetric sidelobe level on each side of the main beam. The method is based on subtracting or adding two patterns obtained from the

main and auxiliary antennas. The side lobes on one side of the main beam were significantly suppressed by adjusting the value of an attenuator and the separation distance between the two auxiliary elements [12].

In 2005 Aboud and Sayidmarie used an auxiliary antenna in conjunction with the primary array. The applied auxiliary antenna for sidelobe reduction has a radiation pattern that is identical to the original phased array's sidelobe structure. A good reduction in sidelobes was obtained for auxiliary antennas with two, four, or eight elements [13]. In the same year, for minimum sidelobe level and null control, three design examples were proposed by Majid M. Khodier et al, in the synthesis of linear array configuration, demonstrated the use of the PSO algorithm and the optimization aim in each example. The results of the PSO algorithm are checked by comparing them with obtaining results using the quadratic programming method (QPM) [1].

A DE algorithm and a binary-coded GA were presented by Carlos Rocha-Alicano et al, in 2007 to the method of synthesizing an SLL reduction planar array factor. SLL minimization requires a highly complex problem of nonlinear and non-convex dependency between the array factor and its element parameters. A binary-coded genetic algorithm was proposed for the synthesis of planar arrays when such external planar array elements are removed, the level of the sidelobe of the planar array reduces without a noticeable change in direction. When implemented together, both algorithms demonstrate the minimization of planar arrays by the sidelobe level [3].In 2008, Yanhui Liu et al, presented a method for reducing the number of array elements based on the matrix pencil method

(MPM). The method was applied to the non-uniform linear arrays to synthesize pre-specified radiation patterns with a limited number of elements [14]. In the same year Huaijun Wang et al, presented a narrowband MIMO imaging radar with two orthogonal linear T/R arrays where they were able to get an image resolution with a small number of array elements that are close enough to that of the conventional two-dimensional planar array that uses all of the array elements [15].

In 2011, Wenji Zhang et al, presented the Bayesian compressive sensing to minimize the number of the array elements. They were able to achieve the required radiation patterns of both linear and planar arrays with a minimum number of array elements[16].

To minimize the SLL of the antenna array pattern, in 2012, Lahcene Hadj Abderrahmane et al, discuss the use of the CE method for synthesizing planar antenna arrays. The method is validated and is shown to be useful on arrays of both isotropic and non-isotropic elements. Simulated results appear to produce SLL elements. Therefore, the CE-designed array had a lower beam width of -22.7 dB for isotropic elements and -32.17 dB for non-isotropic elements [4].

In 2013, an advanced technique has been proposed by Khalil H. Sayidmarie et al, for generating large nulls to resolve the adverse effects of frequency volatility. From the results of the simulation, it is noted that for a much wider bandwidth, the proposed array will retain appropriate null [17].

In 2014, Mohammed, J. R. et al, presented an SLL cancellation for the uniformly excited planar array over a wide angular range. The technique

is to constantly adjust the edge elements' amplitude only and phase-only excited while leaving the rest of the elements unchanged. Simple formulas are provided for computing the necessary amplitude and phase excitations of these edge elements [18]. In the same year, Yilong Lu et al, designed a MIMO cross array with azimuth-elevation combination beamforming capability by the use of DBF systems. They greatly reduced the number of the elements compared to the conventional two-dimensional rectangular array of one-way and two-way beamforming. Their proposed configuration was able to reduce the size of the designed array from (M x N) to only (M+N+4) elements [19]. In 2017, the GA and PSO are separately presented by J.R. Mohammed, to find the optimal values of the amplitude only and phase-only excitations for edge elements for sector sidelobe nulling in the equally spaced linear array pattern with uniform excitations except for elements of edge, it has also been suggested that optimized elements can be increased by using planar arrays instead of linear arrays. In this case, the optimized parameters are the boundary elements of planar arrays [20],In the same year, M. J. Martínez Silva et al analyzed the performance of the square planar arrays in terms of their radiation patterns with that of the cross array. They found that, although the square planar arrays have better efficiency, the cross array was able to provide good directivity for the applications of a 5G mobile handset at 28 GHz [21]. In 2018, Jafar Ramadhan Mohammed proposed a method for uniformly excited large arrays by only adjusting the amplitude and phase of a relatively small number of elements on the extremes of the array by means of (GA). A number of the optimized elements were chosen and fixed to a certain value before the optimization process. Thus, the

6

optimized array patterns were found to be satisfactory only if the chosen value of the optimized elements was found to be sufficient to form the required constraints [22]. In 2019, three applications were presented for the optimization of the Firefly Algorithm by Eduardo Yoshimoto et al, for the synthesis of a non-uniformly spaced linear antenna array, a non-uniformly spaced planar array, and a uniformly spaced planar microstrip array. Strong agreement was obtained between the desired constraint and the optimized patterns in the three cases considered[6].

In 2020, Jafar R. Mohammed, suggested different optimization methods and configurations control only the amplitude and the phase excitations of a number of the selected elements instead of all of the array elements. Thus, a great reduction in the array weight, cost, and feeding complexity was obtained without any loss in the directivity [23-24], In the same year Ahmed J. Abdulkader et al, suggested optimizing the phase-only excitations of the array elements instead of both amplitude and phase excitations to simplify the design process of the array feeding network and reduce the number of the optimized variables [25]. In 2020, Jafar R. Mohammed et al, proposed convex optimization in these methods, only the perimeter elements of the planar arrays were allowed to be iteratively adjusted during the optimization process to obtain the desired radiation patterns with particular nulls and sidelobe levels [26], In the same year, Boxuan Gu et al, also presented the convex optimization to design the crossed array with a minimum number of array elements to achieve the required radiation pattern [27].

1.3.Problem Statement

Some of the modern radar and communication systems use planar array configurations due to their flexibility and the possibility of freely scanning their main beam directions in both azimuth and elevation planes instead of reducing or minimizing the number of the planar array elements, it is possible to select a certain number of the planar array elements to be controllable with required RF components such as variable attenuators, variable phase shifters, and other hardware to control the array radiation patterns according to the required goals, also, in some applications such as MIMO wireless communication and 5G mobile handset, the weight of the used antenna array needs to be as small as possible and takes a small space. Thus, designing such arrays with a fewer number of elements while maintaining a good radiation characteristic is highly desirable. Other advantages of such antennas with a fewer number of array elements include lower cost and greater simplification in the array feeding network.

1.4.Objectives and aims of the dissertation

✓ To study the performance of the rectangular fully filled planar arrays and some other planar configurations such as cross arrays.

✓ The performance of all considered arrays will be analyzed and compared in terms of half Power Beamwidth (HPBW), Fist Null Beamwidth (FNBW), Directivity, Peak side lobe level (SLL), Null direction, and the visual radiation patterns.

✓ Use the Genetic Algorithm to optimize the array performance under some desired constraints on the array radiation pattern.

✓ To simplify the planar array as simple as possible for easy implementation in practice.

✓ To reduce the problems of interfering signals by controlling the null directions which are playing important role in limiting the performance of the current and future wireless communication systems.

✓ To verify the performance of some optimized planar arrays by taking into account the mutual coupling, element type, scattering, and many other practical issues by using CST STUDIO SUITE software.

1.5. Organization of the Thesis

This thesis is organized as follows. The first chapter contains an introduction and discusses the previous research and the general analysis of the latest literature techniques, which act as the inspiration for writing this dissertation. The second chapter gives the theoretical background of planar arrays, GA as a tool for optimization proposed designs. Chapter three presents the design of a proposed Planar array Optimization with amplitude only excitations, Phase-only excitations, and complex excitations using the GA codes in MATLAB the test results are also verified by using CST STUDIO SUITE software in this chapter. Chapter four presents the design of two orthogonal linear antenna arrays (cross-array) with five proposed designs uniform, triangular, Dolph, Taylor distributions or numerically through the use of GA, by amplitude-only excitation, then comparing MATLAB results with verified results of CST in this chapter. Chapter Five offers a conclusion of the thesis and a list of future considerations.

CHAPTER TWO
BACKGROUND THEORY

This chapter explains the background theory of the planar antenna arrays as well as the basic principles of the optimization algorithm.

2.1. Introduction

The radiation of single-element antennas is typically wide pattern, i.e., they have relatively low directivity. Antennas with high directivity are also required in far-distance communications. It is possible to build such antennas by enlarging the radiating physical dimensions. However, this approach can lead to multiple side lobes appearing. Besides the antenna is normally large and hard to design. Another way of raising an antenna's electrical size is to synthesize it as an arrangement of radiating elements in a proper electrical and geometrical configuration known as an antenna array [28].

2.2. Antenna array

An array of antennas simply means a set of antennas placed in some geometric arrangement. An antenna array can have a fixed main beam direction, or by changing the relative phases between antennas, it can scan the main beam in space. The benefit of antenna arrays is that they can generate highly directive beams, where high antenna gain is needed to resolve high propagation losses at high frequencies, so using of antenna arrays is a core idea [28].

2.3. Parameters of Antenna array

Descriptions of different parameters are required to explain an antenna array performance. Some of these parameters that are required for the analysis in this thesis are the following:

2.3.1. Radiation Pattern

An antenna array radiation pattern is a graphic representation of an antenna's radiation properties, which may provide details on the radiated field's energy distribution, phase, and polarization. We are often most interested in plots on spheres surrounding the antenna of the relative energy distribution, and such graphs are referred to as power patterns and field patterns are referred to as plots of field magnitude. We can also plot, normalized patterns. We refer to the area of intense radiation when plotting an antenna array pattern as the "main beam" of the antenna array. Radiation exists in the form of sidelobes in other directions. As shown in Figure 2.1. [28] , [29].
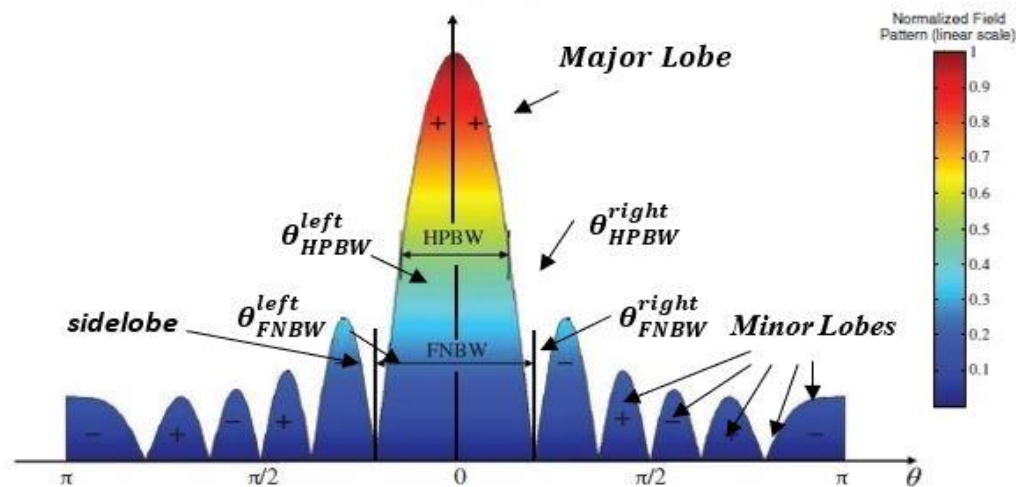
Figure. 2.1. Rectangular plot of normalized radiation pattern.

11

2.3.1.1. Half Power Beam Width (HPBW)

The (HPBW) of an antenna is defined by IEEE as: "In a plane containing the direction of the maximum of a beam, the angle between the two directions in which the radiation intensity is the one-half value of the beam.", it is explained in equation (2.1),[28].

$$HPBW = \left|\theta_{HPBW}^{right}\right| + \left|\theta_{HPBW}^{left}\right| \quad \ldots (2.1)$$

2.3.1.2. First Null Beam Width (FNBW)

The **(FNBW)** is definition by IEEE as: "The angular span between the first pattern nulls adjacent to the main lobe, is called as the First Null Beam Width." it is explained in equation(2.2),[28].

$$FNBW = \left|\theta_{FNBW}^{right}\right| + \left|\theta_{FNBW}^{left}\right| \quad \ldots (2.2)$$

2.3.1.3. Side Lobe Level

The **(SLL)** the ratio of the radiation intensity in the direction of the largest sidelobe which is usually, but not always, the first sidelobe adjacent to the main antenna beam to the maximum radiation intensity is recognized as the sidelobe level (SLL) of an antenna. It is explained in equation (2.3),[28].

$$SLL = \frac{U_{SLL} \; of \; Minor \; Lobe}{U_{max} \; of \; Major \; Lobe} \quad \ldots (2.3)$$

SLL less than -13dB is accepted, Achieve of SLL less than -20dB is the one aim of the thesis being carried out in the field of the cross-array antenna. Proper design and structure of antenna array are necessary to obtain a minimum sidelobe level.

2.3.1.4. Average Side Lobe Level (ASLL)

The (**ASLL**) is a power average create by combining the power in all minor lobes outside the major lobe and expressing it in decibels (dB)it is explained in equation (2.4) [30]. Low average sidelobe levels have been achieved in this thesis with careful design and optimization processes.

$$(ASLL) = 10 \log_{10} \left(\begin{array}{c} average \ power \ of \ minor \ lobes \\ outside \ the \ major \ lobe \end{array} \right) \dots (2.4)$$

2.3.1.5. Taper Efficiency

Is a relative figure of eligibility, giving the loss of directivity due to array amplitude and phase weighted coefficients, and it is a valuable design tool, it is explained in equation (2.5), [31].

$$Taper \ Efficiency = \frac{1}{M} \frac{|\sum w_n|^2}{\sum |w_n|^2} \qquad \dots (2.5)$$

Where M is the number of elements, w_n is the coefficients weights.

2.3.2. Directivity

The main objective of an antenna array designer is to design a response or beam pattern such that radiation in a certain direction is strong and the reception in other directions is suppressed and it is a useful measure of the intensity. The array directivity is defined as the ratio of the intensity of radiation in a given direction from the antenna to the average intensity of radiation in isotropic. The mean intensity of radiation is equal to the total power divided by 4π radiated by the antenna. The direction of maximum radiation intensity is inferred if the direction is not specified. More precisely put, the directness of a non-isotropic source is equal to the ratio in a given direction of its radiation intensity to that of an isotropic source in the situation of array synthesis, as the losses in antennas and antenna

circuits are not beholding, array gain is frequently used reciprocally with array directivity. It is explained in equation(2.6),[28].

$$D_0 = \frac{U_{max}}{U_0} = \frac{4\pi U_{max}}{P_{rad}} \qquad \ldots. (2.6)$$

where

D_0 = directivity (dimensionless).

U_{max} = maximum radiation intensity (Watt/unit solid angle).

U_0= an isotropic source radiation intensity (Watt/unit solid angle).

P_{rad} = total radiated power (Watt).

For broadside planar arrays, the directivity can be computed by the equation (2.7)[28].

$$D_{planar} = \pi \cos \theta_0 D_x D_y \ldots. (2.7)$$

Where

D_x The directivity of the broadside linear array, x-axis

D_y The directivity of the broadside linear array, y-axis

D_x and D_y, can be obtained by the equation (2.6).

2.4. Antenna array configuration

The antenna array is categorized into linear and planar structures according to the geometric configuration, considering the location of array elements. In general, to achieve the desired radiation pattern, the identical radiators are arranged in a linear, rectangular, circular, and cross lattice, etc., as shown in Figure 2.2, with periodic spacing between them. The efficiency of the array beam-forming depends on the choice of array

14

configuration, the physical structure of each element, amplitude and phase excitations of the array elements, and the separation distances between the array elements [28], [33].

The study in this thesis will focus on two types of antenna array configuration, which are the rectangular array and the cross array in terms of studying performance and optimization to them in different ways using optimization by GA.

a-linear array

b- rectangular array

c-circular array

d-cross array
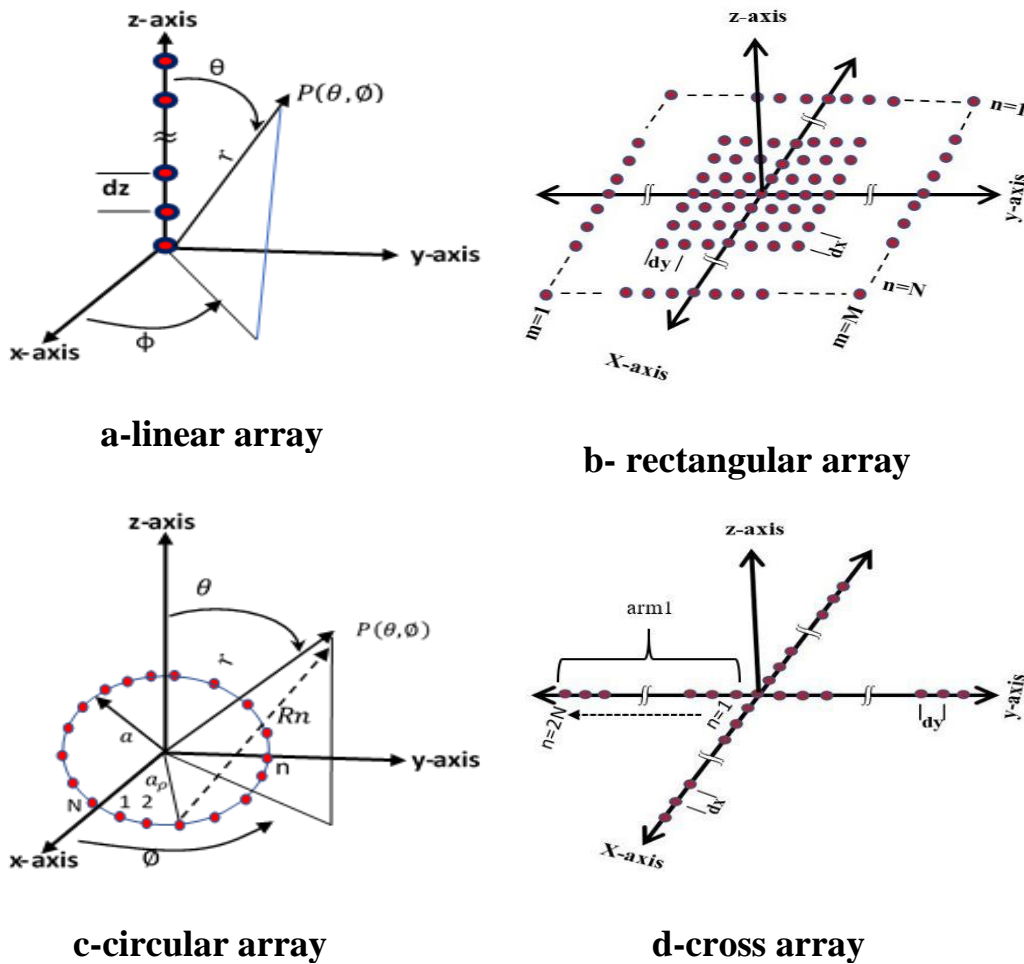
Figure 2.2. geometric configurations of antenna array.

2.4.1. Rectangular Array

Specific radiators may be placed along a rectangular grid to form a rectangular or planar array, in addition to positioning elements along a line to create a linear array. Additional rectangular arrays have additional details for variables that can be used to guide the array pattern and to shape it. Rectangular arrays are more flexible and, with lower side lobes, can have more symmetrical patterns, as mentioned below, some distinct advantages of rectangular arrays over other traditional arrangements such as Linear Arrays are [28].

- Elevated flexibility
- better symmetry in beam patterns,
- Lower levels of Sidelobe
- Higher directivity; narrower main lobe
- The main beam can be scanned basically towards in space.

rectangular arrays are commonly used in a variety of applications because of these benefits, such as radar detection, remote sensing, wireless communications, etc. For 5G MM wave wireless communications, they are considered the most appropriate antenna configuration [33].

2.4.1.1. Rectangular Planar Arrays' Mathematical Analysis

The elements were organized into a two-dimensional geometric structure in planar arrays. The simplest type of planar arrays, as shown in Figure 2.2 (b), is the uniformly spaced rectangular array. As in the case of linear arrays, by summing the electric fields of all elements together, the array factor of a rectangular array can also be determined, treating the rows

16

and columns as independent linear arrays for a uniformly spaced rectangular array. The array factor is explained in equation (2.8) [28].

$$AF(\theta, \emptyset) = \sum_{n=1}^{N} a_{1n} \left[\sum_{m=1}^{M} a_{m1} e^{j(m-1)(kd_x \sin\theta \cos\emptyset + \beta_x)} \right] \times \\ e^{j(n-1)(kd_y \sin\theta \sin\emptyset + \beta_y)} \quad \dots (2.8)$$

can be simplified equation (2.8) as:

$$AF = S_{X_M}.S_{Y_N} \qquad \dots (2.9)$$

Where S_{X_M} and S_{Y_N} are

$$S_{X_M} = \sum_{m=1}^{M} a_{m1} e^{j(m-1)(kd_x \sin\theta \cos\emptyset + \beta_x)} \qquad \dots (2.10)$$

$$S_{Y_N} = \sum_{n=1}^{N} a_{1n} e^{j(n-1)(kd_y \sin\theta \sin\emptyset + \beta_y)} \qquad \dots (2.11)$$

where a_{m1} and a_{1n} are the amplitudes excitation of the elements in x- and y-axis, respectively, d_x and d_y are the spacings of element in x- and y-axis and β_x and β_y are the progressive phase shifts in x- and y-directions. The parameters appear in Figure 2.2 (b), [28].

A rectangular array's radiation pattern varies from that of a linear array. The three-dimensional pattern of radiation of a linear array is the same as omnidirectional, i.e., any plane and directional pattern in every orthogonal plane has a non-directional pattern. On the other hand, the radiation pattern of a rectangular array is much more of a directive.

Another benefit of rectangular arrays over linear arrays is that the beams can be steered three-dimensionally, i.e., in both directions of azimuth and elevation. This can be understood by considering the rectangular sequence in Equations (2.10) and (2.11). The beam can be steered in any direction

with respect to the x-direction by adjusting the progressive phase change between the elements in the x-direction. Likewise, the beam can be steered in relation to the y-directions by changing the progressive phase shifts between the elements in y-direction [31].

In Figure 2.3, for instance, three- dimensions beam pattern for uniform excitation a (9x9) broadside rectangular array.
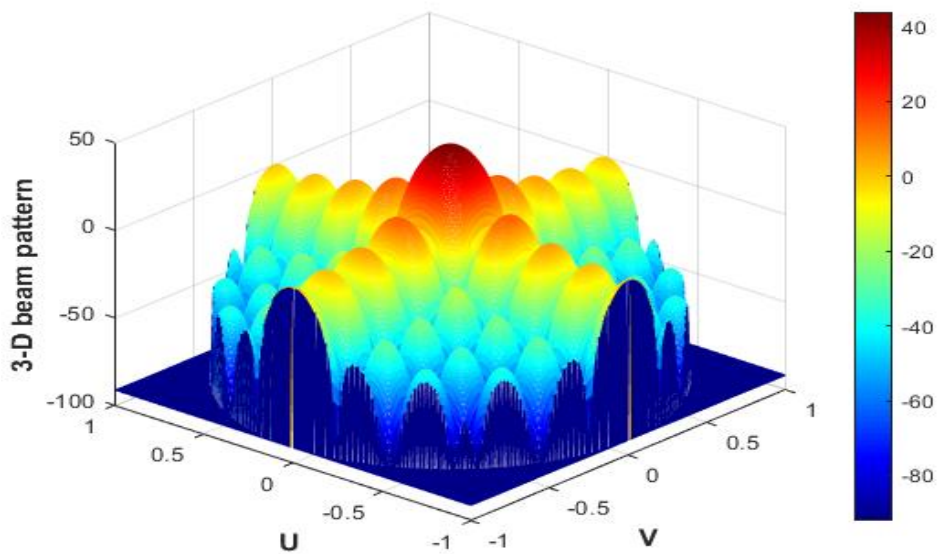
Figure 2.3. (9x9) pattern of broadside rectangular

2.4.2. Cross Array

The cross array consists of two linear arrays that are located at right angles to one another in the form of a cross. As explained in the Figure 2.2, (d). The beam pattern of each linear array is a cross beam that is broad in the plane orthogonal to the array axis and when the responses of the two arrays are combined in the same phase, the resulting beam pattern is the composition of the patterns of each array [35].

18

The array factor of the symmetric two orthogonal linear arrays can be written as [35]: -

$$AF(\theta, \emptyset) = 2 \times w_0 + 2 \sum_{n=1}^{n=2N} w_n \left[\cos\left(n(kd_x \sin\theta \cos\phi)\right) + \cos\left(n(kd_y \sin\theta \sin\emptyset)\right) \right] \dots (2.12)$$

where w_n, is the coefficients of the amplitude element excitation, d_x is the spacing between elements along the x-axis and d_y is the spacing between elements along the y-axis, $k = 2\pi/\lambda$ and λ is the wavelength in free space.

If the element weightings w_n are all uniformly excited, then the resultant radiation pattern will have usually high sidelobe level [35]. Figure 2.4, shows the radiation patterns in three-dimension of cross array with size $(4(2N) + 1)$ for $(N = 2)$ and uniform excitations, i.e., $w_n = 1$ for all elements.
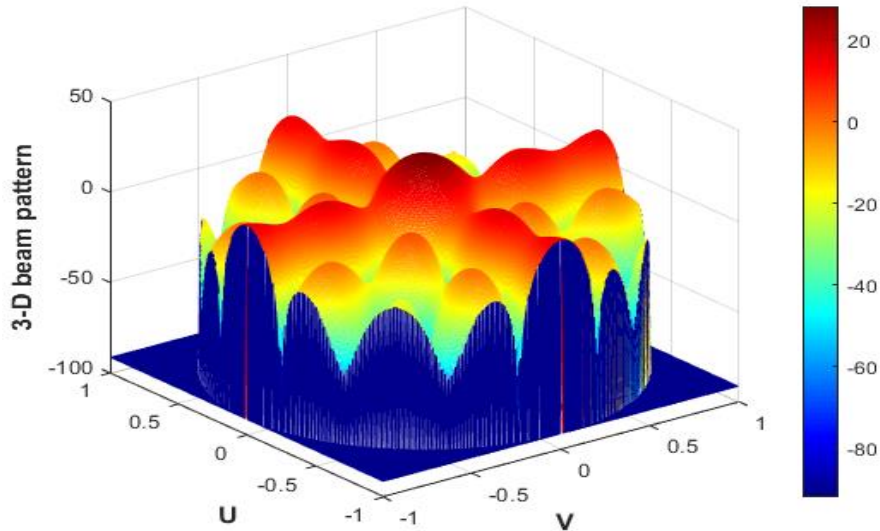
Figure 2.4. pattern of crossed array with size $4(2N) + 1 = 17$

It can be seen that the radiation pattern of the crossed array with uniform excitation has a relatively high sidelobe level. Thus, we need to redesign or recalculating the amplitude element excitations of the crossed array such that the sidelobes can be reduced. These procedures and techniques will be implemented later in Chapter Four of this thesis.

2.5. Genetic Algorithms (GA)

In recent times, unique genetic-based optimization schemes a variety of electromagnetic problems have been solved using algorithms (GA). Adaptive heuristic search algorithms are programming techniques that, are based on the evolutionary ideas of natural selection and genetics. most of the early work on genetic algorithms was pioneered by J. Holland. Since then, several scholars have contributed a wealth of information to the analysis and use of genetic algorithms (GAs) [36].

A definitive work, finished by D. Goldberg is currently the predominant curriculum of choice for the analysis of GAs in 1989. In an area where there is a very large range of candidate solutions and where the search space is uneven and has several peaks and valleys, genetic algorithms begin to evolve[37].

So, the **GA** can be defined as a global optimization algorithm inspired by the process of natural selection. Genetic algorithms are commonly used to generate high-quality solutions to optimization and search problems by following the principles and parameters set by Darwin GAs. By depending on biological operators such as selection, chromosomes, genes, mutation, and crossover, are used to achieve an optimal solution,[38].

2.5.1. Why genetic algorithms?

Consider the relationship between GA optimizers and more conventional and potentially more familiar optimizers in order to answer this query. This relationship is depicted in Figure 2.5. Genetic algorithms are classified as global optimizers, whereas more popular conventional methods are categorized as local optimizers, such as Steepest descent, Davidson‑Fletcher‑Powell(DFP),Broyden‑Fletcher‑Goldfarb‑Shanno (BFGS),and Nelder‑Mead downhill simplex (NMDS)[38] .

The difference between the local and the global quest for optimization techniques is that the outcomes of the local techniques are largely dependent on the starting point or initial guess, whereas the global techniques are highly independent of the original conditions.
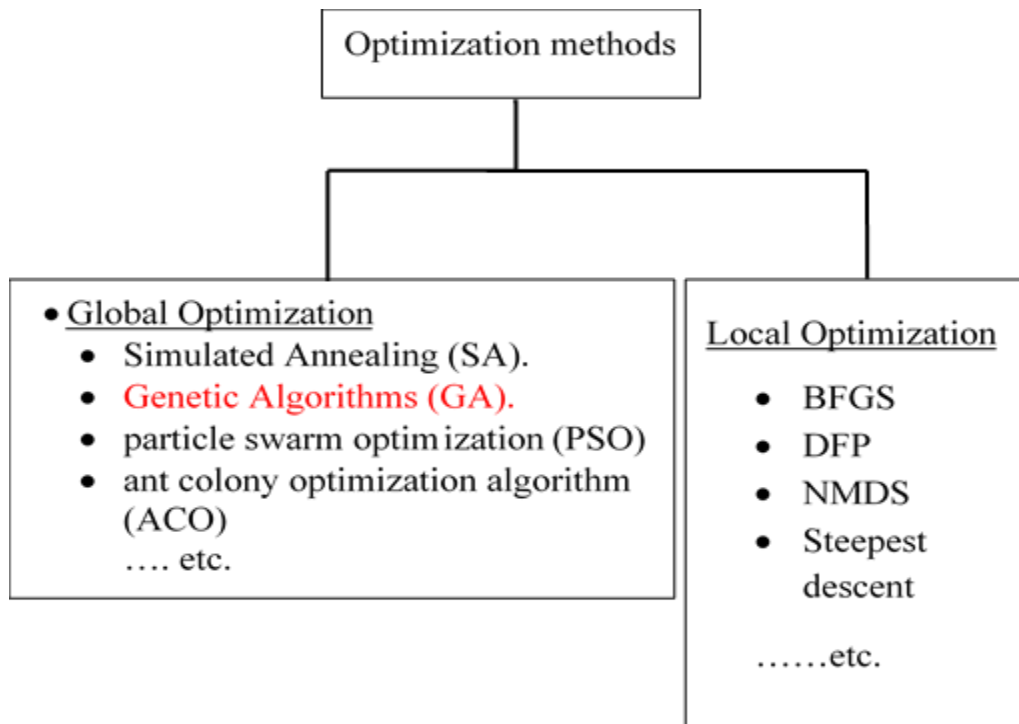
Figure 2.5. some of the optimization methods classification

Although they have the characteristic of being quick in convergence, local techniques, especially the (Davidson–Fletcher–Powell (DFP), Broyden–Fletcher–Goldfarb–Shanno (BFGS) techniques, are directly dependent on the presence of at least the first derivative. They also impose constraints on the space of the solution, such as differentiability and consistency, conditions that are difficult or even impossible to deal with in practice the form of the gradient, conjugate gradient techniques rely either explicitly or implicitly on a derivative. On the other hand, global techniques are essentially independent of the solution space and impose few constraints on it[38].

2.5.2. Benefits of (GA).

A GA has many benefits over conventional approaches to numerical optimization, as well as the reality that it.

1) Fits for a large number of variables .
2) Suitable for parallel computers .
3) Optimizes variables with cost surfaces of extreme complexity .
4) Provides a list, not just a single solution, of optimum parameters.
5) Optimization of parameters that are continuous or discrete .
6) The parameters can be encoded, and the optimization is done with Parameters Encoded .
7) Works with data generated numerically, experimental knowledge, or analytical functions.
8) Searches from a large sampling of the cost surface at the same time.
9) Doesn't need derivative data.

Using computers, genetic algorithms are usually implemented experiments where an issue of optimization is defined. For this thesis, using an abstract representation called chromosomes, representation of a space of optimal solution, called individuals, are represented. GA consists of an iterative mechanism that progresses towards an objective function, or fitness function, a functioning group of chromosomes called a population. Solutions are typically represented using strings of fixed length, real number encoding strings, but other encodings are listed later [37]–[39].

2.6. The Main Terms Associated with the GA

Some important terms and principles of GA optimizers are presented in the following sections, several of which are to be dealt with in more detail later on.

2.6.1. Genes and chromosomes

A gene string is called a chromosome. It is possible to code chromosomes as strings of real number or as binary number strings. The gene is the GA's basic component. The sample chromosome shown in Figure 2.6 is composed of 3 genes with each gene containing 7 binary digits[40].

chromosome = 1010010 1100111 1100110
g1　　　g2　　　g3
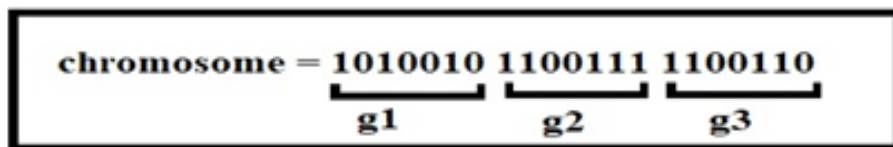
Figure 2.6. composed of 3 genes with 7 binary digits in each gene.

2.6.2. Encoding

The solutions to the issue of chromosomes in GA encoding are a key problem. John Holland used a single string of binary bits. The issue encoding is linked to the fact that certain chromosomes can correspond to the solutions that are infeasible or unconstitutional. For constrained optimization problems and combinatorial optimization problems, this can become very serious. An infeasible solution is one that lies beyond the feasible area of a given problem. In order to treat infeasible chromosomes, penalty methods may be used. To transform an unauthorized chromosome to a legal one, repair techniques are generally adopted. Today, several different genetic information encoding methods are in general use; gray encoding, real-value arrays, permutations, and so on, Processes of encoding can be classified in general as follows [41].

2.6.2.1. Encoding Real-Number

The encoding of real numbers works better than binary encoding for optimization of functions and constrained issues of optimization. The structure of the genotype space is similar to that of the phenotype in real number encoding. It is therefore easy to build effective genetic operators by borrowing important methods from traditional methods.

2.6.2.2. Binary encoding

Most of the new theory of GAs is based on the premise that binary encoding is used. In the phenotype space, the binary code does not maintain the position of points.

2.6.3. An Initial Population and Generation

A matrix of the chromosomes is a population; a collection of randomly selected members (chromosomes) begins with the GA. The original population is called this set. generations are called the iterations in GA. The optimum solution is a random "guess" for each row. If the output of the cost function is determined using a number of variables, then a chromosome in the initial population consists of a number of random variables allocated to these variables. For example, produces a random population matrix of 5 population chromosomes each having 4 variables with encoding of real numbers is shown in Figure 2.7 [38].

$$
\text{population} =
\begin{bmatrix}
\text{gene-1} & \text{gene-2} & \text{gene-3} & \text{gene-4} \\
0.213 & 0.352 & 0.389 & 0.745 \\
0.756 & 0.402 & 0.664 & 0.545 \\
0.365 & 0.512 & 0.775 & 0.776 \\
0.399 & 0.554 & 0.977 & 0.654 \\
0.112 & 0.436 & 0.844 & 0.742
\end{bmatrix}
\begin{matrix}
\\
\text{chromosome-1} \\
\text{chromosome-2} \\
\text{chromosome-3} \\
\text{chromosome-4} \\
\text{chromosome-5}
\end{matrix}
$$

Figure 2.7. A random population matrix of 5 population chromosomes each having 4 variables gene.

2.6.4. Fitness (or Objective) Function

The objective function defining the goal of optimization calls the fitness function. Use a numerical solver to measure properties such as Directivity, Bandwidth, sidelobe level, etc.

It assigns "good" or "badness" to the various members' quality' of chromosomes in the population, the chromosomes are allocated to the assessment role of the cost function. Then every chromosome has a related cost an extremely important step in optimization is formulating the cost function. As the function must be called several times in order to calculate the expense of the members of the community, there is generally a tradeoff between the precision of the measurement and the time of the assessment. Only the related variables of the cost function should be used in order to minimize convergence time[41].

2.6.5. Selection

Selection refers to the process of deciding the number of times a single person is selected for reproduction and, thus, the number of children that an individual can produce. Both Binary GA and real coded GA share the same selection strategies as these strategies apply to chromosomes regardless of the type they take. The selection provides the driving force in GA. The genetic search would terminate prematurely, with too much force. The evolutionary change would be slower than necessary, though with too little force. In this way, the genetic search is oriented towards promising regions in the search space and will increase the efficiency of genetic algorithms [40], [41], the most prevalent types are:

2.6.5.1. Tournament selection

It is a more efficient selection process. N participants are selected at random in tournament selection. The strongest members are chosen from this category of N chromosomes. The procedure is replicated until the participants are chosen for the next, identically sized, population.

Tournament selection facilitates the selection of both weak and strong representatives of the population When 3 chromosomes are chosen for each tournament, Figure 2.8 diagrams the tournament selection process.
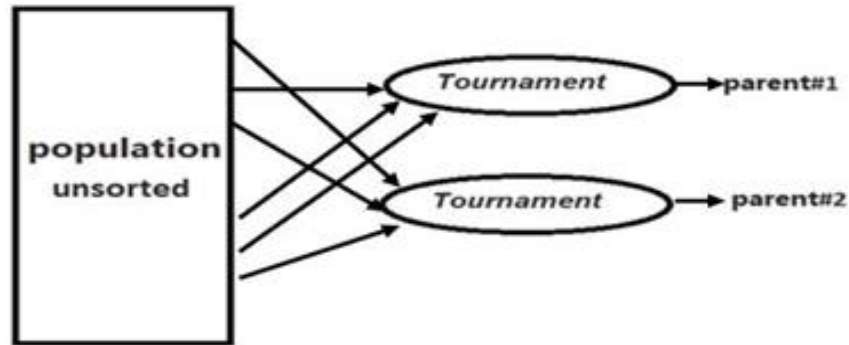
Figure 2.8. Diagrams the tournament selection.

2.6.5.2. Roulette wheel selection

It is the most common method of selection used for crossover and mutation in genetic algorithms for selecting potentially useful chromosomes (solutions). As in all selection methods, possible solutions are allocated to fitness by the fitness function in the roulette wheel selection shown in Figure 2.9 that shows a roulette wheel for 8 parents in the mating pool. This fitness level is used to associate a selection probability with each individual. Although it would be less likely that candidate solutions with a higher fitness will be eliminated, there is still a possibility that they will be. There is a possibility that certain weaker solutions may be possible with roulette wheel selection. The philosophy is that people are chosen based on the probability of equation selection (2.13).

$$probability\ of\ selection = \frac{f(parent_i)}{\sum_i f(parent_i)} \qquad ....(2.13)$$

Where the $f(parent_i)$ is the fitness value at $parent_i$.
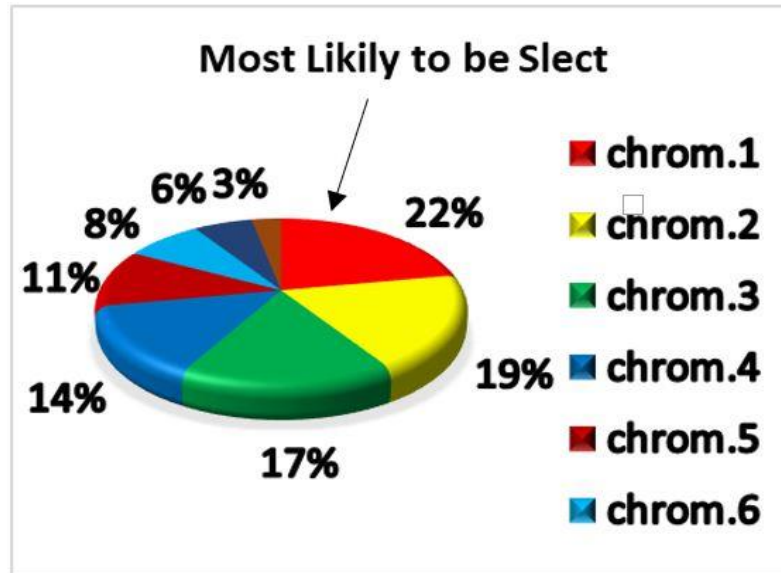
Figure 2.9. Roulette wheel for 8 parents in the mating.

2.6.5.3. Rank selection

In the selection of rankings, as shown in Figure 2.10, the chromosomes in the selection according to their health principles, the population is sorted from best to worse. A numerical rank based on fitness is allocated to each chromosome in the population, and selection is based on this ranking rather than fitness differences. The benefit of this method is that, at the cost of less fit people, it may prevent very fit people from achieving superiority early, which would decrease the genetic diversity of the population and could impede attempts to find an appropriate solution. The downside to this approach is that the entire population has to be sorted by rank, which is a potentially time-consuming process[42].

28
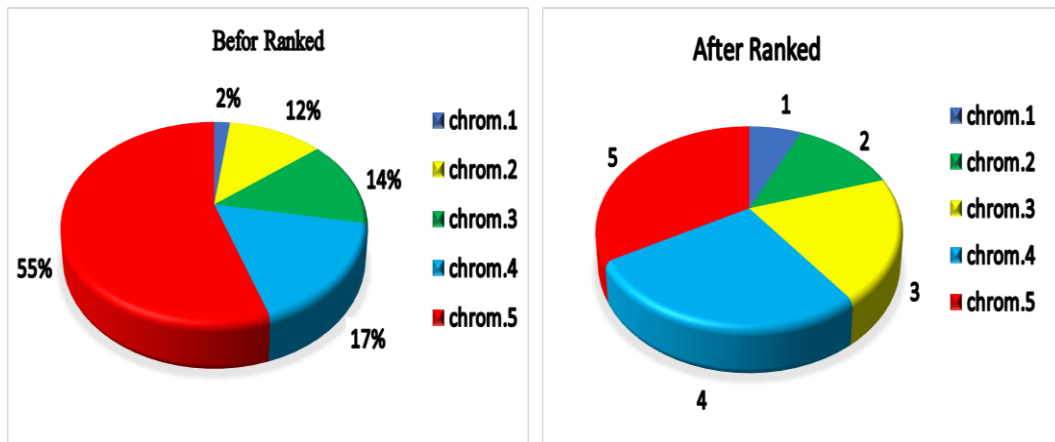
Figure 2.10. Rank selection for 5 parents in the mating.

2.6.6. Crossover (Mating)

This procedure is carried out by randomly choosing members of the population. A crossover point is randomly chosen and a cross probability is mated between the two parents. In the design and execution of robust natural changes, crossover plays an important role. In most GAs, chromosomes are represented by strings of fixed length and crossover operates on pairs of chromosomes (parents) by exchanging segments from the strings of the parents to produce new strings (offspring). The number of crossover points (defining how many segments are exchanged) has historically been set at a very low constant value of 1or 2, where schemes vary from binary to real coded GA.

2.6.6.1.Single point crossover:

A widely used crossover approach is called single-point This is the crossover shown in Figure 2.11, a single point in this system the crossover position (called crossover point) is randomly selected and the pieces of two

parents are exchanged to form two descendants after the crossover position[38].
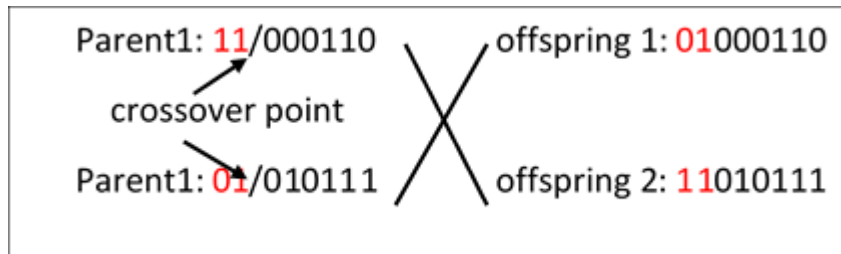
Figure 2.11. A single point crossover.

2.6.6.2 Multi point crossover:

A multi-point crossover is a single-point crossover generalization, a larger number of crossover points will be added. Multiple locations are picked at random in this case and the segments between them are traded, as shown in Figure 2.12[38].

The crossover consists of taking part of the features provided by the first parent in the real GA code and completing the other part with features from the other parent. Those characteristics are selected randomly. The newly generated kids would be a mixture of the properties of their parents. The equations governing this system are[40].
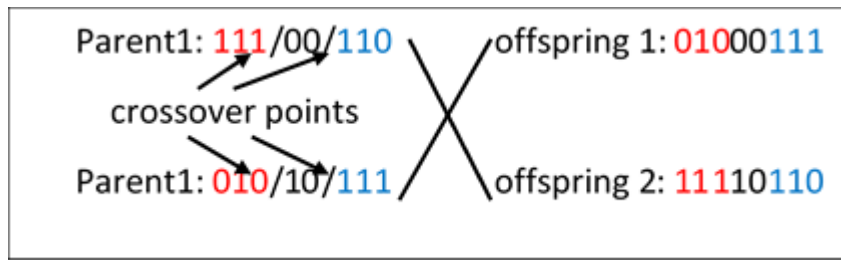
Figure 2.12. A Multi points crossover.

$$\text{offspring1} = \rho \times \text{Parent1} + (1 - \rho) \times \text{Parent2} \ \dots \ (2.14)$$

$$\text{offspring2} = (1 - \rho) \times \text{Parent1} + \rho \times \text{Parent2} \ \dots (2.15)$$

Where ρ is a random number. $(0 \leq \rho \leq 1)$.

2.6.6.3. Uniform crossover

Usually, each bit is chosen from either parent with equal probability in the uniform crossover. Other mixing ratios are often used, resulting in offspring which inherit more genetic information from one parent than the other as shown in Figure 2.13[43].
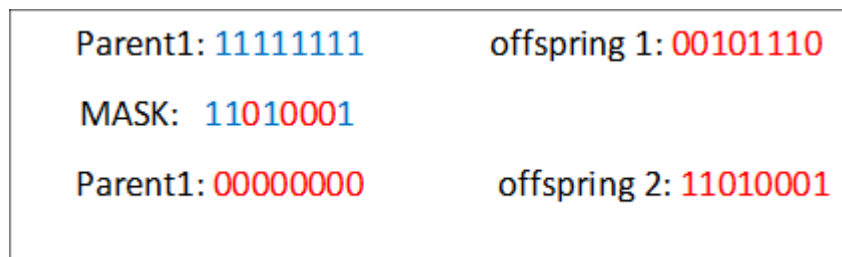
Figure 2.13. Uniform crossover.

2.6.7. Mutation

Is random change in chromosome at the bit level is much as in nature and occur by switching "1" to "0" or "0" to "1". Mutations are important because they allow the algorithm to search beyond the current solution region and increase the probability that the genetic algorithm can explore

31

the entire solution space. Figure 2.14 shown the mutation of single gene and Multi gene[38].

Parent:11111111 ⟶ offspring:11101111 (Single gene mutation)

Parent:11111111 ⟶ offspring:10101111 (Multi gene mutation)
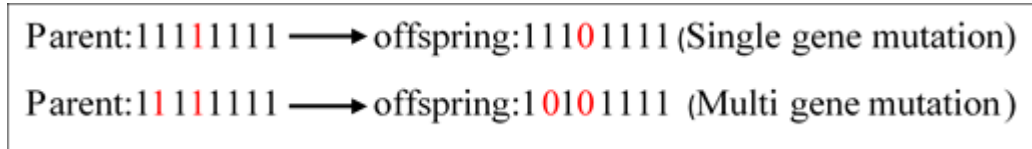
Figure 2.14. mutation of Single gene and Multi gene.

2.7.Flow Chart of basic GA

The flow of a simple genetic algorithm can be illustrated by the description of the flowchart as shown in the Figure 2.15 [41].
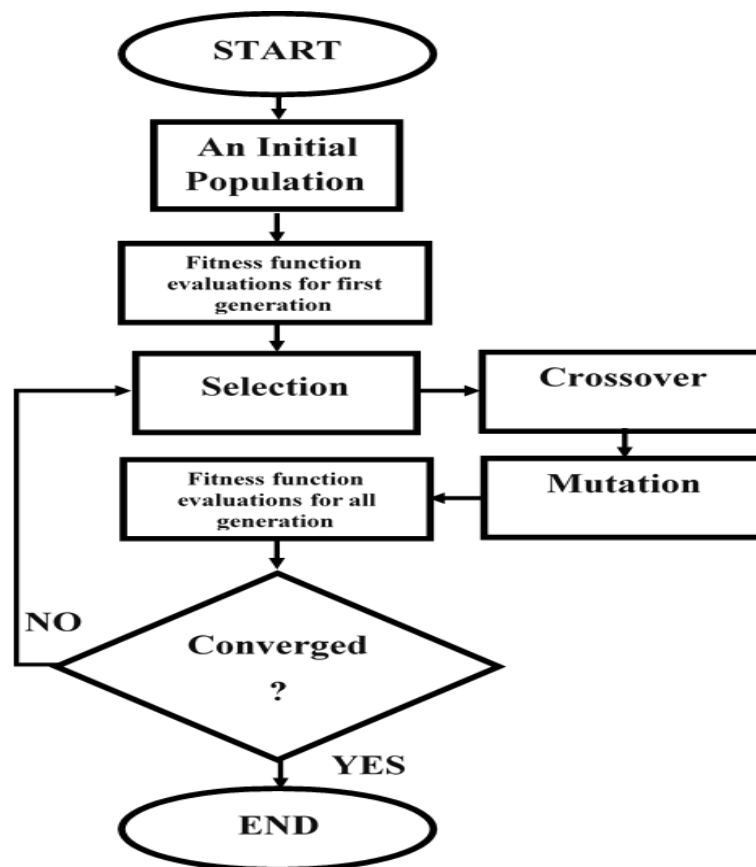
Figure 2.15. Flow Chart of basic GA.

2.8.Parameters of (GA)

Choosing the installation parameter settings is one of the most difficult aspects of using GA. The biggest influence on search performance is the population size, crossover rate, and mutation rate. These are used to govern the running of a GA. They can affect the GA portion of the population and reproduction[40].

2.8.1. population size

It is one of the most important parameters that play an important role in genetic algorithm efficiency. The number of chromosomes in the population is determined by the population size. At the cost of having further fitness tests, greater population sizes increase the amount of variance present in the initial population. The best population size is found to be both based on applications and linked to their number, of chromosomes in a good population of chromosomes comprising a diverse range of possible basic components, resulting in better exploration[44].

2.8.2. Crossover Rate

For chromosomes in one generation, the number of times a crossover happens, i.e., the probability that two chromosomes swap some of their parts, 100% crossover rate means that all offspring are made by crossover. If it is 0 %, the entirely new generation of the older population, except those arising from the mutation process, The crossover rate is usually high and 'application dependent'. Many researchers suggest crossover rate to be between 0.6 and 0.95.[45].

2.8.3. Mutation rate

The mutation rate determines the likelihood that there will be a mutation. The mutation is used to provide the population with new

knowledge to discover new chromosomes and also prevent the population from being filled with identical chromosomes, simply to prevent premature convergence. Application-based is the strongest rate of mutation. The mutation rate for most applications is between 0.001 and 0.1[46].

CHAPTER THREE

PLANAR ARRAY OPTIMIZATION WITH AMPLITUDE, PHASE, AND COMPLEX EXCITATIONS

3.1. Introduction

Several modern radar and communication systems use planar arrays rather than a simple linear array due to their flexibility and the possibility of freely scanning their main beam directions in both azimuth and elevation planes. Generally, an effective optimization algorithm can be used to design such planar arrays and find the optimum values of the amplitudes and/or phases of the array elements that correspond to the desired radiation characteristics. The optimization of all array elements is referred to as fully optimized planar arrays. In such types of arrays, the current excitations in terms of amplitudes or phases of all the array elements are adjusted iteratively during the optimization process to achieve the desired radiation pattern. Thus, the fully optimized planar arrays are usually difficult to be practically implemented and time-consuming. Therefore, simpler methods are highly advised.

This chapter presents a simple technique for designing partially optimized planar arrays that are capable of providing almost the same desired radiation characteristics as that of the traditional fully optimized planar arrays. The technique is based on dividing a planar array into two contiguous sub-planar arrays symmetrical about the array center. The element excitations in terms of either amplitudes and/or phases of the outer sub-planar array are made adaptive and are optimized to form the desired radiation pattern. The number of the optimized square rings in

the outer sub-planar array is also made adaptive to provide a sufficient number of the optimized elements required to meet the constraints. The elements excitations of the inner sub-planar array that have less impact on the array pattern reconfiguration are made constant. Thus, the convergence time of the optimizer in the partially optimized technique is effectively reduced compared to its fully optimized counterparts. The results demonstrate the capability of the proposed technique to form the required radiation pattern with a smaller number of optimized elements.

3.2 . Formulation Technique

3.2.1. Fully Optimized planar Array

Consider a symmetrical broadside planar array of isotropic elements with an even number $N \times M$ as shown in Figure 3.1. The array factor expression of such rectangular array can be obtained by multiplying the two linear array factor expressions according to [28].as follows:

$$\mathbf{AF(\theta, \emptyset)} = \sum_{n=1}^{N} \mathbf{a_{1n}} \mathbf{e^{j\rho_{1n}}} \left[\sum_{m=1}^{M} \mathbf{a_{m1}} \mathbf{e^{j\rho_{m1}}} \mathbf{e^{j[(m-1)\psi_x]}} \right] \mathbf{e^{j[(n-1)\psi_y]}} \ . \ (\mathbf{3.1})$$

where a_{nm}, and ρ_{nm} are the amplitude and phase elements excitation coefficients, $\psi_x = kd_x \sin\theta \cos\phi$, $\psi_y = kd_y \sin\theta \sin\phi$, d_x is the spacing between elements along the x-axis and d_y is the spacing between elements along the y-axis, $k = 2\pi/\lambda$ and λ is the wavelength in free space.

From equation (3.1), it can be seen that all the amplitudes and/or phases of the array elements are needed to be optimized to obtain the desired radiation pattern according to the pre-specified constraints. Here in this method, the amplitude-only control (i.e., a_{nm} are optimized whereas ρ_{nm} are set to zeros), or the phase-only control (i.e., ρ_{nm} are

36

optimized and a_{nm} are set to ones) are adopted, or the complex- control (i.e., ρ_{nm} and a_{nm} are optimized).
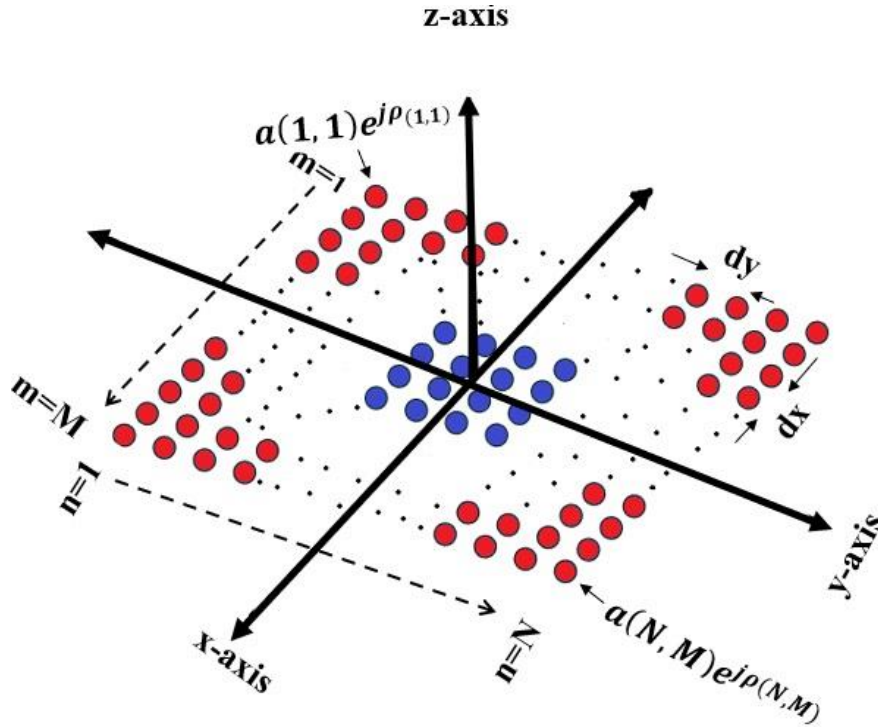
Figure 3.1. Planar Array (rectangular) Configuration.

Instead of optimizing the amplitudes, a_{nm}, and/or phases, ρ_{nm}, of all the array elements, it is possible to efficiently optimize only part of the array elements while maintaining the same radiation characteristics as that of the fully optimized planar arrays.

3.2.2Partially Optimized Planar Array

The fully planar array can be divided into two contiguous sub-planar arrays symmetrical about the array center. For simplicity, assume a square array with $N = M$ and suppose that the number of the square rings in the outer sub-planar array is equal to L. Thus, the number of the elements that need to be optimized in the outer sub-planar array is equal to $2\{2L(N - L)\}$. These element excitations are used to meet the desired constraints. The amplitudes and/or phases of the remaining

elements are made to be ones and zeros respectively. The array factor of the equation (3.1) can be rewritten to express such division into inner and outer sub-planar arrays.

$$AF(\theta, \emptyset) = \underbrace{\sum_{n=1}^{N-2L} \sum_{n=1}^{N-2L} e^{j[(n-1)(\psi_x + \psi_y)]}}_{\text{inner sub-planar array}}$$

$$+ \underbrace{\sum_{n=N-2L+1}^{N} \sum_{n=N-2L+1}^{N} a_{nn} e^{j\rho_{nn}} e^{j[(n-1)(\psi_x + \psi_y)]}}_{\text{L outer square rings}} \quad \dots (3.2)$$

As mentioned earlier, the values of a_{nm} and ρ_{nm} in the inner sub-planar arrays are chosen to be 1 and 0 respectively, for amplitude–only control, the values of a_{nn} in the outer sub-planar array is only optimized, for phase-only-control, the values of ρ_{nn} in the outer sub-planar array are only optimized, for complex-control, both the values of $\rho_{nn} and a_{nn}$ in the outer sub-planar array are optimized. The GA is used to perform the optimization process to find an appropriate value of outer square rings, *L*, and then the overall array radiation pattern that best fulfils the pre-specified constraints.

3.3 Constrained Genetic Algorithm

The GA was previously mentioned in Chapter -Two with detail is used to optimize either the amplitudes and/or the phases of the (fully and partially) planar array elements. The cost function minimizes the difference between the desired radiation pattern according to the pre-specified constraints and the pattern generated from the optimized elements. The constraints represent the (fitness function) and impose the width and direction of the desired nulls, peak sidelobe level, and the width of the main beam as follows:

$$\left| AF_n(\theta_i, \emptyset_i) \right| \leq 0 \text{ dB} \quad , for \ (-1/Nd_x) \leq \theta_i \leq (1/Nd_x) \dots (3.3)$$

$$\left|AF_n(\theta_i, \emptyset_i)\right| \leq SLL \quad , for \ (-1/Nd_x) \geq \theta_i \geq (1/Nd_x) \ .... (3.4)$$

$$\left|AF_n(\theta_j, \emptyset_j)\right| \leq Null_{(Depth,j)} \ , \quad for \ j = 1, 2, ..., J \quad .... (3.5)$$

Where $AF_n(\theta_i, \emptyset_i)$ is the normalized array factor, $1/Nd_x$ is the first null position, θ_j is the null directions, and J is the total number of the required nulls. The constraint in equation (3.3) represents the limits on the required main beam, while the constraints in equations (3.4), and (3.5) represent the limits on the peak sidelobe level and the null directions respectively.

The flowcharts of the optimization process of the fully and partially planar arrays can be summarized in Figure 3.2, and Figure 3.3, respectively.
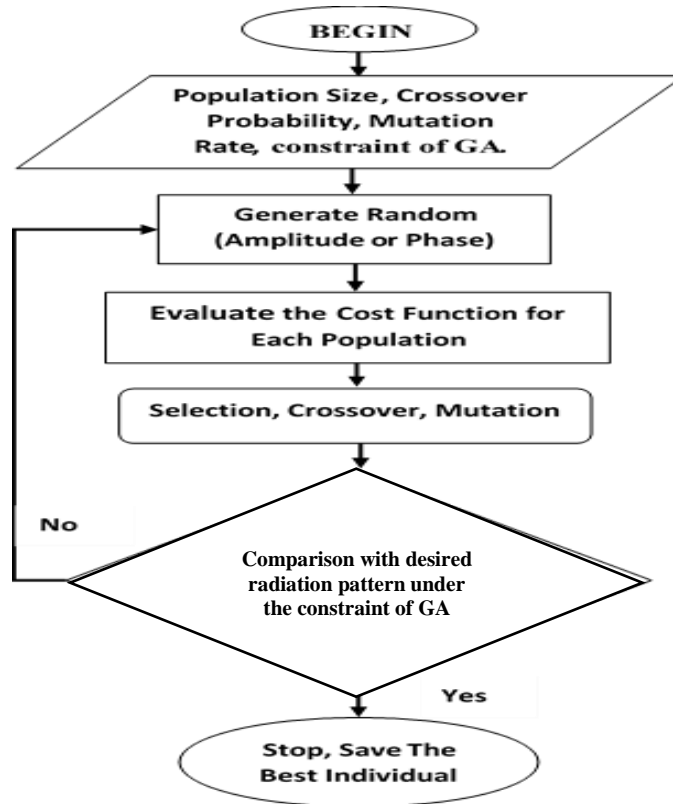
Figure 3.2. flowchart for fully optimized planar arrays.
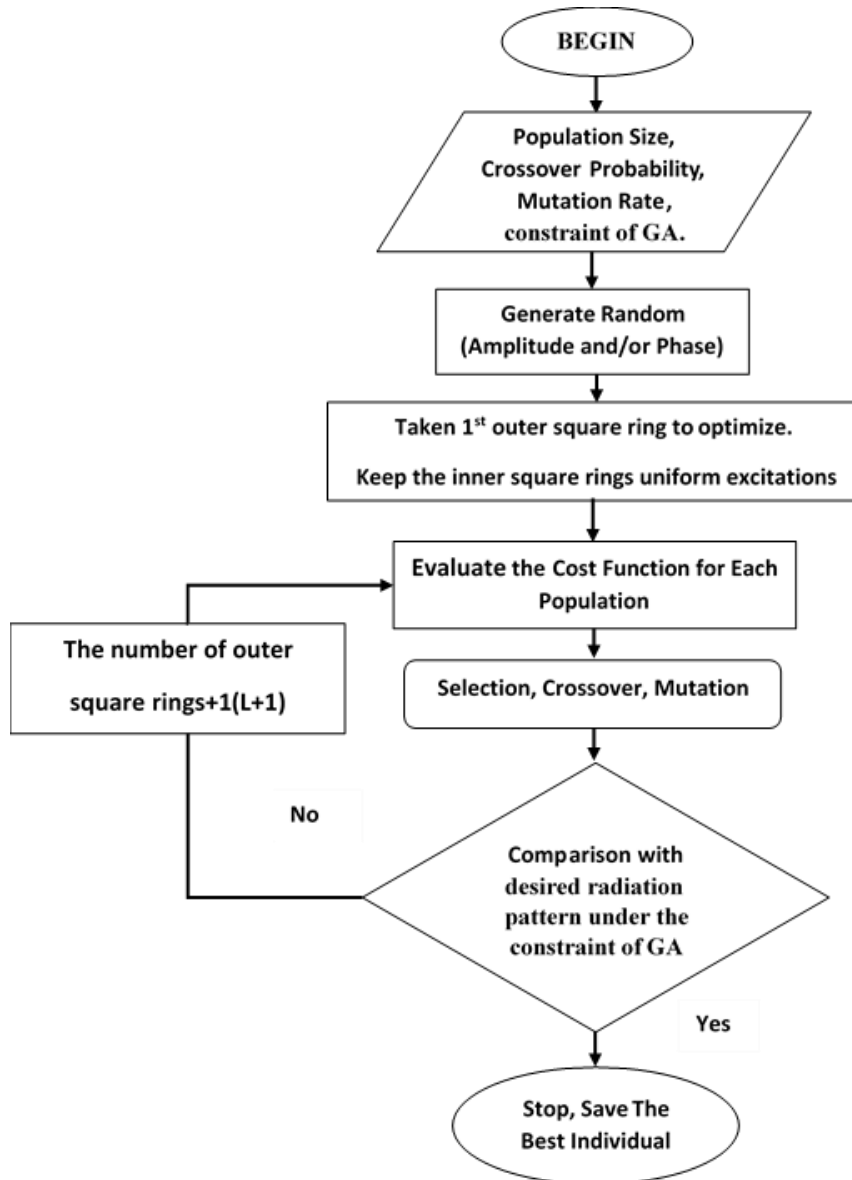
Figure 3.3. flowchart for partially optimized planar arrays.

After a number of attempts to adjust the algorithm settings, the main parameters of GA were chosen as: population size **(50)**; the selection is Tournament; crossover is two points; mutation rate is **(0.2)**; the mating pool is **(10)**. The upper and lower values of the excitation amplitudes are bounded between (**0** and**1**), while the phases are bounded between (**-π/2** and **π/2**).

3.4 Results and Dissections

To demonstrate the capability of the proposed technique, various illustrative scenarios have been simulated. The elements of the considered planar array are divided into two sub-planar arrays symmetrical about the center of the array. The elements of the outer square rings sub-planar array which have more contribution to the pattern reconfiguration are used to form the desired radiation pattern. The computations were performed in a large planar array of 20x20 elements with half-wavelength spacing in both x and y axes and the main beam directed toward the broadside. the required constraints for all scenarios are two wide nulls at center directions of (20°) both with depth (-50dB) and peak SLL=-14.23dB.

3.4.1. First scenario (amplitude-only control)

In the first scenario, the author used amplitude-only control to optimize the fully planar array elements and compare their performance to that of the partially optimized planar array with changing (L) outer square rings as shown in the Table (3.1).

Table (3.1) the results of the optimization partially planar array using amplitude -only control.										
L	NO. elements fixed	NO. elements optimized	Complexity	Directivity [dB]	Taper Efficiency	Average Side Lobes [dB]	HPBW degree	FNBW degree	SSL [dB]	Depth of Null
1	324	76	19%	26.26	0.813	-19.6	5.64	12.6	-13.2	-32
2	256	144	36%	26.59	0.751	-19.9	5.6	12.8	-14.2	-48.7
3	196	204	51%	26.6	0.757	-19.88	5.58	12.8	-15.4	-51.3
4	144	256	64%	26.3	0.543	-20.6	5.8	14	-18.5	-54.3
5	100	300	75%	26.4	0.537	-20.3	6	14.2	-19	-56.5

41

6	64	336	84%	25.5	0.37	-20.5	6.45	16	-20.5	-60
7	36	364	91%	26.22	0.384	-19.1	5.6	14	-21	-63
8	16	384	96%	26.4	0.256	-18.4	5.3	13.2	-22.6	-57
9	4	396	99%	26	0.232	-18.1	5.6	14	-22.6	-57
10	0	400	100%	26.44	0.217	-19.2	5.5	13.4	-21.1	-52

As can be seen from Table (3.1), when the value of (L = 3) outer square rings a performance is obtained similar to that of the fully optimized planar array (last row) according to the required constraints previously placed in the GA.

Figure 3.4(a, b), and Figure 3.5, shows the radiation patterns and the corresponding amplitude excitations of the fully and partially optimized planar arrays.
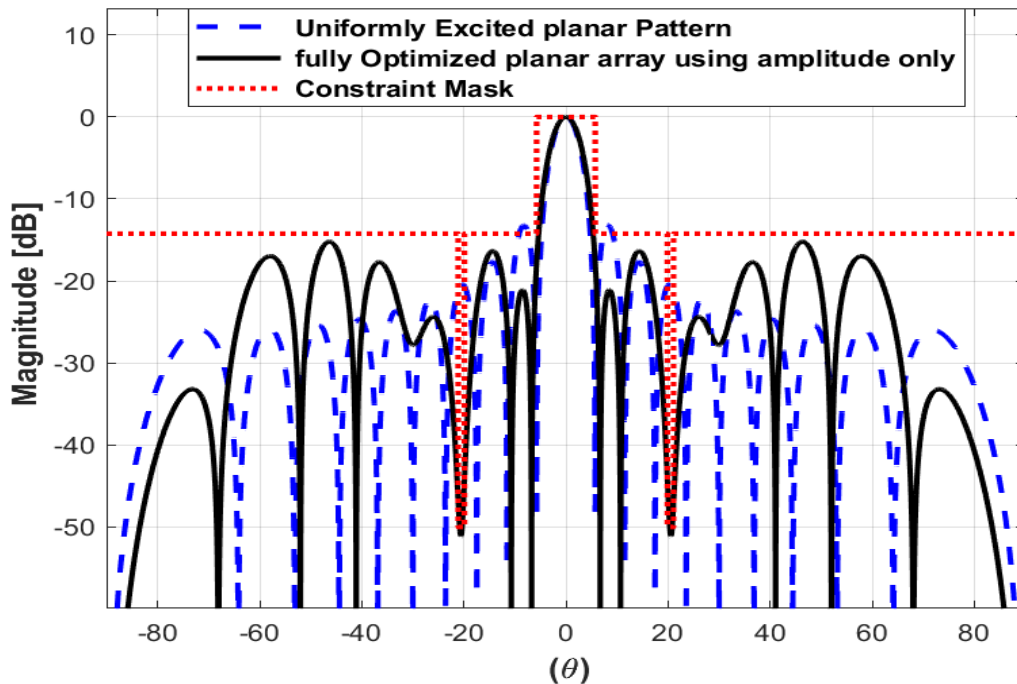
Figure 3.4.(a) The radiation patterns of 20x20 planar array for amplitude-only control, fully optimized
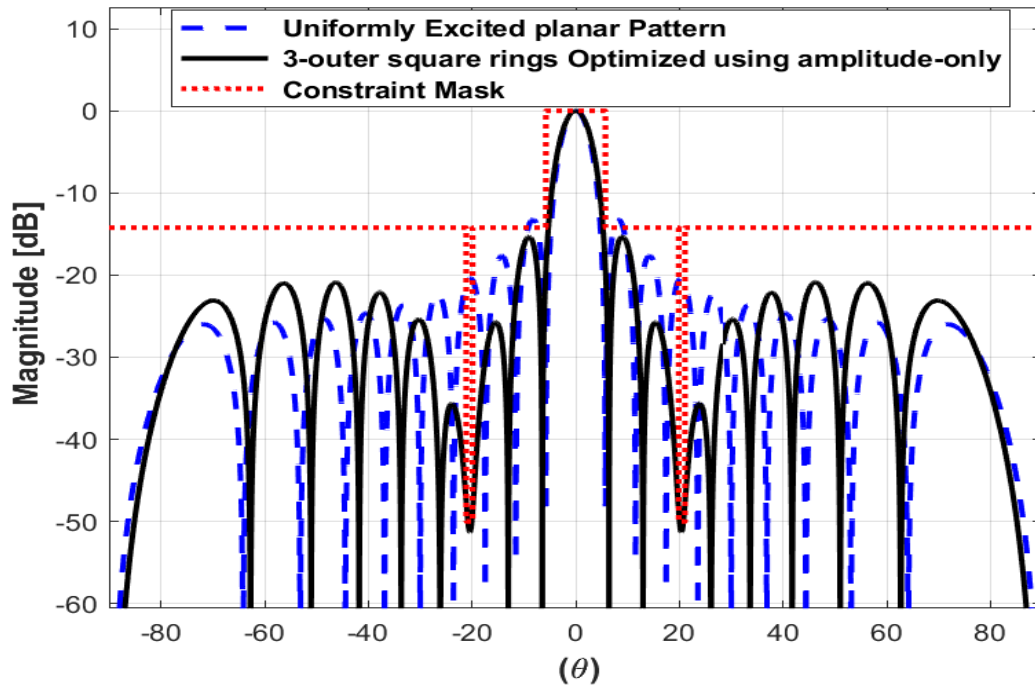
Figure 3.4.(b) The radiation patterns of 20x20 planar array
for amplitude-only control, partially optimized at (L=3).

From figure 3.4(a, b), it can be seen that the radiation patterns of the
fully and partially optimized planar arrays are both within the constraint
limits but not exactly the same in the sidelobe regions.
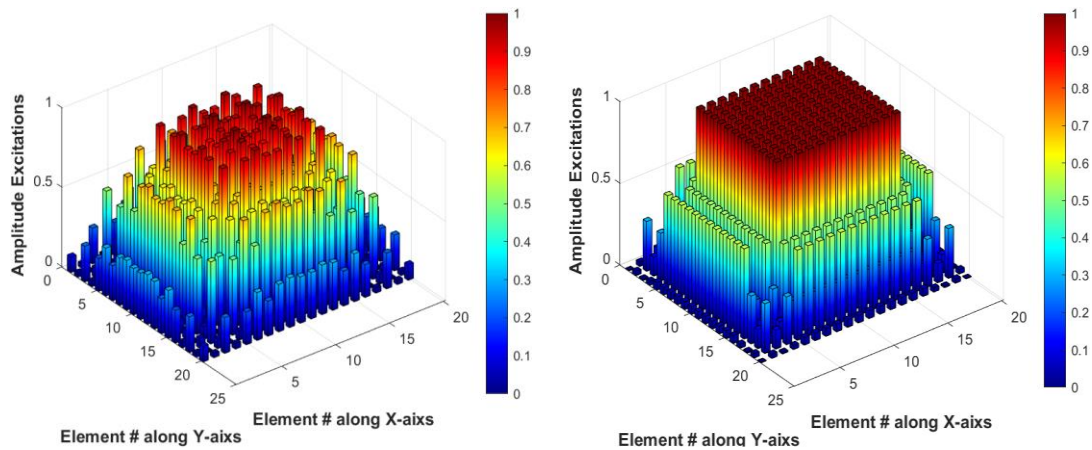
Figure 3.5. The amplitude excitations of 20x20 planar array
for amplitude-only control, (left) fully optimized, (right)
partially optimized at (L=3).

The three-dimensional patterns and contour plot in [dB] of fully and partially optimized illustrated in Figure 3.6, and Figure 3.7. They clearly show the depth and width of the nulls.
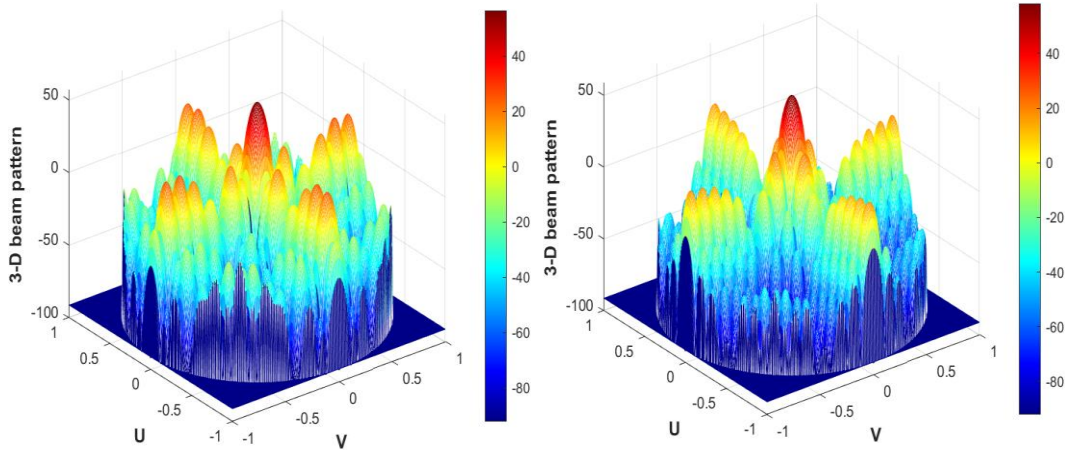
Figure 3.6. The three-dimensional of 20x20 planar array for amplitude-only control. (left) fully optimized, (right) partially optimized at (L=3).
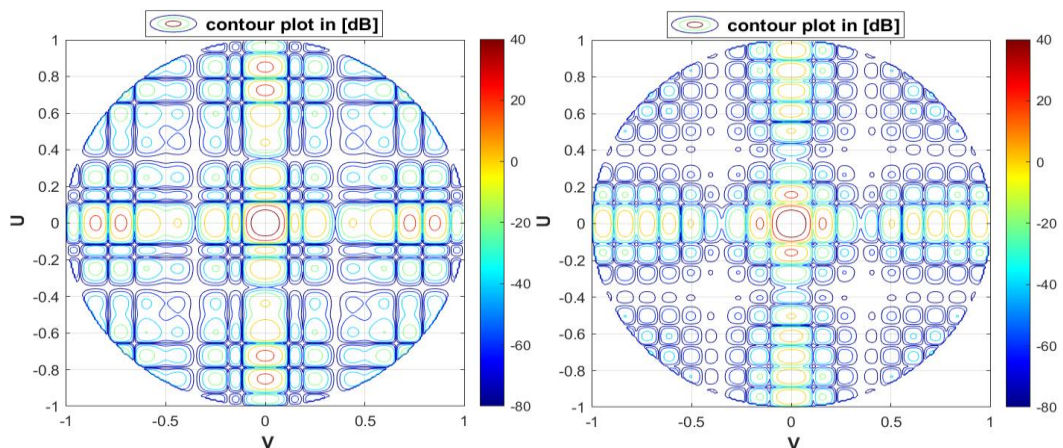
Figure 3.7. The contour plot in [dB] of 20x20 planar array for amplitude-only control. (left) fully optimized, (right) partially optimized at (L=3).

The convergence of the algorithm for maximum reduction in the relative sidelobe level and generating the nulls with required depth and width of 20x20 planar array for an amplitude-only control   is depicted in figure 3.8
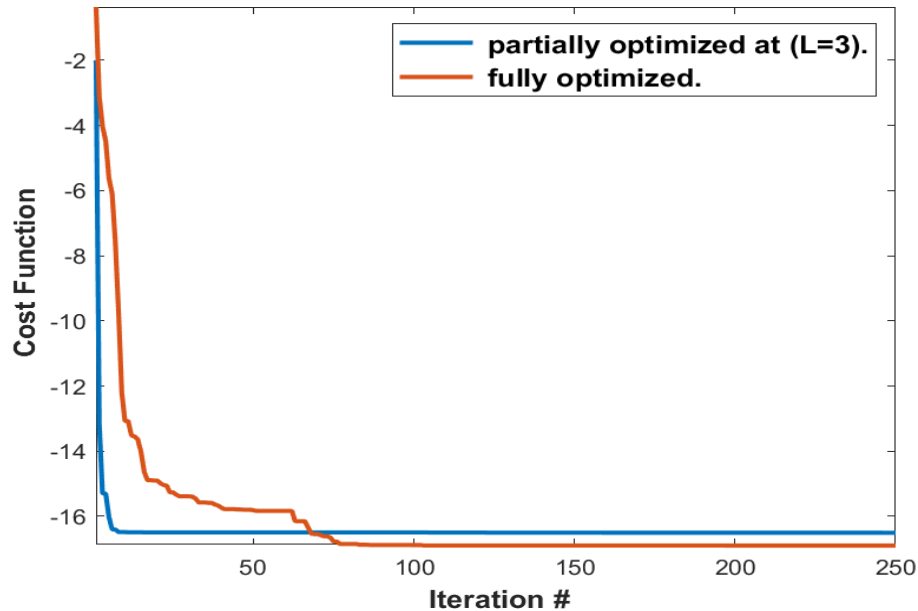
Figure 3.8. The cost function vs. iteration of 20x20 planar array for amplitude-only control, fully optimized and partially optimized at (L=3).

Also note that the number of iterations to achieve the fitness function in the partially optimized state is much less than the fully optimized.

By comparing the results of the two cases and considering the difference of the number of iterations and the time taken to optimize the planar array, whereas the time elapsed for fully optimized is (18.94) seconds and for partially optimized is (12.66) seconds, we conclude that our results are reasonable.

3.4.2. Second scenario (phase-only control)

In the second scenario, the author used phase-only control to optimize the fully planar array elements and compare its performance

to that of the partially optimized planar array with changing (L) outer square rings as shown in the Table (3.2).

Table (3.2) the results of the optimization partially planar array using phase -only control.										
L	NO. elements fixed	NO. elements optimized	Complexity	Directivity [dB]	Taper Efficiency	Average Side Lobes [dB]	HPBW degree	FNBW degree	SSL [dB]	Depth of Null
1	324	76	19%	26	1	-17.4	5.46	12.5	-13.4	-23
2	256	144	36%	25.4	1	-16.6	5.68	13.08	-13.9	-36
3	196	204	51%	25.3	1	-16.5	5.8	13.68	-15.4	-51.9
4	144	256	64%	25.5	1	-16.8	5.72	13.4	-15	-57.5
5	100	300	75%	25.5	1	-16.4	5.54	13.22	-17.1	-60.6
6	64	336	84%	25.1	1	-16	5.76	13.68	-16	-52
7	36	364	91%	25.4	1	-16.2	5.64	13.32	-16	-53
8	16	384	96%	25.4	1	-15.8	5.46	12.9	-15.77	-60.7
9	4	396	99%	25.8	1	-16.9	5.5	12.96	-16	-54.3
10	0	400	100%	25.5	1	-16.0	5.5	13.07	-17.1	-52

As can be seen from Table (3.2), when the value of (L = 3) outer square rings a performance is obtained similar to that of the fully optimized planar array according to the required constraints previously placed in the GA.

Figure 3.9.(a, b), and Figure 3.10, shows the radiation patterns and the corresponding phase excitations of the fully and partially optimized planar arrays.
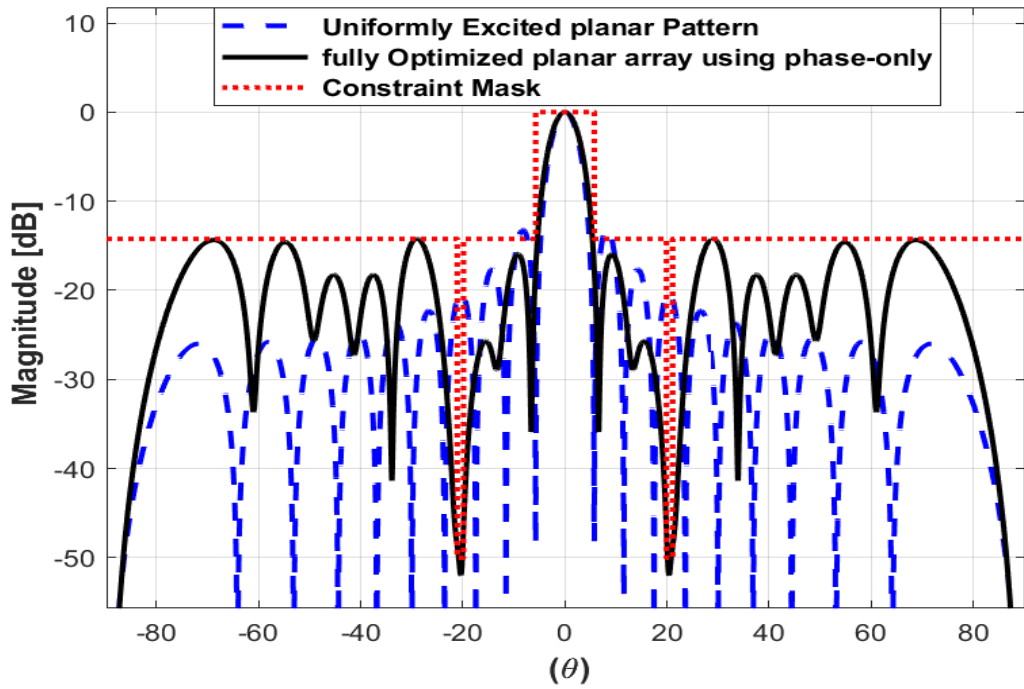
Figure 3.9.(a) The radiation patterns of 20x20 planar array for phase-only control, fully optimized
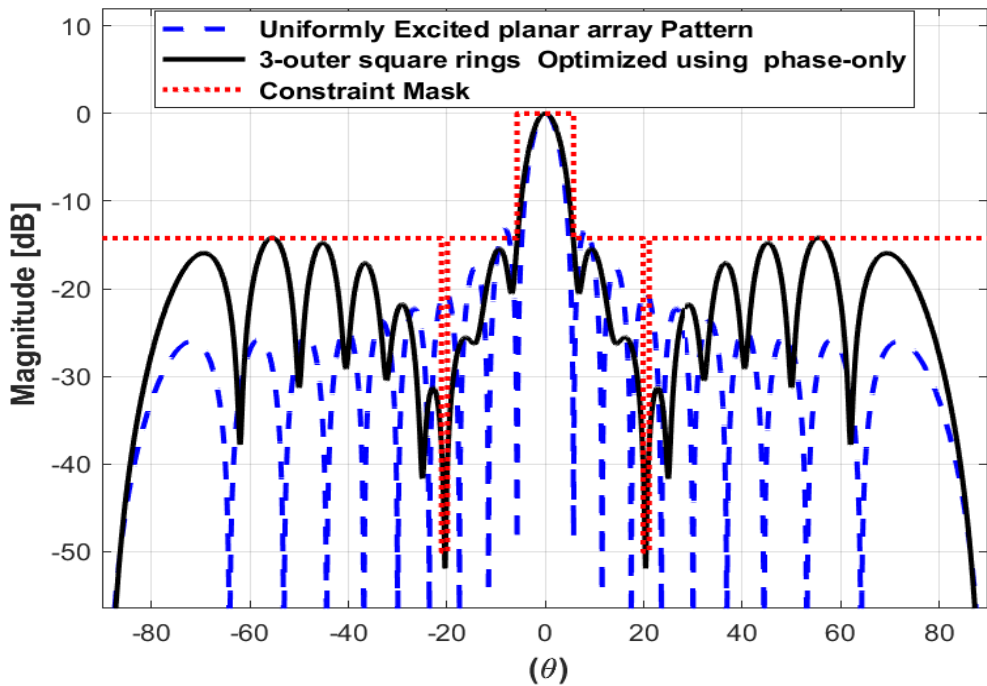
Figure 3.9.(b) The radiation patterns of 20x20 planar array for phase-only control, partially optimized at (L=3).

47

From figure 3.9(a, b), it can be seen that the radiation patterns of the fully and partially optimized planar arrays are almost the same and within the constraint limits. Moreover, the phase distributions of the fully and partially optimized arrays in figure 3.10, are approximately the same, especially for elements close to the array center.
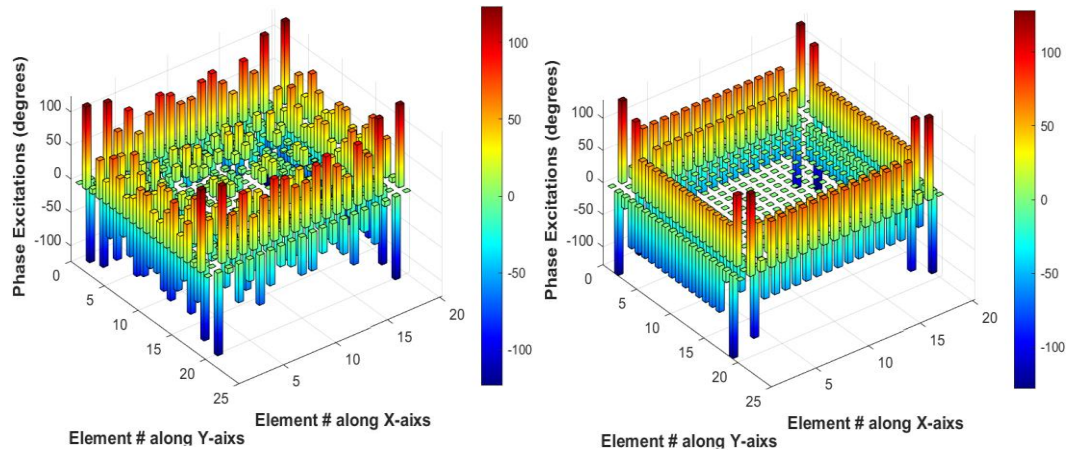
Figure 3.10. The phase excitations of 20x20 planar array for phase-only control. (left) fully optimized, (right) partially optimized at (L=3).

The three-dimensional pattern and contour plot in [dB] of fully and partially optimized illustrated in Figure 3.11, and Figure 3.12, They clearly show the depths and widths of the nulls.
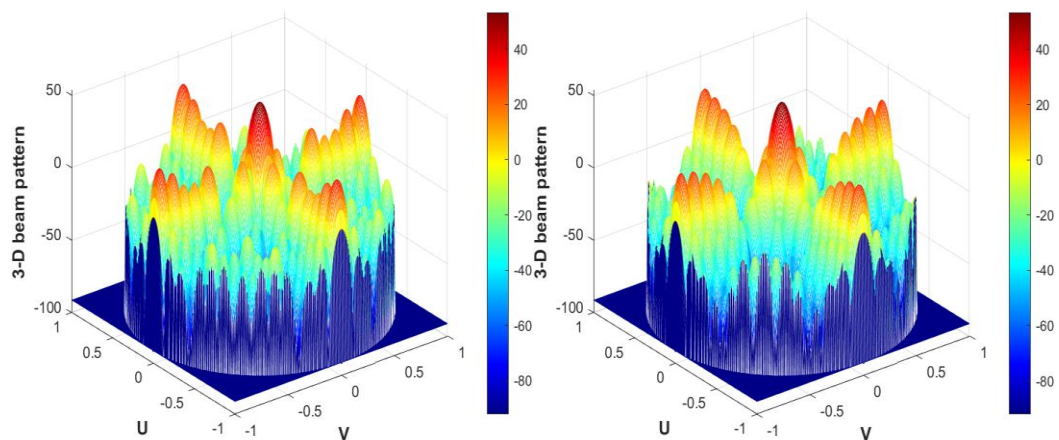
Figure 3.11. The three-dimensional of 20x20 planar array for phase-only control. (left) fully optimized, (right) partially optimized at (L=3).
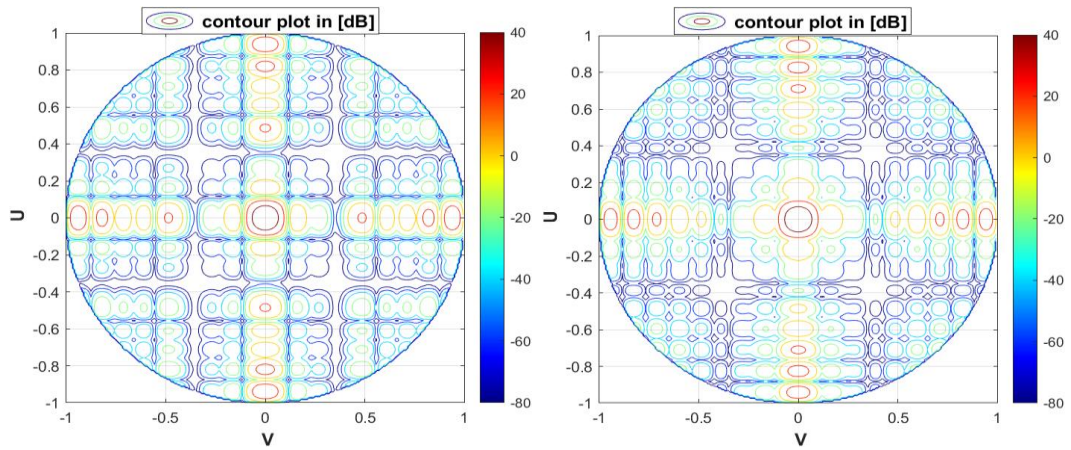
Figure 3.12. The contour plot in [dB] of 20x20 planar array for phase-only control. (left) fully optimized, (right) partially optimized at (L=3).

The convergence of the algorithm for maximum reduction in the relative sidelobe level and generating the nulls with required depth and width of 20x20 planar array for phase-only control is depicted in Figure 3.13
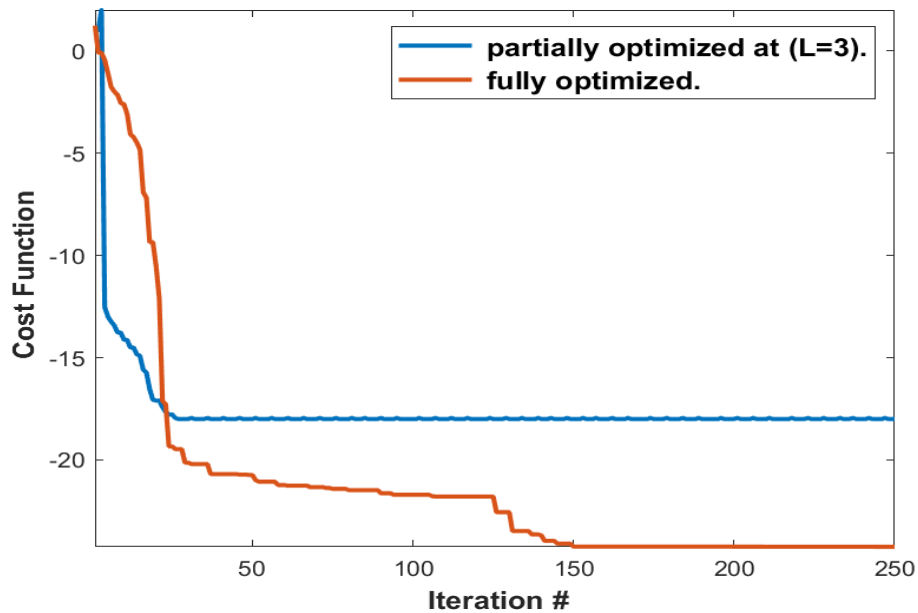
Figure 3.13. The cost function vs. iteration of 20x20 planar array for phase-only control, fully optimized and partially optimized at (L=3).

49

Also note that the number of iterations to achieve the fitness function in the partially optimized state is much less than the fully optimized.

By comparing the results of the two cases and considering the difference of the number of iterations and the time taken to optimize the planar array, whereas the time elapsed for fully optimized is (15.87) seconds and for partially optimized is (11.35) seconds, we conclude that our results are reasonable.

3.4.3. Third Scenario (Complex- Control)

In this scenario, the author used complex- control to optimize the fully planar array elements and compare their performance to that of the partially optimized planar array with changing (L) outer square rings as shown in the Table (3.3).

Table (3.3) the results of the optimization partially planar array using complex- control.										
L	NO. elements fixed	NO. elements optimized	Complexity	Directivity [dB]	Taper Efficiency	Average Side Lobes [dB]	HPBW degree	FNBW degree	SSL [dB]	Depth of Null[dB]
1	324	76	19%	26.25	0.813	-19.5	5.6	12.6	-13.2	-39
2	256	144	36%	26.2	0.694	-20	5.7	13.2	-14.23	-44
3	196	204	51%	26.6	0.735	-19.5	5.4	12.9	-16.2	-51.6
4	144	256	64%	26	0.5	-21.5	6	14.8	-17.9	-50.3
5	100	300	75%	24.8	0.625	-17	6.2	14.9	-18.2	-51
6	64	336	84%	24.3	0.256	-19.1	7.2	20	-26.3	-50
7	36	364	91%	26	0.362	-18.6	5.8	13.8	-18.6	-51
8	16	384	96%	26.3	0.344	-17.8	5.2	12.5	-16.5	-53
9	4	396	99%	25.7	0.326	-16.4	5.3	12.4	-16.6	-52
10	0	400	100%	25.6	0.232	-16.9	5.6	13.2	-16.7	-50.5

As can be seen from Table 3.3, when the value of (L = 3) outer square rings a performance is obtained similar to that of the fully optimized planar array according to the required constraints previously placed in the GA.

Figure 3.14(a, b), show the radiation patterns, figure 3.15, and figure 3.16, shows the corresponding complex excitations (amplitude, phase) of the fully and partially optimized planar arrays.
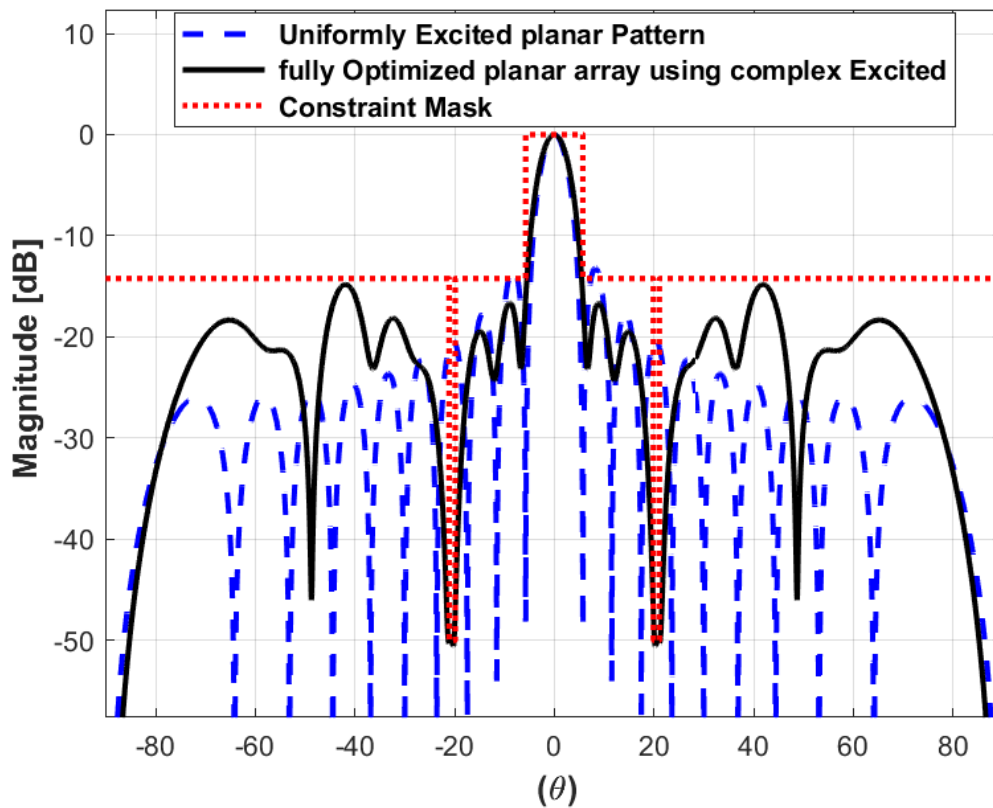

Figure 3.14(a). The radiation patterns of 20x20 planar array for complex- control, fully optimized.
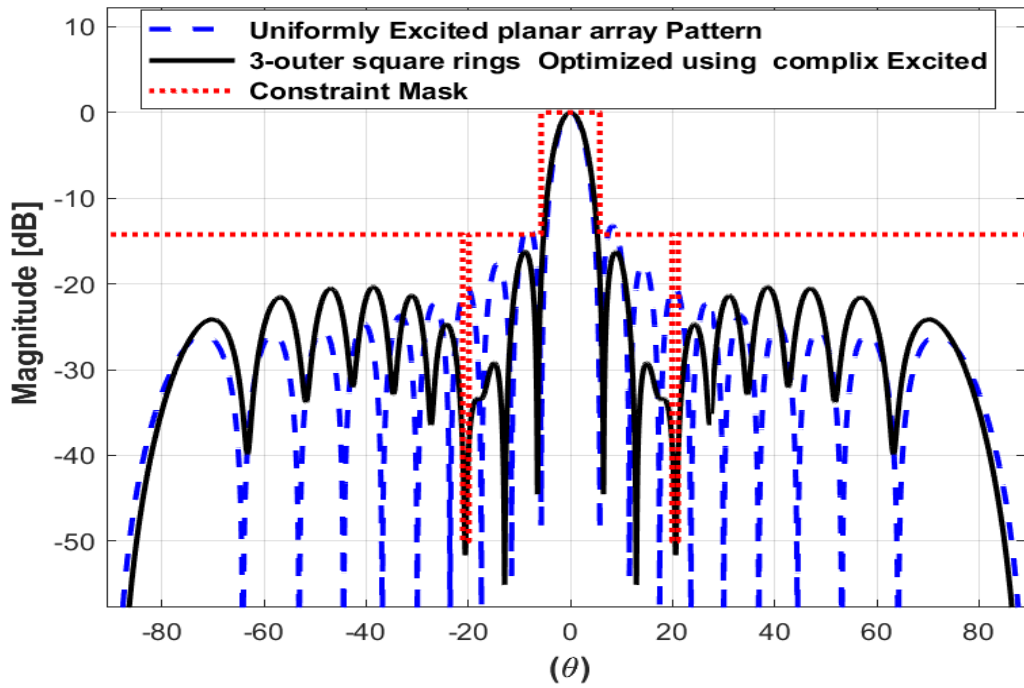
Figure 3.14(b). The radiation patterns of 20x20 planar array for complex- control, partially optimized at (L=3).
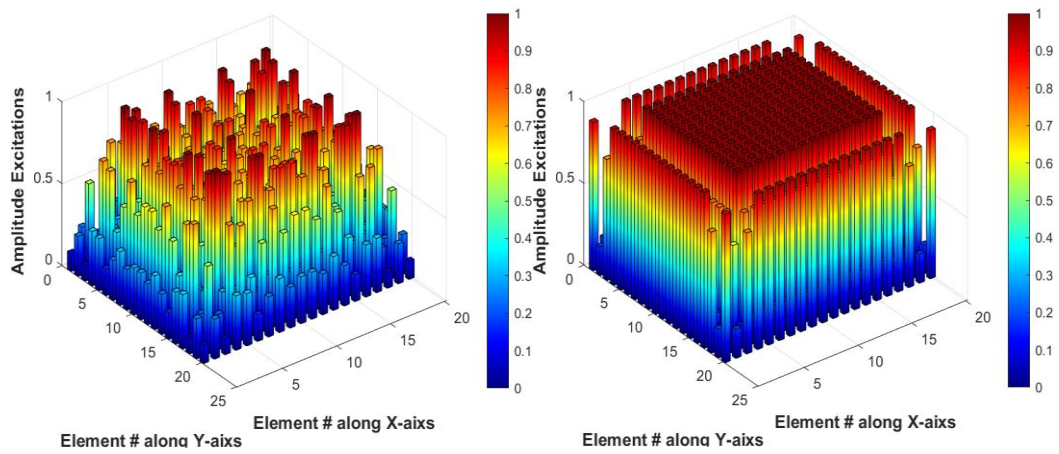
Figure 3.15. The amplitude excitations of 20x20 planar array for complex-control. (left) fully optimized, (right) partially optimized at (L=3).
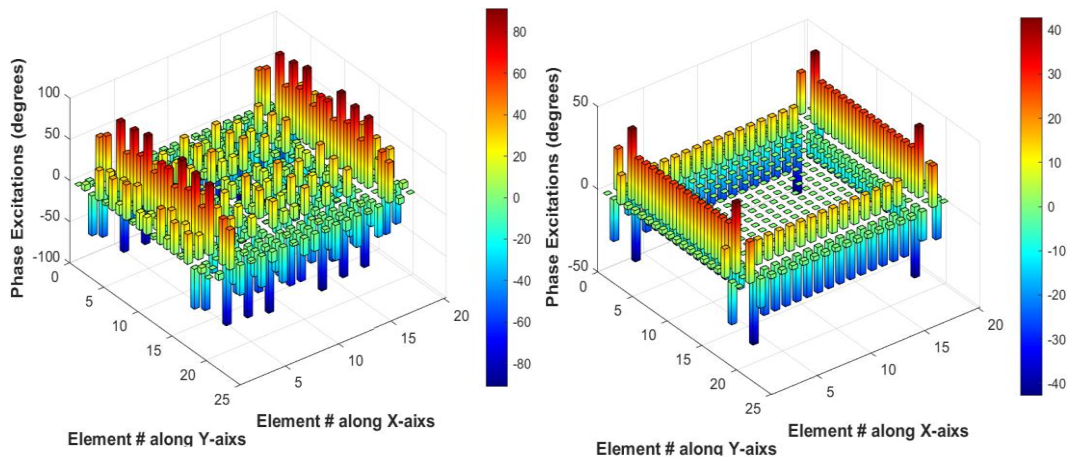
Figure 3.16. The phase excitations of 20x20 planar array for complex-control. (left) fully optimized, (right) partially optimized at (L=3).

From Figure 3.14, it can be seen that the radiation patterns of the fully and partially optimized planar arrays are almost the same and within the constraint limits. But not exactly the same in the sidelobe regions Moreover, the duration time of optimizing this scenario more than the time of (amplitude-only control) and (phase-only control), also the complexity of the design feeding network and the cost.

The three-dimensional pattern and contour plot in [dB] of fully and partially optimized illustrated in Figure 3.17 and Figure 3.18. They clearly show the depths and widths of the nulls.
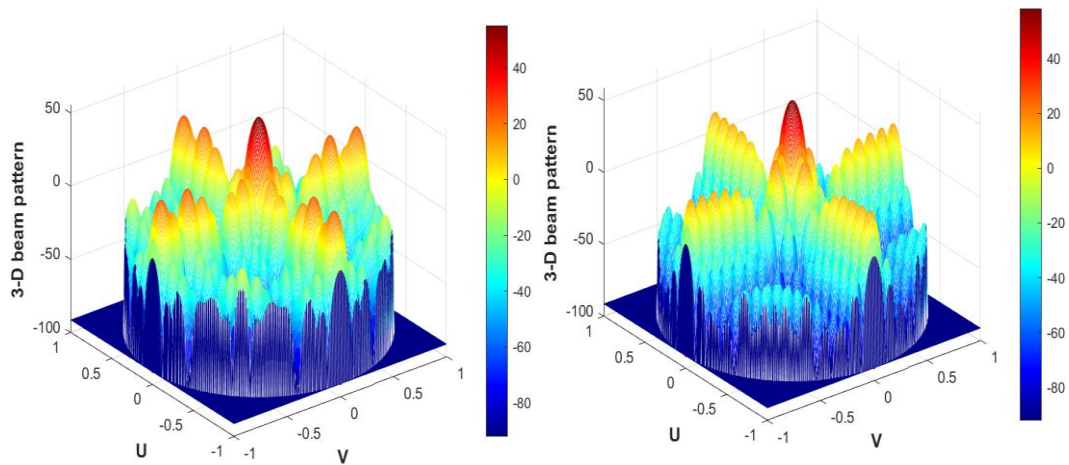
Figure 3.17. The three-dimensional of 20x20 planar array for complex- control. (left) fully optimized, (right) partially optimized at (L=3).
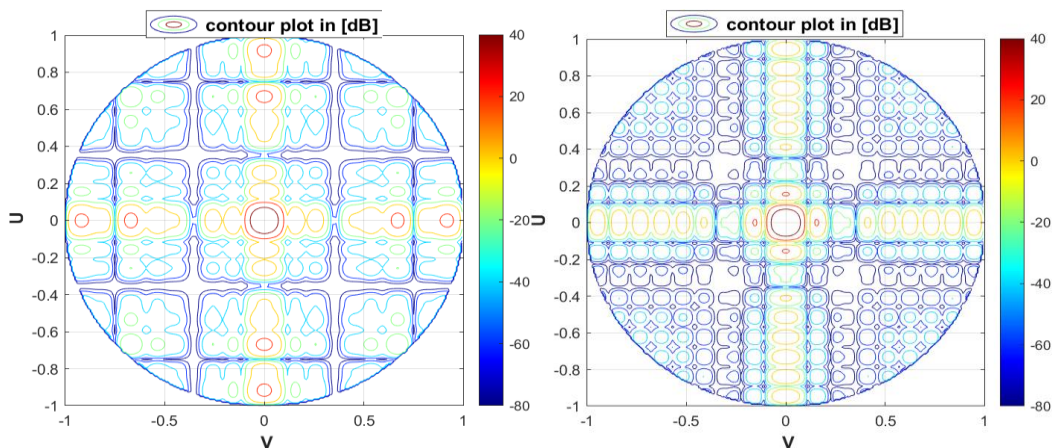
Figure 3.18. The contour plot in [dB] of 20x20 planar array for complex- control. (left) fully optimized, (right) partially optimized at (L=3).

The convergence of the algorithm for maximum reduction in the relative sidelobe level and generating the nulls with required depth and width of 20x20 planar array for complex-control is depicted in Figure 3.19.
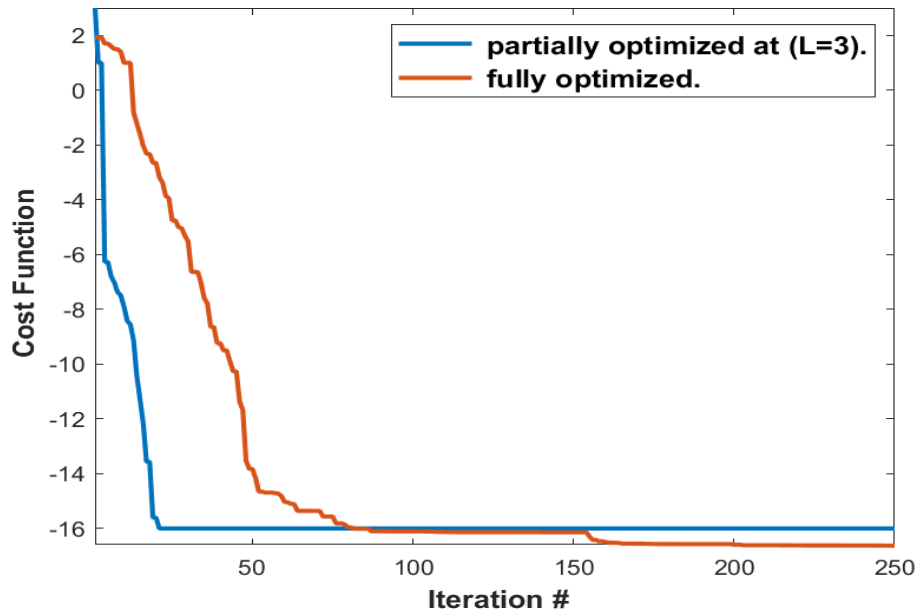
Figure 3.19. The cost function vs. iteration of 20x20 planar array for complex- control. (left) fully optimized, (right) partially optimized at (L=3).

Also note that the number of iterations to achieve the fitness function in the partially optimized state is much less than the fully optimized.

By comparing the results of the two cases and considering the difference of the number of iterations and the time taken to optimize the planar array, whereas the time elapsed for fully optimized is (23.07) seconds and for partially optimized is (14.38) seconds, we conclude that our results are reasonable

3.5. A comparative study

The performances of the proposed partially planar array for three scenarios in terms of directivity, complexity, taper efficiency, average sidelobes, HPBW, and Depth of Nulls versus the number of the optimized elements in the outer square rings are going to be compared.

Aggregation of results for the three scenarios (amplitude -only control, phase-only control, and complex -control) are shown by the following Tables (3.1,3.2, and 3.3) respectively, Figure 3.20 shows the curves.

(a)

(b)

(c)

(d)

(e)

(f)

56
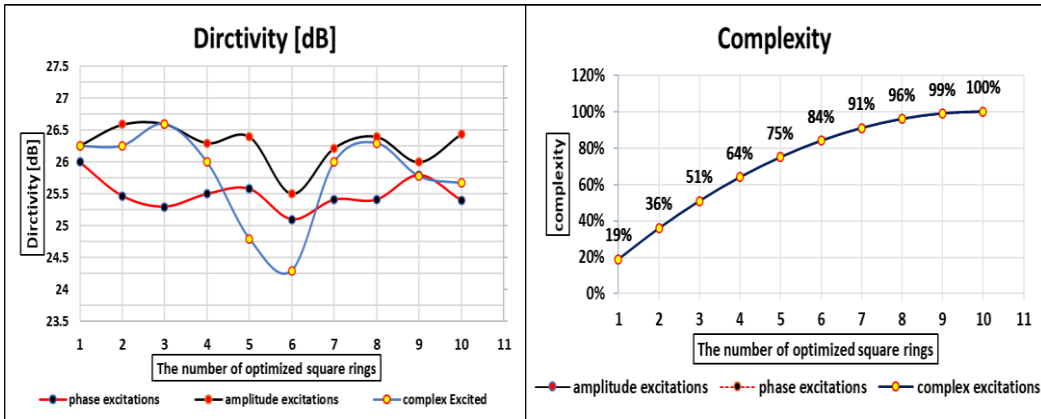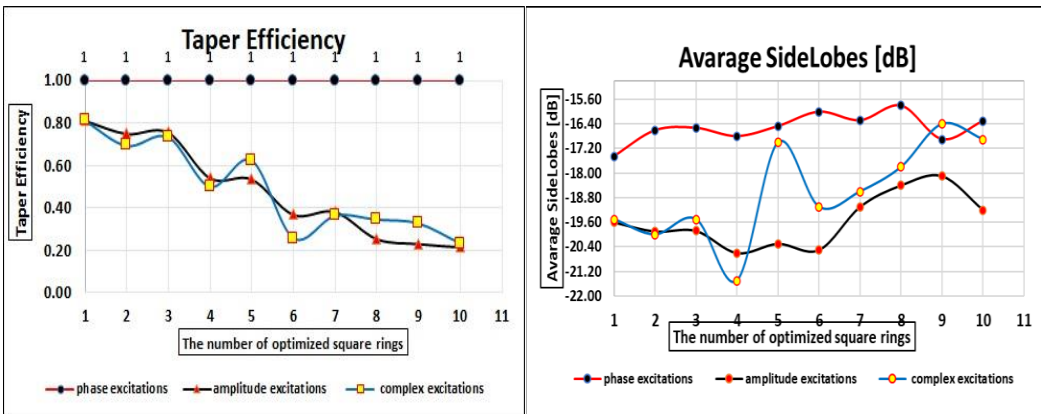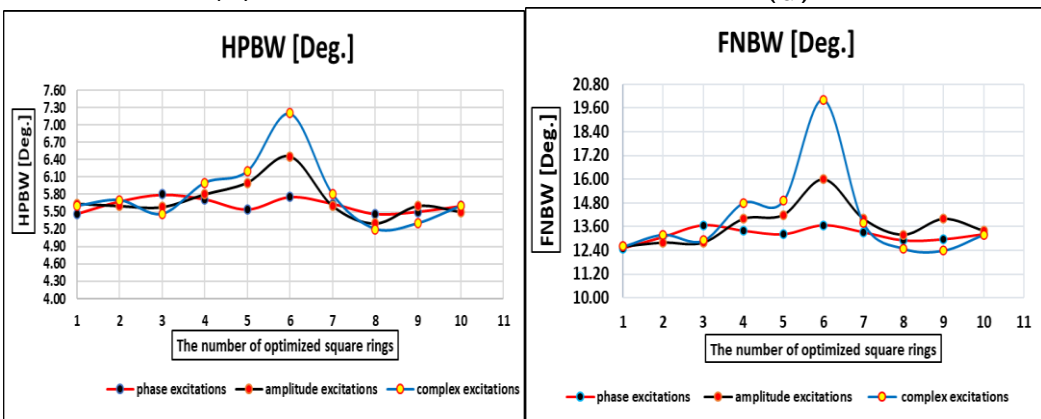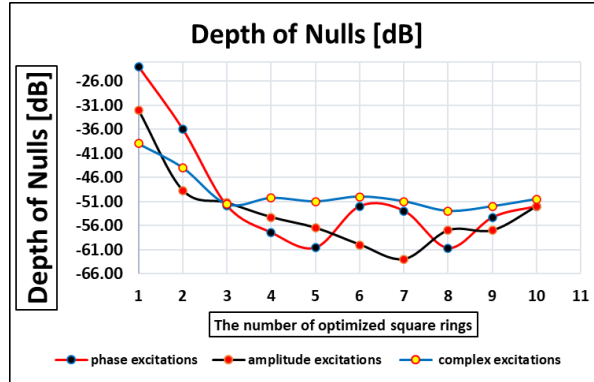
(g)

Figure 3. 20: (**a**)The Directivity, (**b**)Complexity, (**c**)Taper Efficiency, (**d**) Average Side Lobes, (**e**) HPBW, (**f**) FNBW, and (**g**) depth of nulls, the partially optimized planar array versus the number of optimized square rings.

Finally, Table (3.4) shows the numerical comparison between the tested methods. Here, the proposed partially planar array uses 3 outer square rings, i.e., the optimized outer elements were equal to 204 among a total number of elements equal to 400.

Table (3.4). Performances of the Tested Methods for 20x20 planar array.								
scenarios	Directivity [dB]	Average-SLL [dB]	Taper Efficiency	Peak SLL [dB]	FNBW [Deg.]	HPBW [Deg.]	Depth of Null[dB]	Complexity Percentage
Uniformly Excited Array	27.07	-20	1	-13.23	11.46	5.05	-----	----
Amplitude-Only Fully Optimized Array	26.44	-19.2	0.217	-21.1	13.4	5.5	-52	100%
Amplitude-Only Partially Optimized Array with 3 Outer Square Rings	26.6	-19.88	0.757	-15.4	12.8	5.58	-51.3	51%
Phase-Only Fully Optimized Array	25.51	-16.08	1	-17.1	13.07	5.5	-52	100%

Phase-Only Partially Optimized Array with 3 Outer Square Rings	25.3	-16.53	1	-15.4	13.68	5.8	-51.9	51%
complex-Only Fully Optimized Array	25.67	-16.9	0.232	-16.7	12.9	5.6	-50.5	100%
complex-Only Partially Optimized Array with 3 Outer Square Rings	26.6	-19.5	0.735	-16.2	13.2	5.46	-51.6	51%

3.6. Verification

To validate the performance of the proposed technique the rectangular patch elements operating at frequency 2.4GHz are designed and tested under a realistic electromagnetic environment. Figure 3.21, and Table (3.5) show the specification of the designed single patch.
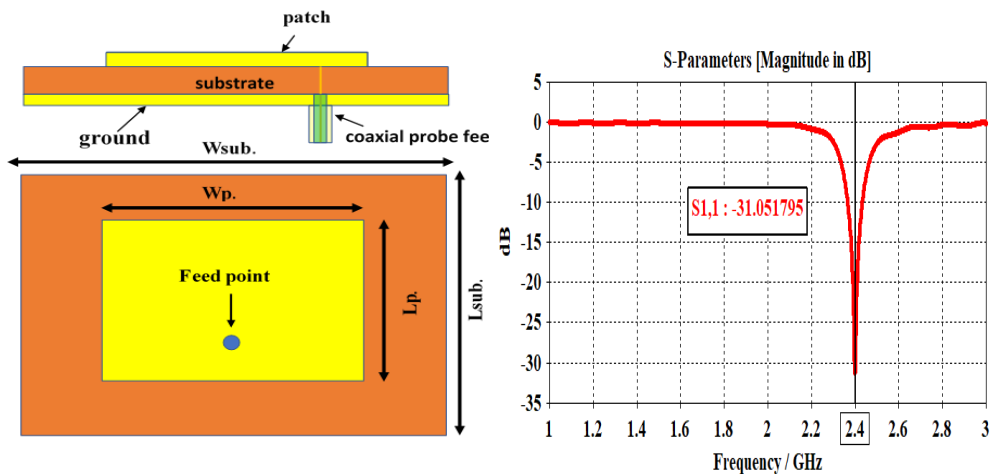
Figure 3.21. (left) a schematic diagram of microstrip patch antenna. (right). S11 versus frequency.

Using CST full-wave modelling. Wherein a planar linear array is designed depending on these patch elements and in different scenarios as mentioned earlier in the theoretical simulation after taking the effect of the patch antenna in MATLAB code, but in different constraints

applied to GA, results are found in good agreement with the theoretical ones and show a realistic array pattern with accurate nulls.

Table (3.5). Dimensions of proposed patch antenna.	
Parameters	Values
Resonant Frequency	2.4 GHz
Feed	Co-axial of 50Ω
Dielectric constant (εr)	4.3
Substrate Height (hsub)	1.6 mm
Substrate	FR4
loss tangent	0.025
Length of Ground Plane (Lg)	38.3 mm
Width of Ground Plane (Wg)	38.3 mm
Substrate Length (Lsub)	38.3 mm
Substrate Width (Wsub)	38.3 mm
Patch Width (WP)	28.7mm
Patch Length (LP)	28.7mm
Inner radius of probe Co-axial	0.5 mm
Outer radius of probe Co-axial	1.674mm
Feed point location can be located at (Xp, Yp)	(0,-6.175)
Dielectric constant (εr) of probe	Teflon 2.1
Length of probe Co-axial	6.607mm

3.6.1. Amplitude-only control

using a planar array with (9x9) elements as shown in Figure 3.22, schematic diagram combined with a three-dimensional pattern of uniform excitations elements, where $d_x = 0.6\lambda_g$ is the spacing between elements along the x-axis, $d_y = 0.6\lambda_g$ is the spacing between elements along the y-axis, $a_{nm} = 1$, and $\rho_{nm} = 0$ for all elements.

The required constraints are two nulls at the center of directions $\pm 37^O$ both with depth $-39dB$, and $peak\ SLL = -17.23\ dB$.

The results of MATLAB obtained as a result of optimizing the GA were used to investigate the design. The Tables (3.6, and 3.7) show the amplitude elements excitation coefficients(a_{nm}) for both fully and

partially optimization, in which the position of the element is the optimization value, they are represented in the tables with the same order for the x and y coordinates.
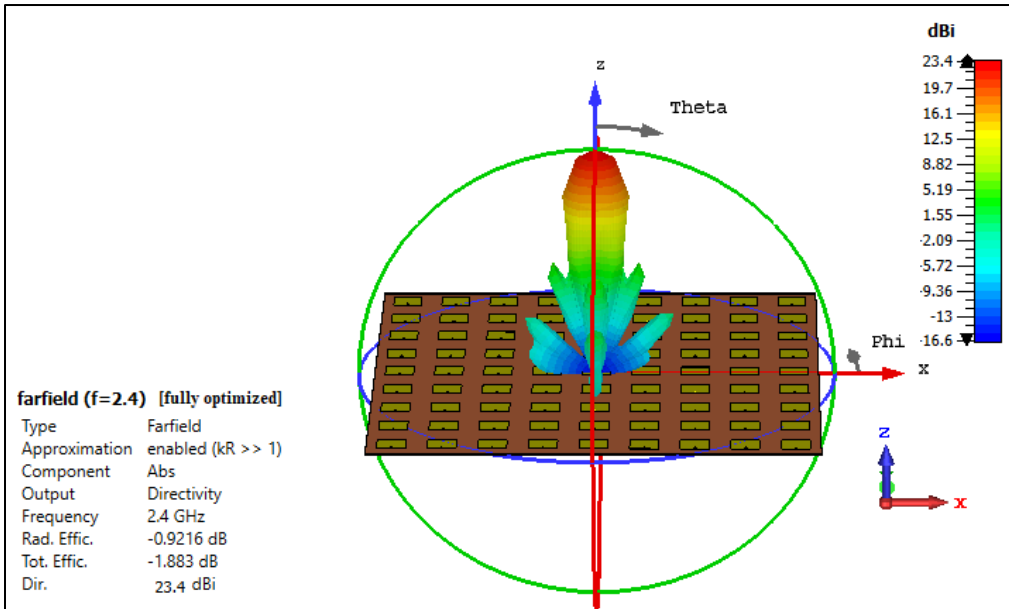
Figure 3.22. a schematic diagram of planar (9x9) microstrip patch coaxial probe fed antenna.

a_{nm}	1	2	3	4	5	6	7	8	9
Table (3.6). the amplitude elements excitation coefficients of planar (9x9) for fully amplitude-only control.									
1	0.1703	0.2742	0.3273	0.354	0.3461	0.3461	0.4127	0.1708	0.1907
2	0.2742	0.4414	0.527	0.57	0.5573	0.5572	0.6644	0.2749	0.307
3	0.3273	0.527	0.6291	0.6804	0.6653	0.6652	0.7931	0.3282	0.3665
4	0.354	0.57	0.6804	0.7359	0.7196	0.7194	0.8579	0.355	0.3964
5	0.3461	0.5573	0.6653	0.7196	0.7036	0.7034	0.8388	0.3471	0.3876
6	0.3461	0.5572	0.6652	0.7194	0.7034	0.7033	0.8386	0.347	0.3875
7	0.4127	0.6644	0.7931	0.8579	0.8388	0.8386	1	0.4138	0.4621
8	0.1708	0.2749	0.3282	0.355	0.3471	0.347	0.4138	0.1712	0.1912
9	0.1907	0.307	0.3665	0.3964	0.3876	0.3875	0.4621	0.1912	0.2135

60

a_{nm}	1	2	3	4	5	6	7	8	9
				Table (3.7). the amplitude elements excitation coefficients of planar (9x9) for (2- outer square rings) amplitude-only control.					
1	0.4995	0.4679	0.7067	0.7067	0.7067	0.7067	0.7067	0.2922	0.4353
2	0.4679	0.4384	0.6621	0.6621	0.6621	0.6621	0.6621	0.2737	0.4078
3	0.7067	0.6621	1	1	1	1	1	0.4134	0.6159
4	0.7067	0.6621	1	1	1	1	1	0.4134	0.6159
5	0.7067	0.6621	1	1	1	1	1	0.4134	0.6159
6	0.7067	0.6621	1	1	1	1	1	0.4134	0.6159
7	0.7067	0.6621	1	1	1	1	1	0.4134	0.6159
8	0.2922	0.2737	0.4134	0.4134	0.4134	0.4134	0.4134	0.1709	0.2546
9	0.4353	0.4078	0.6159	0.6159	0.6159	0.6159	0.6159	0.2546	0.3793

Figure 3.23, shows the actual radiation patterns of the uniform excited, fully optimized, and partially (2- outer square rings) optimized planar arrays according to Tables (3.6, and 3.7) using CST.
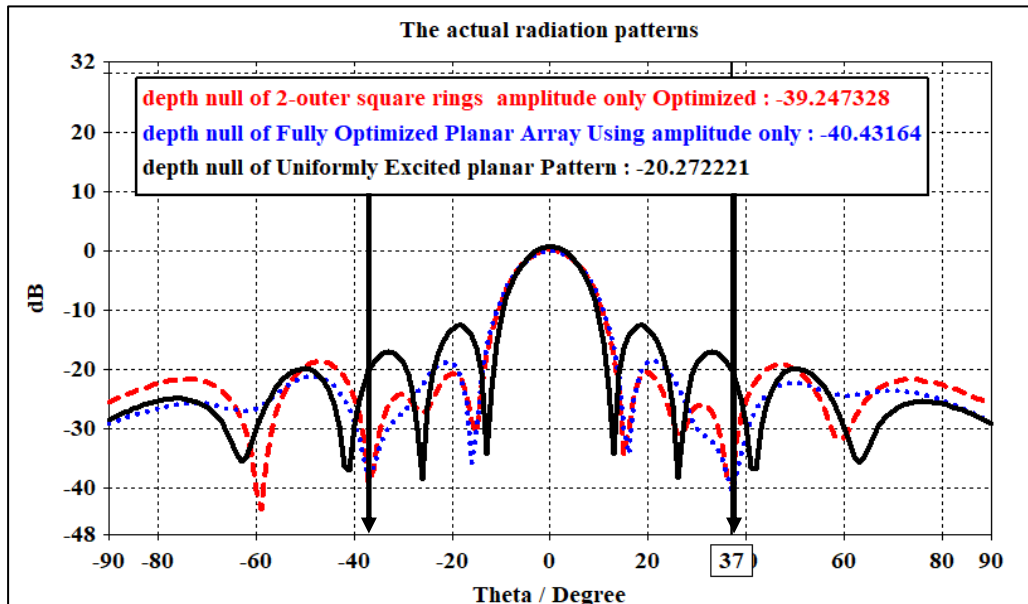
Figure 3.23. The actual radiation patterns of (9x9) planar array for amplitude-only control using CST.

Figure 3.24, shows the comparison of simulated E-plane radiation patterns between the MATLAB program and the CST program.
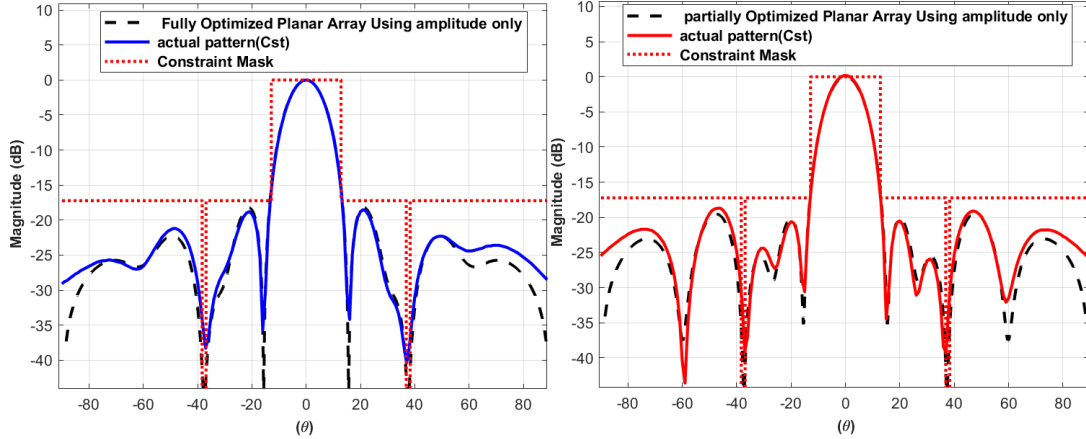
Figure 3.24. The E-plane radiation patterns of 9x9 planar array using MATLAB for amplitude-only control. (left) fully optimized, (right) partially optimized at (L=2).

3.6.2. phase-only control

using a planar array with (9x9) elements as shown in Figure 3.25, schematic diagram combined with a three-dimensional pattern of uniform excitations elements, where $d_x = 0.6\lambda_g$ is the spacing between elements along the x-axis, $d_y = 0.6\lambda_g$ is the spacing between elements along the y-axis, $a_{nm} = 1$, and $\rho_{nm} between = \pm 90°$ for all elements.

The required constraints are one null at center of direction 35.11^O ,with depth $-40 dB$, and $peak\ SLL = -13.23\ dB$.

The results of MATLAB obtained as a result of optimizing the GA were used to investigate the design. The tables (3.8, and 3.9) show the phase elements excitation coefficients(ρ_{nm})in degree for both fully and partially optimization, in which the position of the element is the

optimization value, they are represented in the tables with the same order for the x and y coordinates.
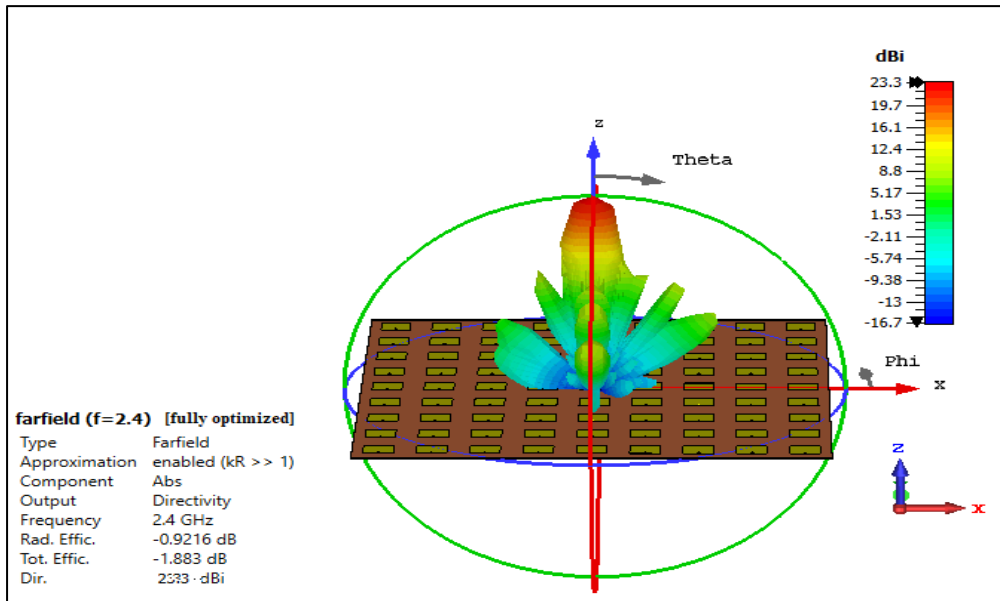
Figure3.25. a schematic diagram of planar (9x9) microstrip patch coaxial probe fed antenna.

Table 3.8. the phase of elements excitation coefficients of planar (9x9) for fully phase-only control.								
ρ_{nm}	1	2	3	4	5	6	7	8	9
1	0	6.59	-20.3	-5.35	-30.2	1.37	-13.1	-46.5	12.1
2	-6.59	0	-26.9	-11.9	-36.8	-5.21	-19.7	-53.0	5.56
3	20.3	26.9	0	14.9	-9.94	21.7	7.12	-26.1	32.4
4	5.35	11.9	-14.9	0	-24.9	6.73	-7.84	-41.1	17.5
5	30.2	36.8	9.94	24.9	0	31.6	17.0	-16.2	42.41
6	-1.37	5.21	-21.6	-6.73	-31.6	0	-14.5	-47.8	10.7
7	13.2	19.7	-7.12	7.84	-17.0	14.5	0	-33.3	25.3
8	46.5	53.0	26.1	41.1	16.2	47.8	33.3	0	58.6
9	-12.1	-5.56	-32.4	-17.5	-42.4	-10.7	-25.3	-58.6	0

ρ_{nm}	1	2	3	4	5	6	7	8	9
1	0	69.8	24.9	24.9	24.9	24.9	24.9	19.3	22.9
2	-69.8	0	-44.9	-44.9	-44.9	-44.9	-44.9	-50.5	-46.9
3	-24.9	44.9	0	0	0	0	0	-5.60	-2.04
4	-24.9	44.9	0	0	0	0	0	-5.60	-2.04
5	-24.9	44.9	0	0	0	0	0	-5.60	-2.04
6	-24.9	44.9	0	0	0	0	0	-5.60	-2.04
7	-24.9	44.9	0	0	0	0	0	-5.60	-2.04
8	-19.3	50.5	5.60	5.6	5.60	5.60	5.60	0	3.56
9	-22.9	46.9	2.04	2.04	2.04	2.04	2.04	-3.56	0

Table 3.9. the phase elements excitation coefficients of planar (9x9) for (2- outer square rings) phase-only control.

Figure 3.26, shows the actual radiation patterns of the uniformly excited, fully optimized, and partially (2- outer square rings) optimized planar arrays according to Tables (3.8, and 3.9) using CST.
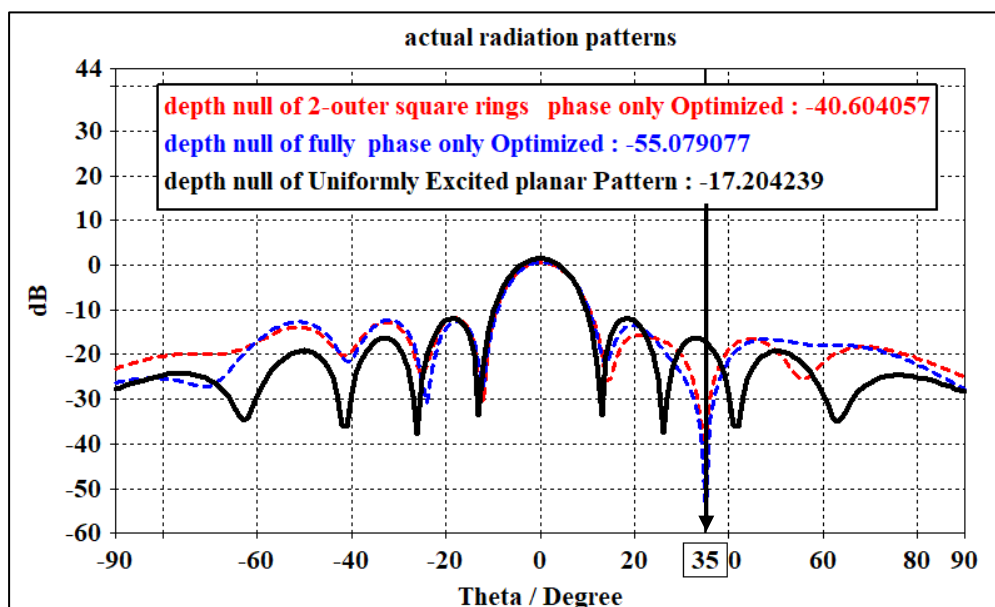
Figure 3.26. The actual radiation patterns. of (9x9) planar array for phase-only control using CST.

Figure 3.27, shows the comparison of simulated E-plane radiation patterns between the MATLAB program and the CST program.
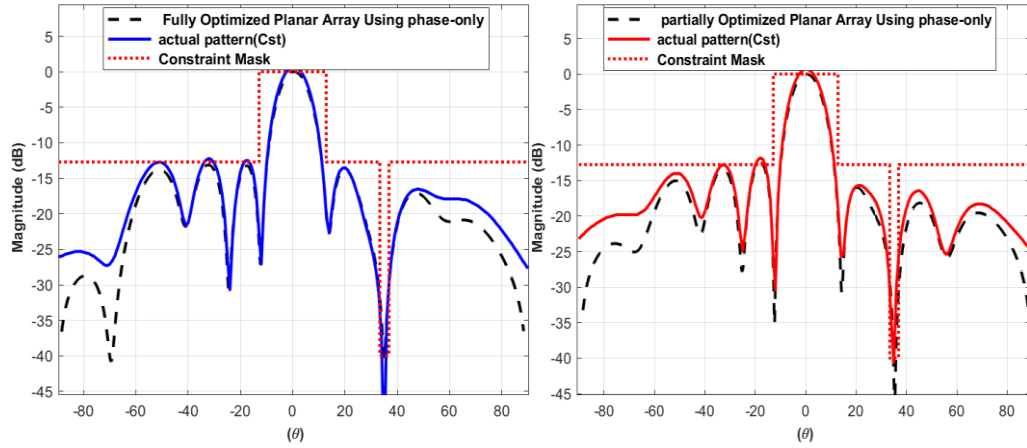
Figure 3.27. The E-plane radiation patterns of (9x9) planar array using MATLAB for phase-only control. (left) fully optimized, (right) partially optimized at (L=2).

3.6.3. Complex-control

Using a planar array with (9x9) elements as shown in Figure 3.28, schematic diagram combined with a three-diminution pattern of uniform excitations elements, where $d_x = 0.6\lambda_g$ is the spacing between elements along the x-axis, $d_y = 0.6\lambda_g$ is the spacing between elements along the y-axis, a_{nm} $between = 0\ and\ 1$, and $\rho_{nm} between = \pm 90°$ for all elements.

The required constraints are two nulls at center of directions $\pm 34^O$ and both with depth $-40dB$,and $peak\ SLL = -14.23\ dB$.

The results of MATLAB obtained as a result of optimizing the GA were used to investigate the design. The tables (3.10,3.11,3.12, and 3.13), shows the amplitude elements excitation coefficients(a_{nm}), and the phase elements excitation coefficients(ρ_{nm})in degree for both fully and partially optimization, in which the position of the element is the

optimization value, they are represented in the tables with the same order for the x and y coordinates.
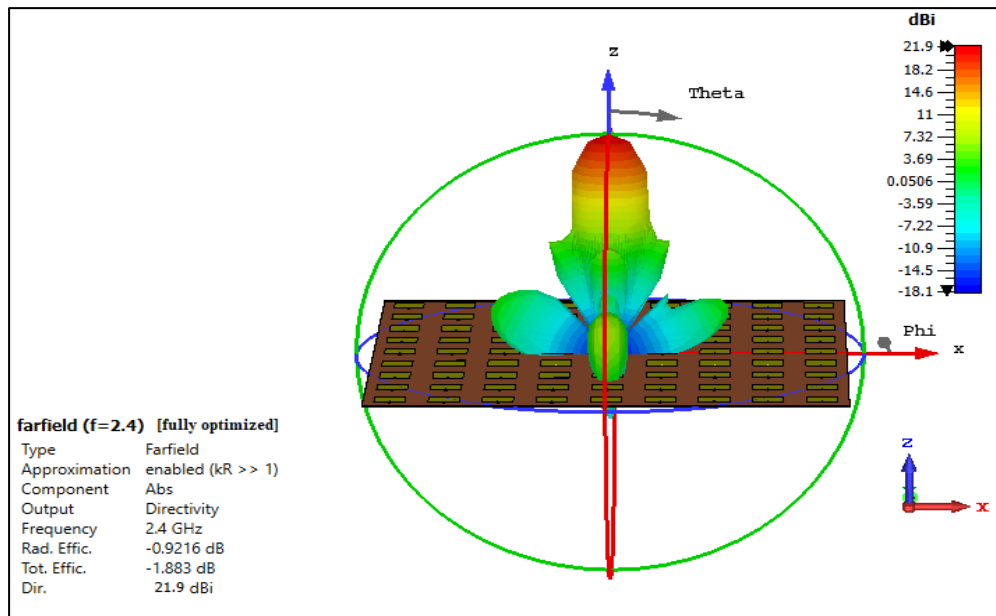
Figure 3. 28. a schematic diagram of planar (9x9) microstrip patch coaxial probe fed antenna.

a_{nm}	1	2	3	4	5	6	7	8	9
1	0.010	0.021	0.078	0.059	0.102	0.057	0.092	0.052	0.047
2	0.021	0.044	0.161	0.123	0.210	0.117	0.190	0.107	0.097
3	0.078	0.161	0.582	0.445	0.763	0.424	0.689	0.387	0.353
4	0.059	0.123	0.445	0.340	0.583	0.324	0.527	0.296	0.270
5	0.102	0.210	0.763	0.583	1.000	0.556	0.903	0.507	0.462
6	0.057	0.117	0.424	0.324	0.556	0.309	0.502	0.282	0.257
7	0.092	0.190	0.689	0.527	0.903	0.502	0.815	0.458	0.417
8	0.052	0.107	0.387	0.296	0.507	0.282	0.458	0.257	0.234
9	0.047	0.097	0.353	0.270	0.462	0.257	0.417	0.234	0.214

Table 3.10. the amplitude elements excitation coefficients of planar (9x9) for fully complex- control.

Table 3.11. the phase elements excitation coefficients of planar (9x9) for fully complex- control.									
ρ_{nm}	1	2	3	4	5	6	7	8	9
1	0	-48.9	-28.4	-33.8	-8.42	-29.3	-9.08	-46.1	-27.6
2	48.93	0	20.3	15.0	40.4	19.5	39.7	2.73	21.2
3	28.49	-20.3	0	-5.37	20.0	-0.85	19.3	-17.6	0.77
4	33.82	-15.0	5.37	0	25.4	4.50	24.7	-12.3	6.14
5	8.422	-40.4	-20.0	-25.4	0	-20.9	-0.67	-37.7	-19.2
6	29.30	-19.5	0.85	-4.50	20.9	0	20.2	-16.8	1.62
7	9.085	-39.7	-19.3	-24.7	0.67	-20.2	0	-37.0	-18.5
8	46.16	-2.73	17.6	12.3	37.7	16.8	37.0	0	18.4
9	27.64	-21.2	-0.77	-6.14	19.2	-1.62	18.5	-18.4	0

Table 3.12. the amplitude elements excitation coefficients of planar (9x9) for (2- outer square rings) complex- control.									
a_{nm}	1	2	3	4	5	6	7	8	9
1	0.734	0.497	0.856	0.856	0.856	0.856	0.856	0.260	0.401
2	0.497	0.337	0.580	0.580	0.580	0.580	0.580	0.176	0.272
3	0.856	0.580	1	1	1	1	1	0.303	0.469
4	0.85	0.580	1	1	1	1	1	0.303	0.469
5	0.856	0.580	1	1	1	1	1	0.303	0.469
6	0.856	0.580	1	1	1	1	1	0.303	0.469
7	0.856	0.580	1	1	1	1	1	0.303	0.469
8	0.260	0.176	0.303	0.303	0.303	0.303	0.303	0.092	0.142
9	0.401	0.272	0.469	0.469	0.469	0.469	0.469	0.142	0.220

ρ_{nm}	1	2	3	4	5	6	7	8	9
Table 3.13. the phase elements excitation coefficients of planar (9x9) for (2- outer square rings) complex- control.									
1	0	25.2	16.8	16.8	16.8	16.8	16.8	61.2	11.6
2	-25.2	0	-8.31	-8.31	-8.31	-8.31	-8.31	35.9	-13.5
3	-16.8	8.31	0	0	0	0	0	44.3	-5.20
4	-16.8	8.31	0	0	0	0	0	44.3	-5.20
5	-16.8	8.31	0	0	0	0	0	44.3	-5.20
6	-16.8	8.31	0	0	0	0	0	44.3	-5.20
7	-16.8	8.31	0	0	0	0	0	44.3	-5.20
8	-61.2	-35.9	-44.3	-44.3	-44.3	-44.3	-44.3	0	-49.5
9	-11.6	13.5	5.20	5.20	5.20	5.20	5.20	49.5	0

Figure 3.29, shows the actual radiation patterns of the uniform excited, fully optimized, and partially (2- outer square rings) optimized planar arrays according to tables (10, 11,12, and 13) using CST.
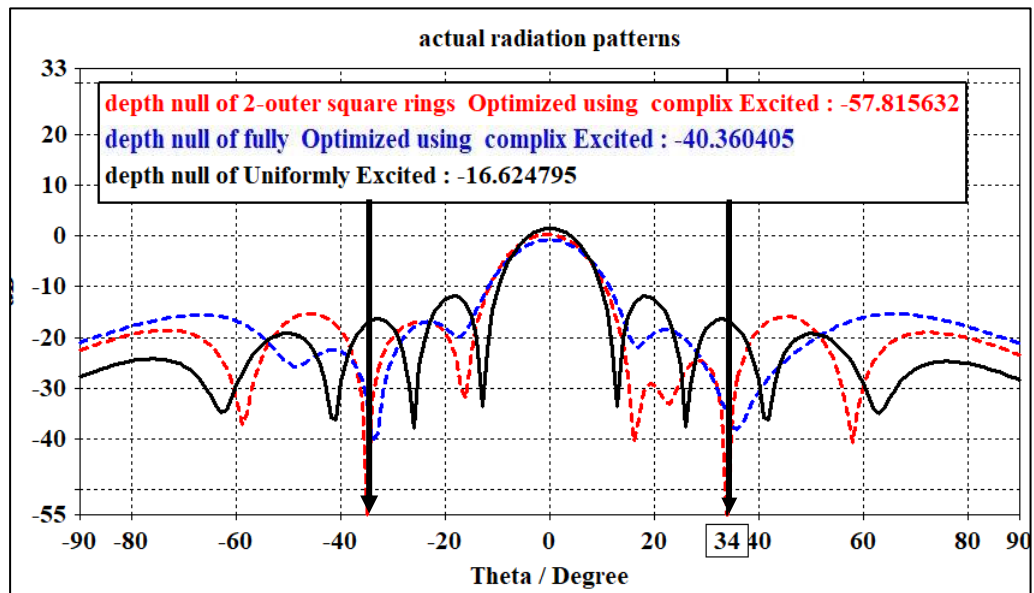
Figure 3.29. The actual radiation patterns. of (9x9) planar array for complex- control using CST.

Figure 3.30, shows the comparison of simulated E-plane radiation patterns between the MATLAB program and the CST program.
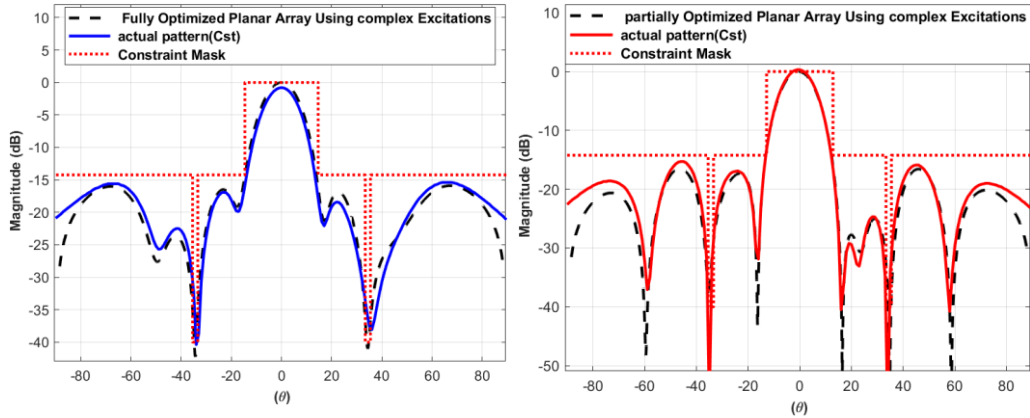
Figure 3.30. The E-plane radiation patterns of (9x9) planar array using MATLAB for complex- control. (left) fully optimized, (right) partially optimized at (L=2).

CHAPTER FOUR
CROSS ARRAY OPTIMIZATION

4.1. Introduction

Conventional rectangular planar arrays with fully filled elements are practically very complicated, especially for large arrays. They usually occupy a large space. Thus, any reduction in the space and the number of the array elements is highly desirable in many applications such as massive MIMO wireless communication and satellite systems. The weight of the used antenna array needs to be as small as possible and takes a small space. Thus, designing such arrays with a fewer number of elements while maintaining good radiation characteristics is highly desirable. Other advantages of such antennas with a fewer number of array elements include lower cost and greater simplification in the array feeding network.

This chapter presents a simple configuration of two crossed arrays along with a proper choice of the element weightings. The radiation pattern of the crossed array which has a very small number of elements can be made the same as that of the conventional rectangular array with a full grid a large number of elements. The element weightings of the proposed crossed array can be computed either deterministically through the use of triangular, Dolph, Taylor distributions or numerically through the use of the GA.

4.2. Principles of The Proposed Cross Array

Consider a fully filled conventional rectangular planar array with odd number of isotropic elements equal to $(2N + 1) \times (2M + 1)$ as shown in Figure 4.1 the array elements are assumed to be located in the x-y

plane and the coordinate system's origin is set to be the array's geometric center. The array factor of this antenna can be expressed as an equation (4.1) [28].

$$AF(\theta, \emptyset) = \sum_{n=1}^{2N+1} \sum_{m=1}^{2M+1} w_{nm}\, e^{j[(m-1)kd_x \sin\theta \cos\phi]} e^{j[(n-1)kd_y \sin\theta \sin\phi]} \quad (4.1)$$

where w_{nm}, is the coefficients of the amplitude element excitation, d_x is the spacing between elements along the x-axis and d_y is the spacing between elements along the y-axis, $k = 2\pi/\lambda$ and λ is the wavelength in free space.
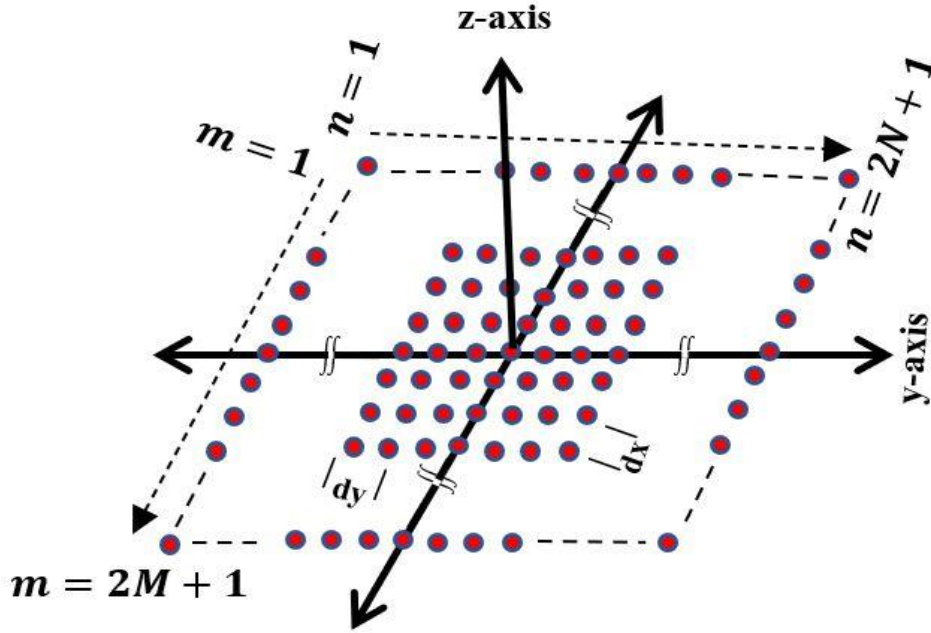
Figure 4.1 Conventional rectangular array.

For simplicity, we will assume the symmetric square planar array with a total number of elements equal to $(2N + 1) \times (2N + 1)$. From equation (4.1), it can be seen that the synthesis of the fully filled

71

rectangular array is complex and computationally intensive, especially when the number of elements is large.

To simplify this complicated array, the author suggests replacing this square planar array with only two orthogonal linear crossed arrays as shown in Figure 4.2, the total number of the elements in the crossed array is made to be $4(2N) + 1$.
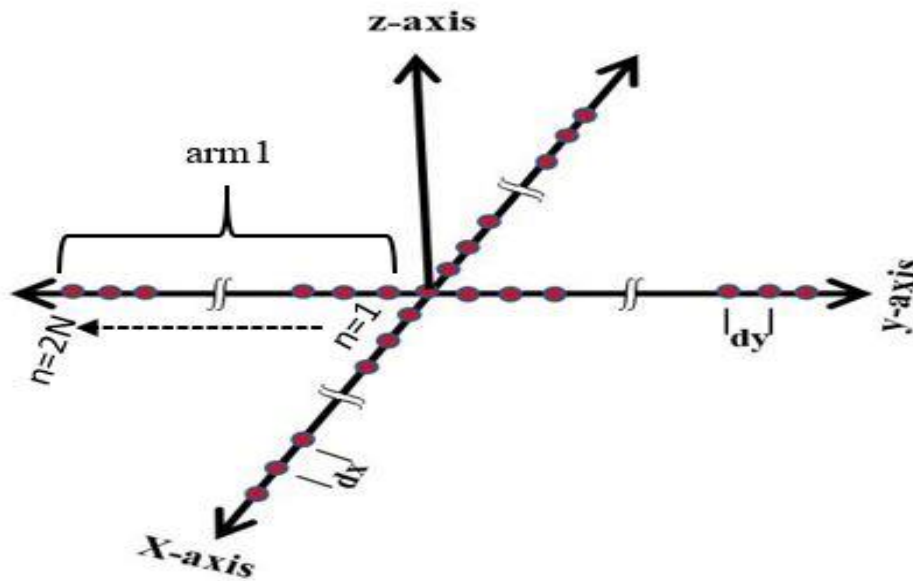
Figure 4.2. Two orthogonal linear arrays.

The patterns of the two crossed linear arrays with a total number of elements $4(2N) + 1$ have been combined to produce an effective pattern that is equivalent to that of the fully filled square planar with a total number of elements $(2N + 1)^2$ to achieve such matching between the radiation patterns of these two antenna arrays, the amplitude elements excitation of the crossed array needs to be properly computed.

The array factor of the symmetric two orthogonal linear arrays can be written as an equation (4.2) [4].

$$AF(\theta, \emptyset) = 2 \times w_0 + 2 \sum_{n=1}^{n=2N} w_n \left[\cos\left(n(kd_x \sin\theta\cos\phi)\right) \right.$$
$$\left. + \cos\left(n\left(kd_y \sin\theta \sin\emptyset\right)\right) \right] \qquad (4.2)$$

If the element weightings w_n are all uniformly excited, then the resultant radiation pattern will have usually a high sidelobe level [14].

Figure 4.3, show the radiation patterns in three-dimension at (N=3) for both conventional planar array with size $(2N + 1) \times (2N + 1)$ and the proposed cross array with size $4(2N) + 1$ and uniform excitations, i.e., $w_n = 1$ for all elements.
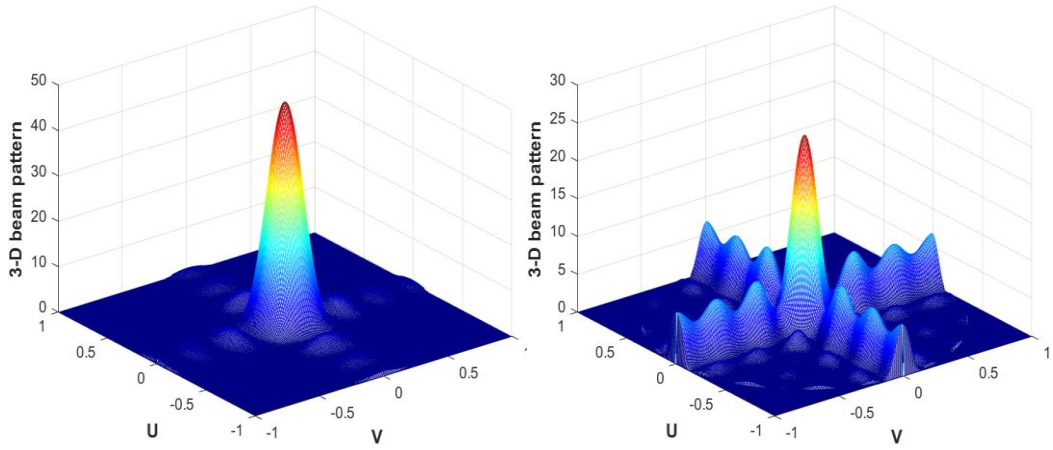
Figure 4. 3. Three-dimension patterns of the uniform planar array 49 elements (left) and the proposed cross array 25 elements (right).

Figure 4.4, and Figure 4.5 show the corresponding amplitude excitations, and radiation patterns for both conventional planar array with size $(2N + 1) \times (2N + 1)$ and the proposed cross array with size $4(2N) + 1$

73
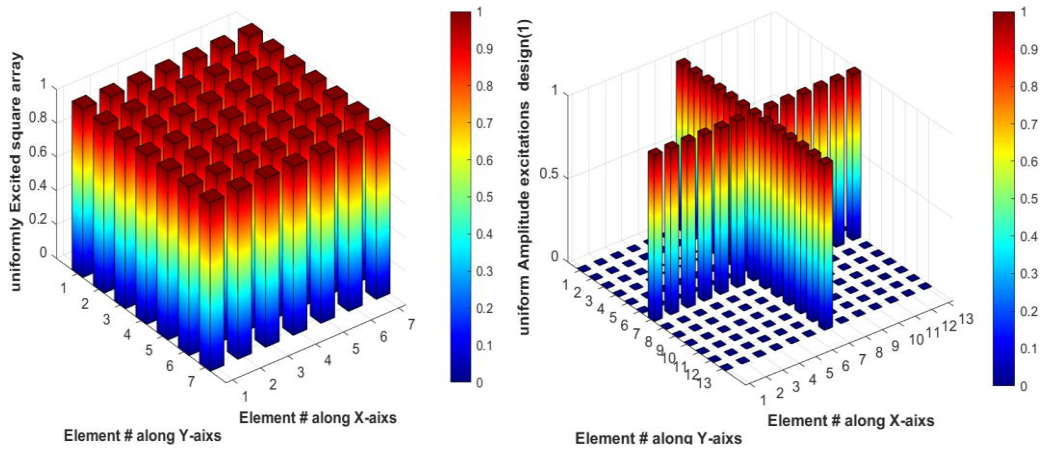
Figure 4. 4. amplitude excitations of the uniform planar array 49 elements (left) and the proposed cross array 25 elements (right).
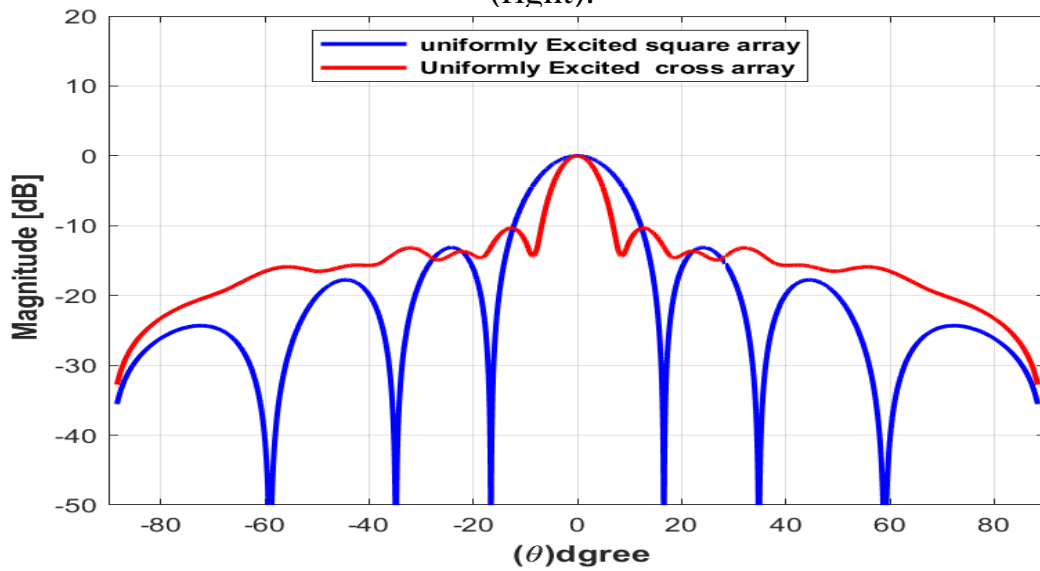
Figure 4. 5. The E-plane radiation patterns of the uniform planar array 49 elements , and the proposed cross array 25

It can be seen that the radiation pattern of the crossed array with uniform excitation has a relatively high sidelobe level. Thus, we need to redesign or recalculating the amplitude element excitations of the crossed array such that the sidelobes can be reduced.

74

4.3. The Techniques of Proposed Designs

The techniques that can be used to reduce the sidelobe level is by selecting the amplitude element excitations of the crossed array according to a specific taper.

The author proposed five design techniques to reduce the number of elements of the planar array as well as reduce the level of side lobes of the cross arrays while achieving similar performance to planar arrays.

The proposed five techniques of the design are:

a) The crossed array with uniform excitations, elements (This design is referred to as Design1).

b) The crossed array with Dolph taper (this design is referred to as Design 2).

c) The crossed array with a Taylor taper (this design is referred to as Design 3).

d) The crossed array with a triangular taper (this design is referred to as Design 4).

e) The crossed array optimized by GA (this design is referred to as Design 5).

Furthermore, the dilution factor has been defined as the percentage ratio of the total number of elements in the proposed design, to the total number of the elements in the conventional square planar array can be expressed as an equation (4.3). Thus, a smaller value of the dilution factor represents the best design .

$$\text{Dilution factor} = \frac{\text{Total element number in the proposed design}}{\text{Total element number in conventional square array}} \times 100\% \ (4.3)$$

4.4. Results and Dissections

To demonstrate the usefulness of the proposed two orthogonal linear crossed array, different examples are illustrated. In the first example, a small size arrays are considered where the amplitude element excitations of all the five designs of the proposed cross arrays and their corresponding radiation patterns are computed and compared.

In the second example, a large size arrays are considered. In these two examples, antennas of an equally spaced linear arrays $d_X = d_Y = \lambda / 2$ is considered, the coefficient weights of this array are also assumed to be uniform (design 1). The coefficient weights of the element excitation are then redesigned using Dolph with required SLL=-20 dB (design 2), Taylor with SLL=-20 dB and nbar =4 (design 3), triangular taper (design 4), and the GA. The main parameters of the GA are chosen as: population size of **(50)**; the selection is Tournament; crossover is two points; mutation rate is **(0.2)**; the mating pool is **(10).** The upper and lower values of the excitation amplitudes are bounded between (0 and1) (design 5). In addition, the amplitude-only control method is used to synthesis the excitation coefficients of the tested arrays. Thus, the phase element excitations are assumed to be zero.

4.4.1. The First Example Small Size Arrays

Assumes (N=2) a small square planar array with a size equal to $(2N + 1) \times (2N + 1) = 25$ elements and the coefficient weights of the element's excitation are assumed to be uniform. The proposed cross array has a size equal to $4(2N) + 1 = 17$ elements.

Accordingly, the dilution factor of the proposed cross array under this case is $^{17}/_{25} = 68$ %.

4.4.1.1. Crossed Array with Uniform Excitations Elements (Design1).

If the elements weighting w_n are all uniformly excited, then the resultant radiation pattern will have usually high SLL. Figure 4.6, and Figure 4.7 shows the comparison of radiation patterns and corresponding amplitude excitations, for both conventional planar array and the proposed cross array (design1).
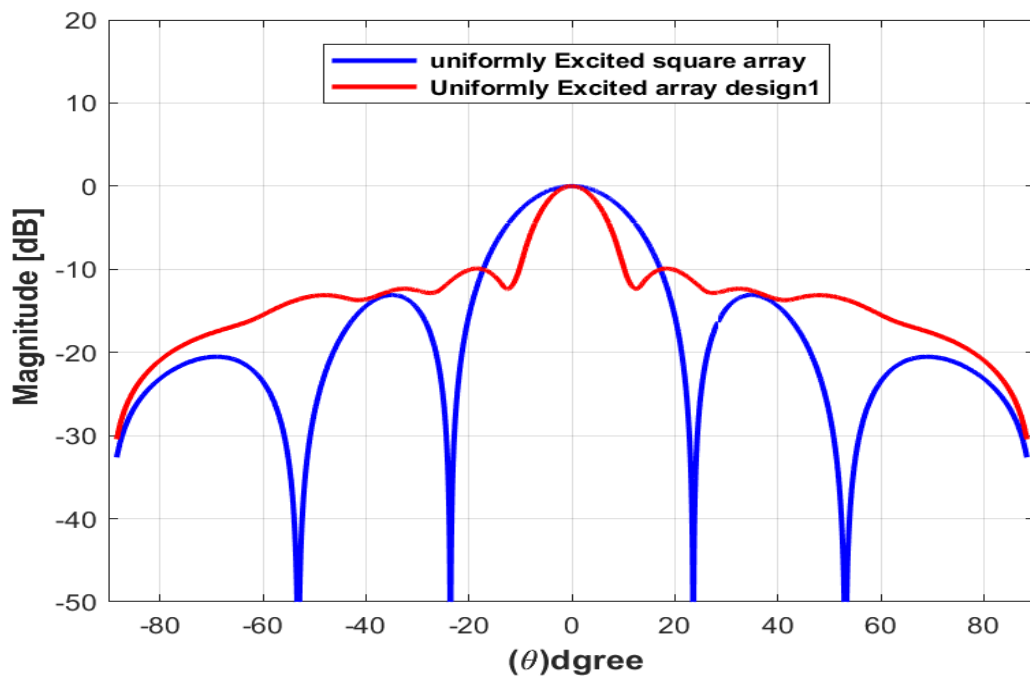
Figure 4. 6. radiation patterns of the uniform planar array 25 elements , and the proposed cross array (design1) 17 elements.
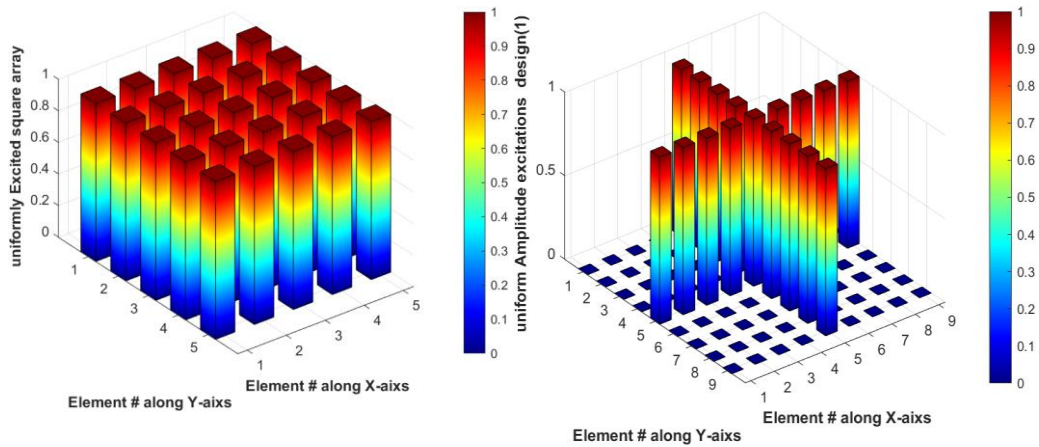
Figure 4. 7. amplitude excitations of the uniform planar array 25
elements (left) and the proposed cross array 17 elements (right)
(design1).

Figure 4.8, show the radiation patterns in three-dimension for both
planar array with size 25 elements and the proposed cross array with
size 17 elements (design1).
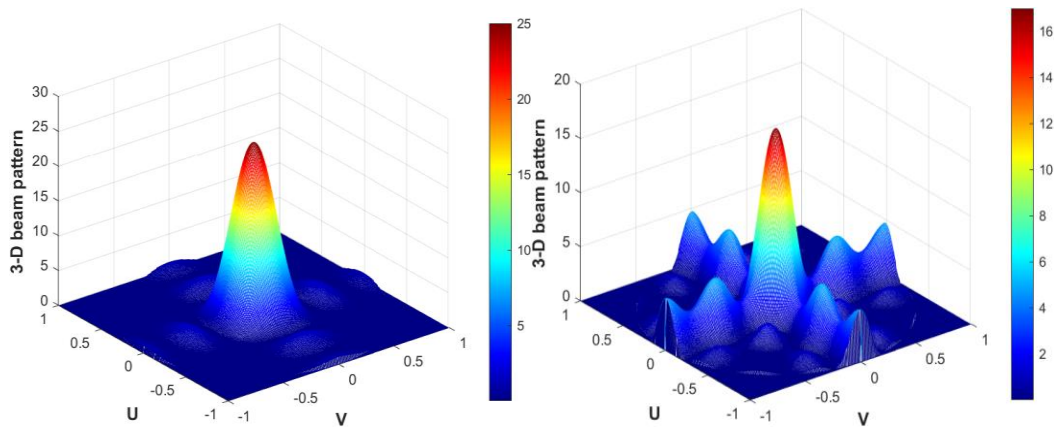
Figure 4. 8. Three-dimension patterns of the uniform planar array
25 elements (left) and the proposed cross array 17 elements
(right) (design1).

The contour plot in [dB] of the uniform planar array 25 elements, and the proposed cross array 17 elements illustrated in Figure 4.9.
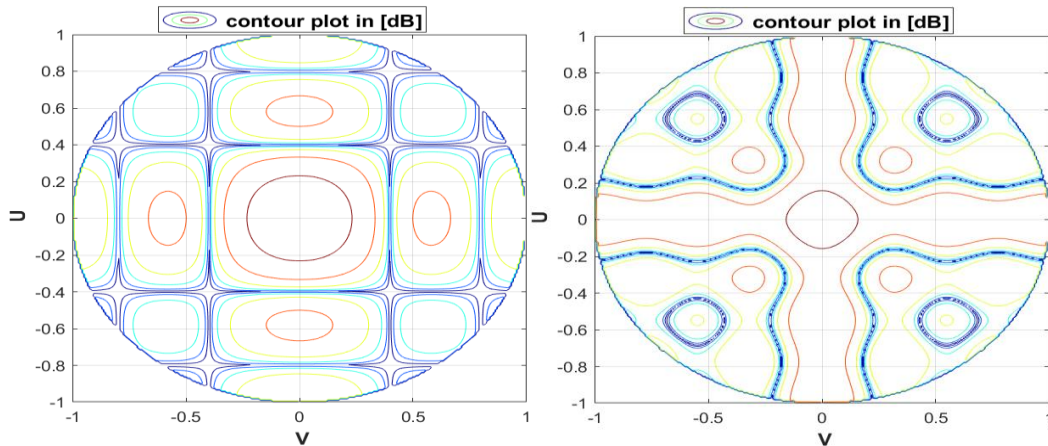
Figure 4. 9 contour plot in [dB] of the uniform planar array 25 elements , and the proposed cross array 17 elements.

The directivity of uniformly excited array design1 is (14.5 dB), the Peak SLL (-9.9 dB), FNBW (24.6º), and HPBW (12º).

The above results indicate the need to recalculate the amplitude element excitations of the crossed array such that the SLL can be reduced.

4.4.1.2. Crossed Array with Dolph taper (Design 2).

To apply another tapering to reduce the SLL such as Dolph the element weightings w_n for proposed two orthogonal linear crossed arrays.

w_n	w_1	w_2	w_3	w_4	w_5	w_6	w_7	w_8	w_9
	0.601	0.615	0.812	0.950	1	0.950	0.812	0.615	0.601

Figure 4.10, shows the comparison of radiation patterns of the uniform planar array, crossed array with uniform excitations (design 1), and Dolph taper (design 2).

79
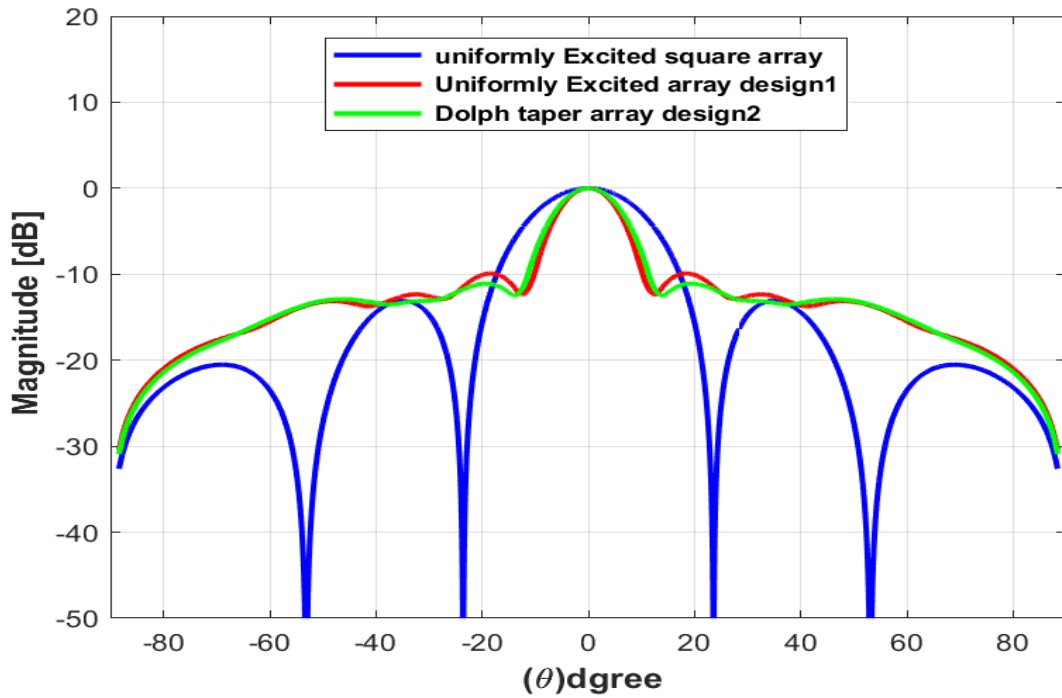
Figure 4. 10 radiation patterns of the uniform planar array that size 25 elements comparison with the proposed cross array that size 17 elements (design 1)and (design 2).

Figure 4.11, shows the corresponding amplitude excitations, and the radiation patterns in three-dimension of the proposed cross array (design2).
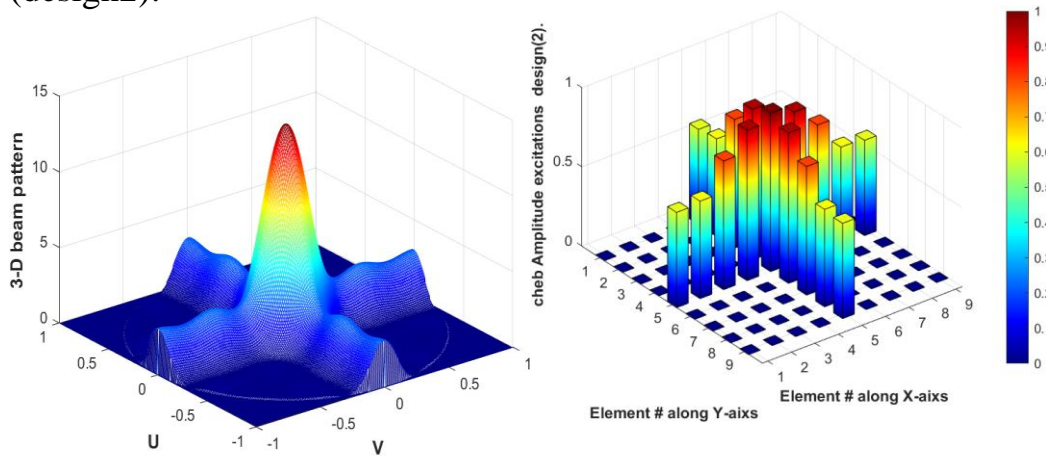
Figure 4. 11. Three-dimension patterns of the proposed cross array with size 17 elements (left), and amplitude excitations (right) (design2).

The Directivity of Dolph taper array design2 is (14 dB), the Peak SLL (-11 dB), FNBW (27.3º), and HPBW (13º).

The above results indicate to reduce the SLL, however, this reduction remains relatively low.

4.4.1.3. Crossed Array with Taylor taper (Design 3).

To apply another tapering to reduce the SLL such as Taylor taper the element weightings w_n for proposed two orthogonal linear crossed arrays.

w_n	w_1	w_2	w_3	w_4	w_5	w_6	w_7	w_8	w_9
	0.764	0.820	1.038	1.234	1.2847	1.234	1.038	0.820	0.764

Figure 4.12, shows the comparison of radiation patterns of the uniform planar array, crossed array with uniform excitations (design 1), and Taylor taper (design 3).
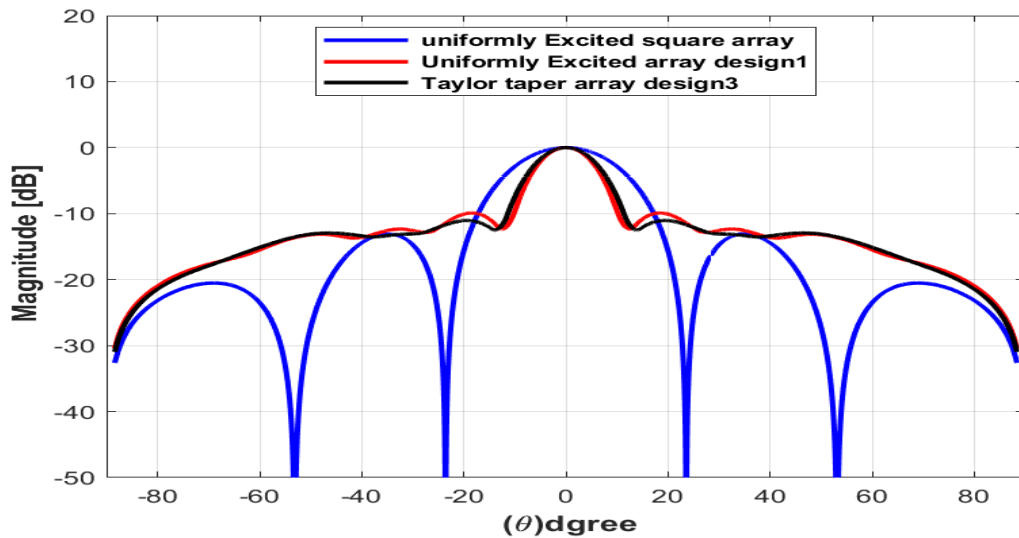
Figure 4. 12 radiation patterns of the uniform planar array that size 25 elements comparison with the proposed cross array that .size 17 elements (design 1)and (design 3).

Figure 4.13, shows the corresponding amplitude excitations, and the radiation patterns in three-dimension of the proposed cross array (design3).
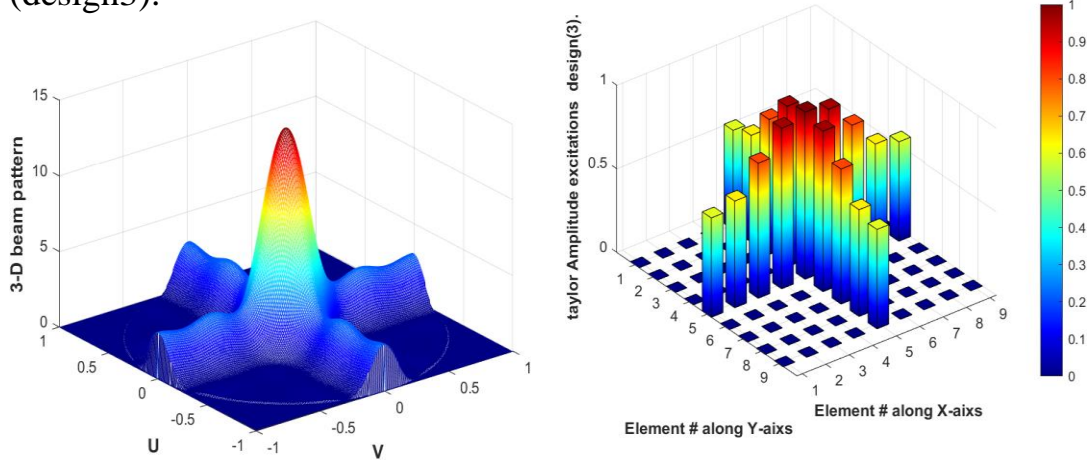
Figure 4. 13. Three-dimension patterns of the proposed cross array with size 17 elements (left), and amplitude excitations (right) (design3).

The directivity of Taylor taper array design3 is (14.07 dB), the Peak SLL (-11 dB), FNBW (27.3°), and HPBW (13°).

The above results indicate to reduce the SLL, however, this reduction remains relatively low.

4.4.1.4. Crossed Array with a triangular taper (Design 4).

One of the simplest techniques that can be used to reduce the sidelobe level is by selecting the amplitude element excitations of the crossed array according to a specific triangular taper as given by the following equation (4.4):

$$w_n = 2N + 1 - |n|, \quad for \quad 0 \le |n| \le 2N \qquad (4.4)$$

Where the weights of the elements at each arm from center to edge of cross array having a tapered linear slope. Further, the above equation represents a straight line with a slope equal to 1.

the element weightings w_n for proposed two orthogonal linear crossed arrays.

w_n	w_1	w_2	w_3	w_4	w_5	w_6	w_7	w_8	w_9
	1	2	3	4	5	4	3	2	1

Figure 4.14, show the comparison of radiation patterns of the uniform planar array, crossed array with uniform excitations (Design 1), and Triangular taper (Design 4).
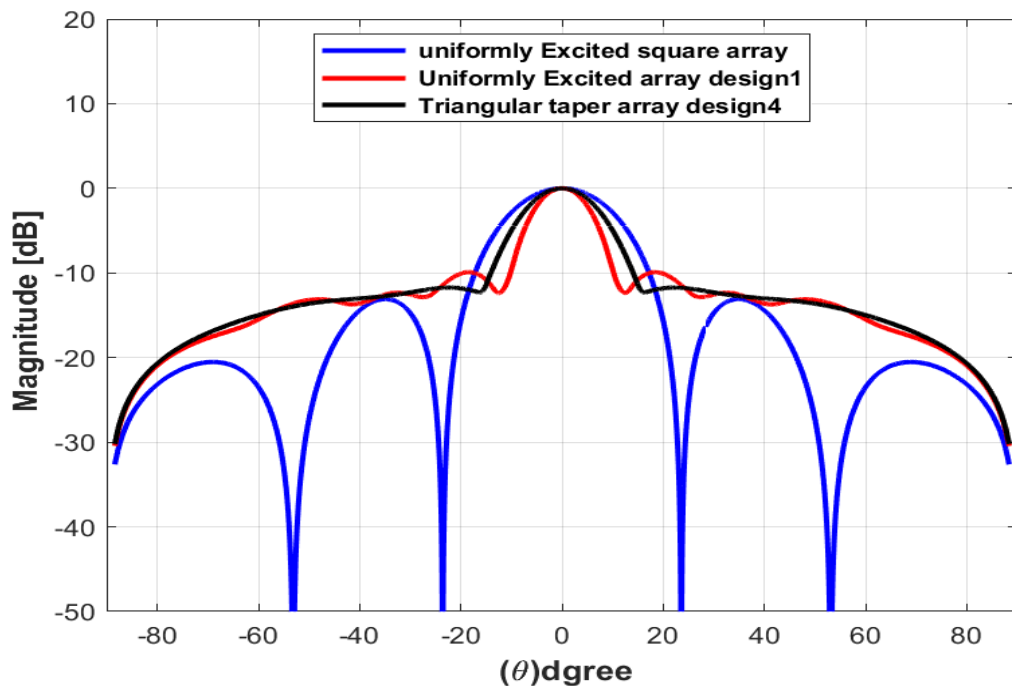
Figure 4. 14 radiation patterns of the uniform planar array that size 25 elements comparison with the proposed cross array that .size 17 elements (design 1)and (design 4).

Figure 4.15, shows the corresponding normalized amplitude excitations, and the radiation patterns in three-dimension of the proposed cross array (design4).
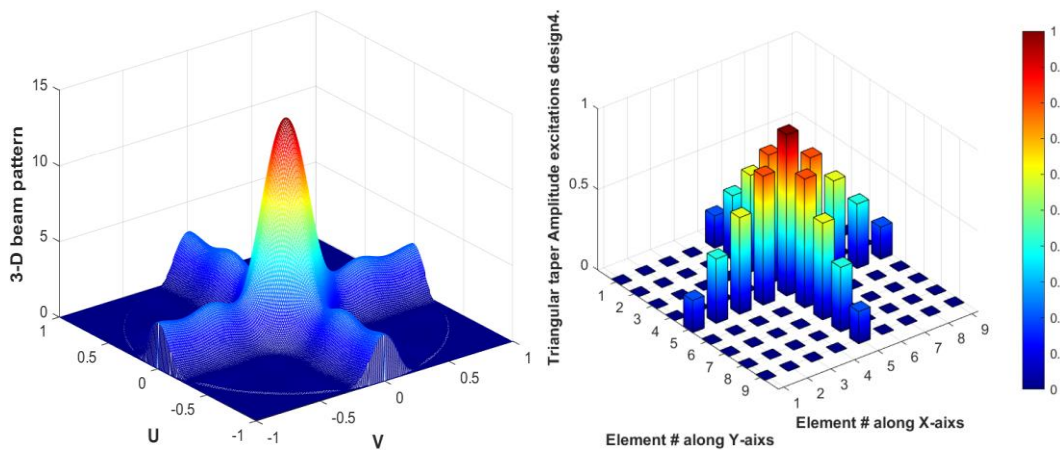
Figure 4. 15. Three-dimension patterns of the proposed cross array with size 17 elements (left), and normalized amplitude excitations (right) (design 4).

The directivity of triangular taper array design4 is (15.1dB), the Peak SLL (-11.7 dB), FNBW (31.8º), and HPBW (15.6º).

The above results indicate a greater reduction in the SLL than in previous designs, however, this reduction remains relatively low.

4.4.1.5. Crossed Array optimized by GA (Design 5).

The amplitude element excitations of the proposed cross array can be reduced sidelobe level numerically through optimized using a GA (design 5). the element weightings w_n for proposed two orthogonal linear crossed arrays.

w_n	w_1	w_2	w_3	w_4	w_5	w_6	w_7	w_8	w_9
	0.101	0.3118	0.5627	0.8193	1	0.9711	0.7074	0.3669	0.1157

Figure 4.16, shows the comparison of radiation patterns of the uniform planar array, crossed array with uniform excitations (design 1), and optimized using a GA (design 5).
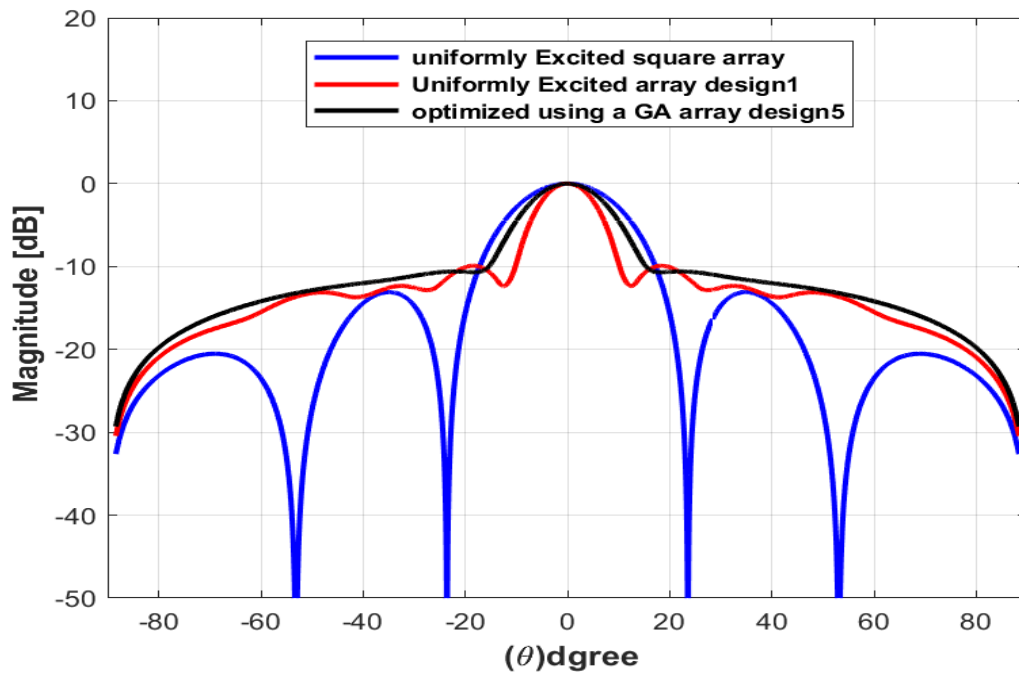
Figure 4. 16 radiation patterns of the uniform planar array that size 25 elements comparison with the proposed cross array that .size 17 elements (design 1) and (design 5).

Figure 4.17, shows the corresponding amplitude excitations, and the radiation patterns in three-dimension for the proposed cross array (design5).
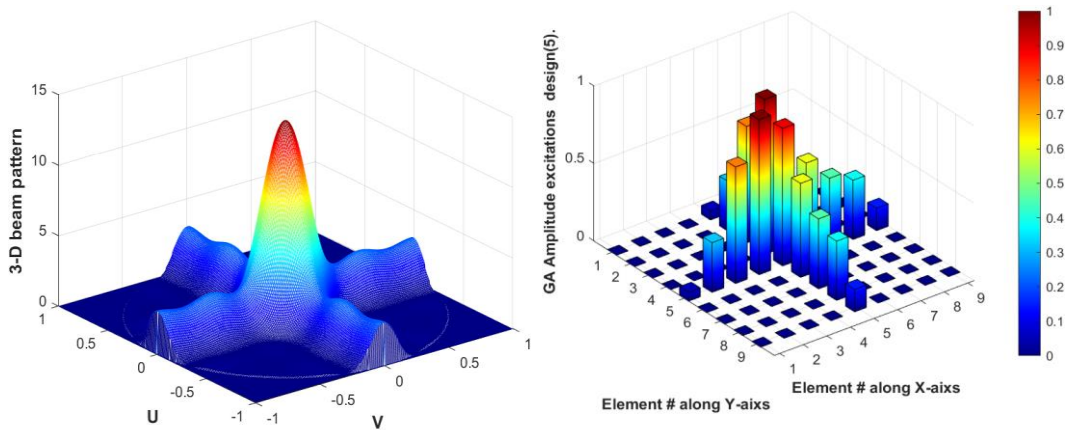
Figure 4. 17. Three-dimension patterns of the proposed cross array with size 17 elements (left), and amplitude excitations (right) (design 5).

The Directivity of optimized using a GA array design 5 is (13.3 dB), the Peak SLL (-11.3 dB), FNBW (31.3º), and HPBW (16º).

The above results indicate to reduce the SLL; However, this reduction remains relatively low.

4.4.2. Comparison Results of Example 1

Figure 4.18 and table 4.1 show the comparison results of these five designs.
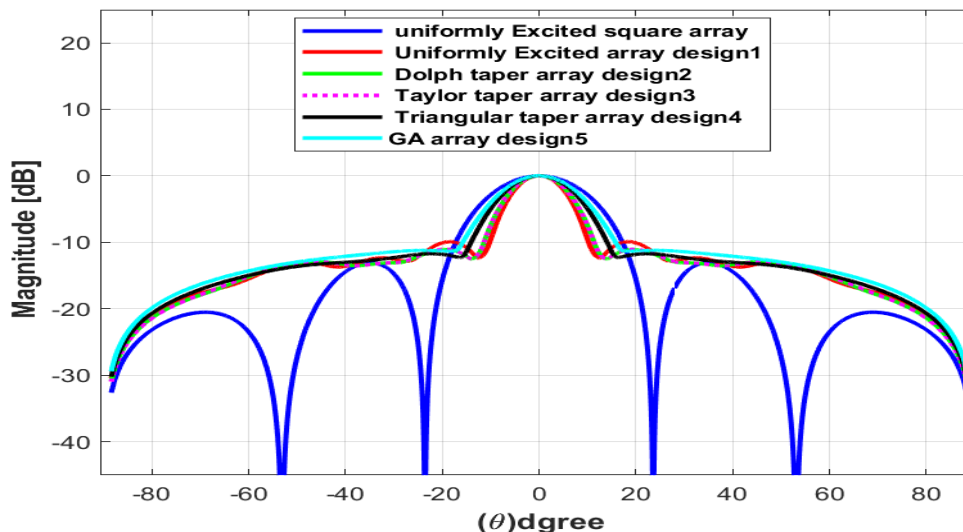
Figure 4. 18. Radiation patterns of the tested arrays for square array with size (2N+1) ×(2N+1) =5 ×5=25 elements and crossed array with size 4(2N) +1=17 elements.

Table (4.1). Performance measures of the proposed designs with 17 elements and the conventional square array with 25 elements				
The Method	**Directivity [dB]**	**Peak SLL [dB]**	**FNBW [Deg.]**	**HPBW [Deg.]**
uniformly Excited square array	**15.5**	**-13.1**	**47**	**20.5**
Uniformly Excited array design1	**14.5**	**-9.9**	**24.6**	**12**
Dolph taper array design2	**14.0**	**-11**	**27.3**	**13**
Taylor taper array design3	**14.07**	**-11**	**27.3**	**13**
Triangular taper array design4	**15.1**	**-11.7**	**31.8**	**15.6**
GA array design5	**13.3**	**-11.3**	**31.3**	**16**

From Figure 4.18 and Table 4.1, it can be seen that the level of the peak sidelobe in the crossed array pattern has been slightly reduced. This reduction can be significantly reduced with larger array sizes as can be seen in the next example. Thus, the proposed crossed array method is found to be more suitable for the applications that require large array sizes such as massive MIMO.

4.4.3. The second Example large Size Arrays.

For example2, assume(N=15) a large square planar array with a size equal to (2N+1) ×(2N+1) =31 ×31 =961 elements, and the coefficient weights of the element excitation are assumed to be uniform as previous. The proposed cross array has a size equal to 4(2N) +1=121elements.

The coefficient weights of the proposed cross array are found using the five design methods as previous.

The dilution factor of this case is $121/961 = 12.59$ %.

4.4.3.1. Crossed Array with Uniform Excitations Elements (Design1).

If the element weightings w_n are all uniformly excited such as design1 in the previous example, although a narrow beam pattern is obtained, the resultant radiation pattern will have usually a high sidelobe level. Figure 4.19, and Figure 4.20 show the comparison of radiation patterns and corresponding amplitude excitations, for both conventional planar array and the proposed cross array (design1).
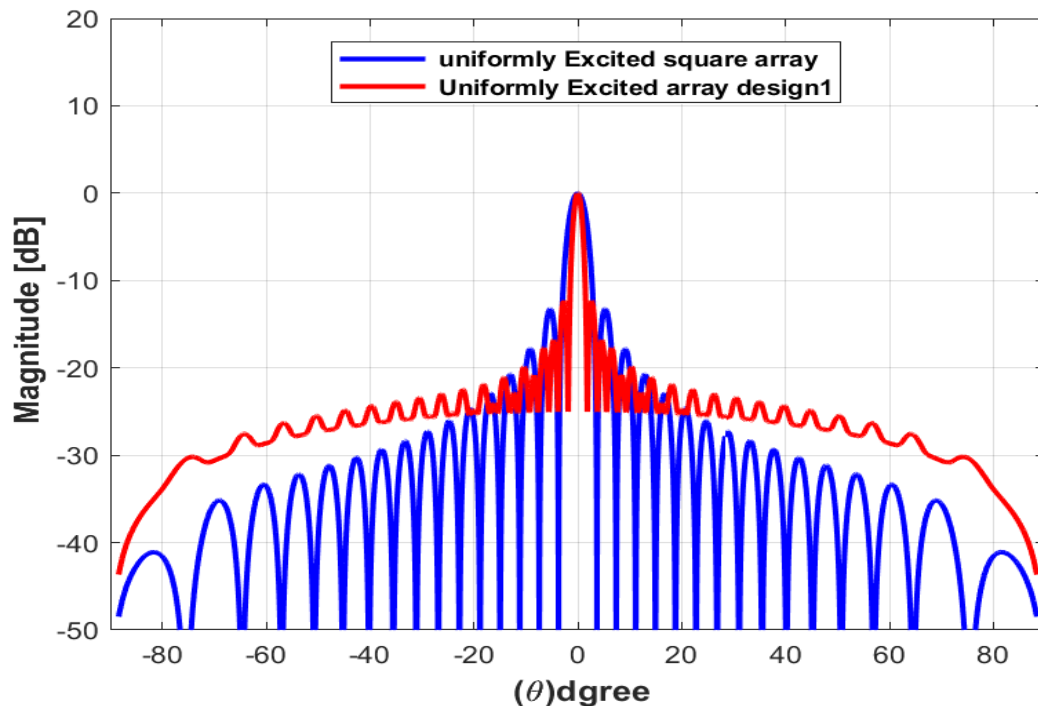
Figure 4. 19. radiation patterns of the uniform planar array 961 elements , and the proposed cross array (design1) 121 elements.
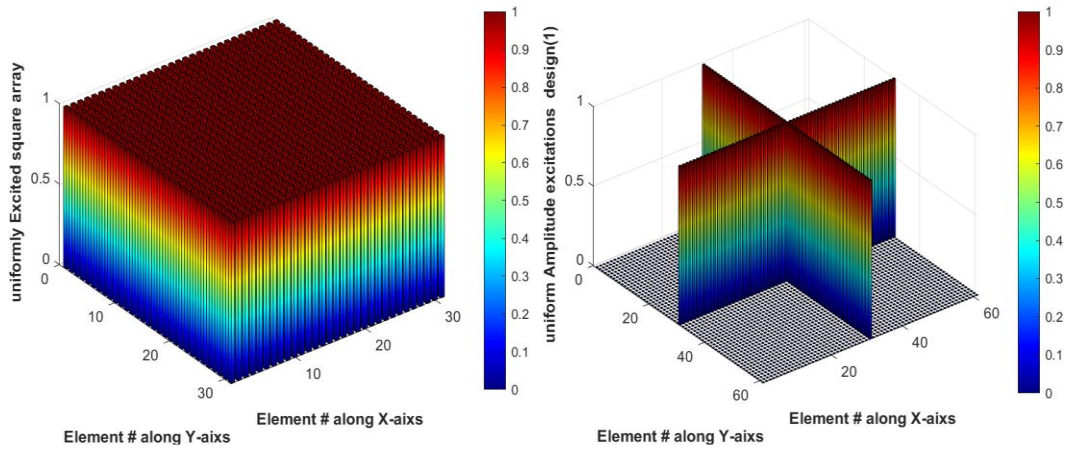
Figure 4. 20. amplitude excitations of the uniform planar array 961 elements (left) and the proposed cross array 121 elements (right) (design1)

Figure 4.21, shows the radiation patterns in three-dimension of both planar arrays with size 961 elements and the proposed cross array with size 121 elements (design 1).
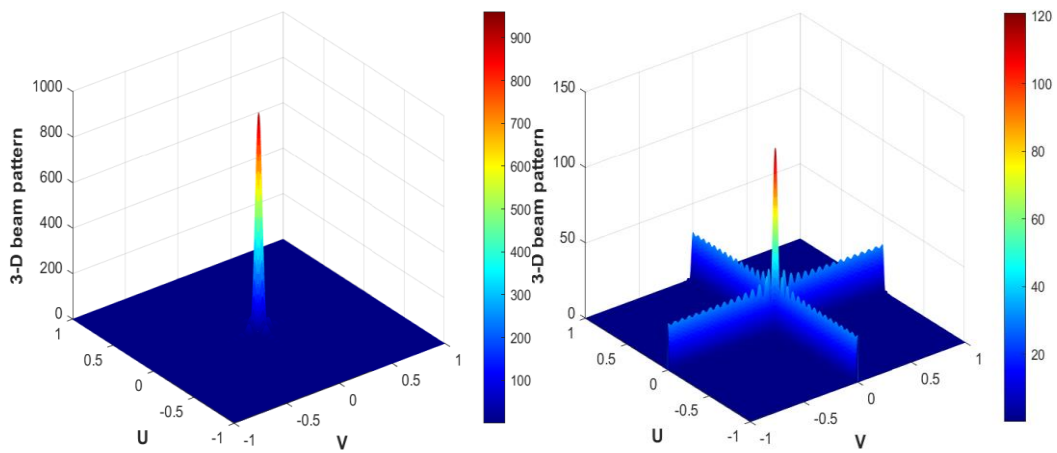
Figure 4. 21. Three-dimension patterns of the uniform planar array 961 elements (left) and the proposed cross array 121 elements (right) (design1).

The contour plot in [dB] of the uniform planar array 961 elements, and the proposed cross array 121 elements illustrated in Figure 4.22.
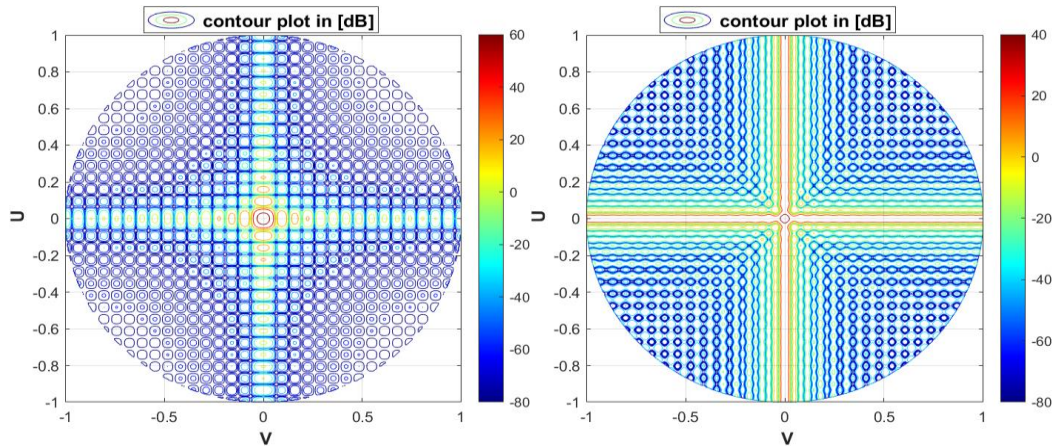
Figure 4. 22 contour plot in [dB] of the uniform planar array 961 elements , and the proposed cross array 121 elements.

The directivity of uniformly excited array design1 is (18.1 dB), the Peak SLL (-12.3 dB), FNBW (3.58°), and HPBW (1.6°).

The above results indicate the need to recalculate the amplitude element excitations of the crossed array such that the SLL can be reduced.

4.4.3.2. Crossed Array with Dolph taper (Design 2).

Apply Dolph tapering to reduce the SLL such as design2 in the previous example, figure 4.23, show the comparison of radiation patterns of the uniform planar array, crossed array with uniform excitations (design 1), and Dolph taper (design 2).
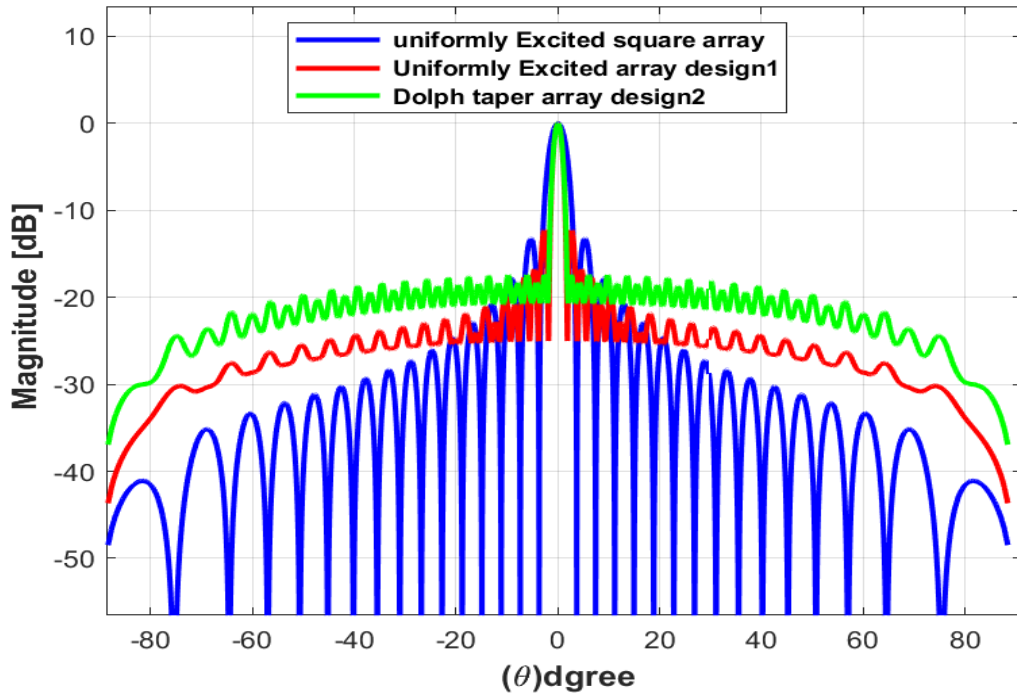
Figure 4. 23 radiation patterns of the uniform planar array that size 961 elements comparison with the proposed cross array that .size 121 elements (design 1)and (design 2).

Figure 4.24, shows the corresponding amplitude excitations, and the radiation pattern in three-dimension of the proposed cross array (design2).
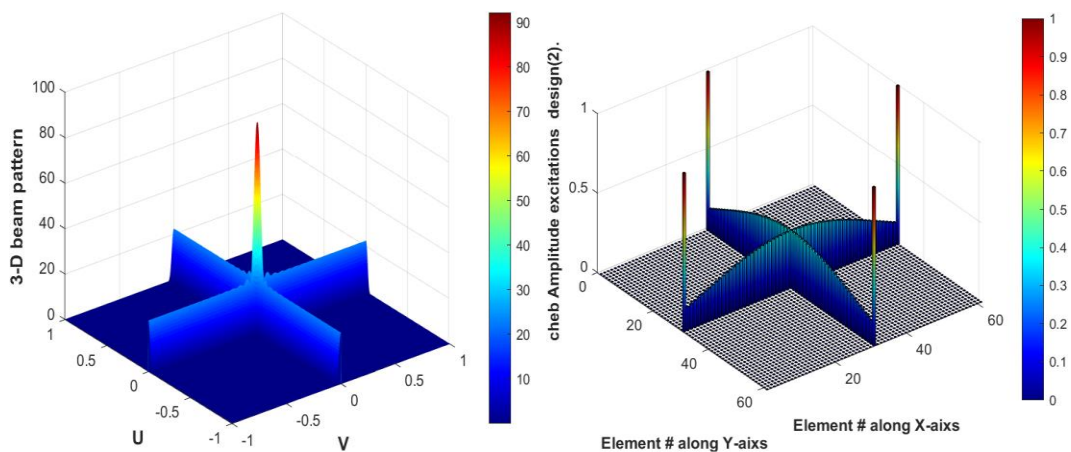
Figure 4. 24. Three-dimension patterns of the proposed cross array with size 121 elements (left), and amplitude excitations (right) (design2).

The directivity of Dolph taper array design2 is (18.4dB), the Peak SLL (-17.5 dB), FNBW (4.02º), and HPBW (1.8º).

The above results indicate a greater reduction in the SLL than in the previous design, however, obtaining a lower reduction by other designs later.

4.4.3.3. Crossed Array with Taylor taper (Design 3).

Apply Taylor tapering to reduce the SLL such as design3 in the previous example, figure 4.25, show the comparison of radiation patterns of the uniform planar array, crossed array with uniform excitations (design 1), and Taylor taper (design 3).

Figure 4. 25 radiation patterns of the uniform planar array that size 961 elements comparison with the proposed cross array that size 121 elements (design 1)and (design 3).

Figure 4.26, shows the corresponding amplitude excitations, and the radiation patterns in three-dimension of the proposed cross array (design3).

92
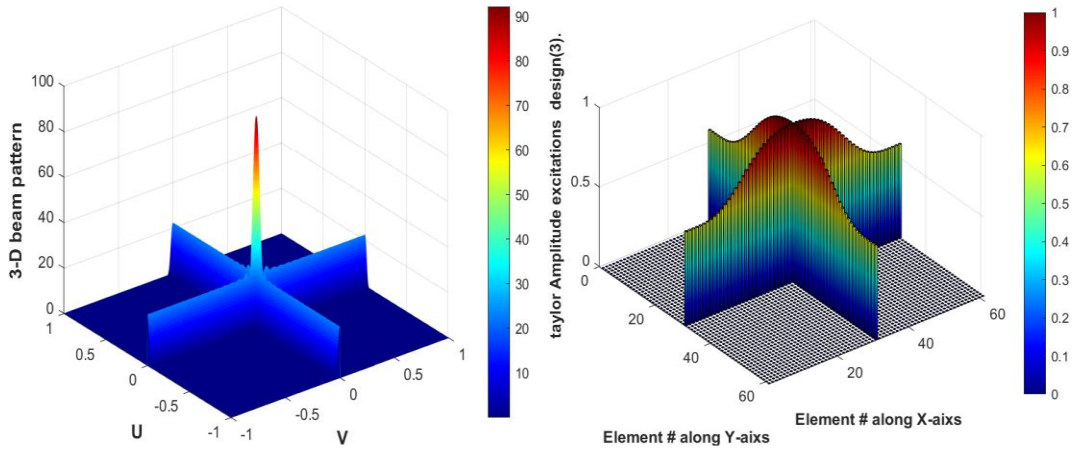
Figure 4. 26. Three-dimension patterns of the proposed cross array with size 121 elements (left), and amplitude excitations (right) (design3).

The Directivity of Taylor taper array design3 is (17.7dB), the Peak SLL (-17.1 dB), FNBW (4.46º), and HPBW (1.84º).

The above results indicate a greater reduction in the SLL and get similar performance in comparison with design 1.

4.4.3.4. Crossed Array with a triangular taper (Design 4).

The technique of a specific triangular taper as is given by the following equation (4.4), that can be used to reduce the SLL as it was described in example 1 (Design 4).

Figure 4.27, show the comparison of radiation patterns of the uniform planar array, crossed array with uniform excitations (design 1), and triangular taper (design 3).
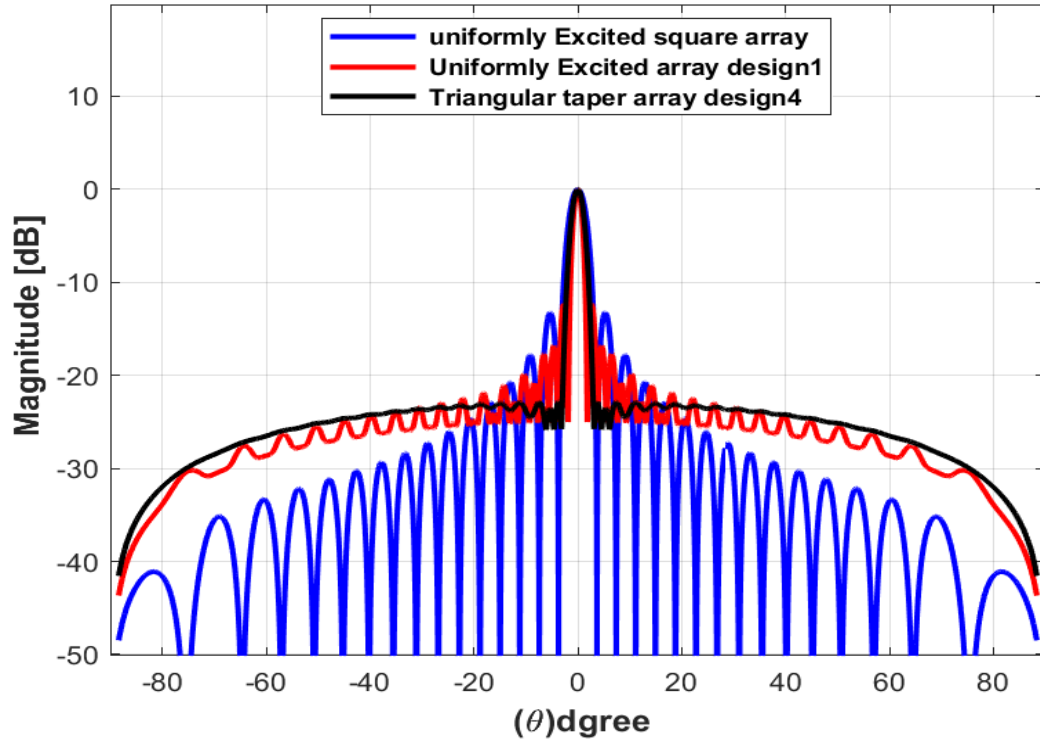
Figure 4. 27 radiation patterns of the uniform planar array that size 961 elements comparison with the proposed cross array that size 121 elements (design 1) and (design 4).

Figure 4.28, show the corresponding normalized amplitude excitations, and the radiation patterns in three-dimension of the proposed cross array (design4).
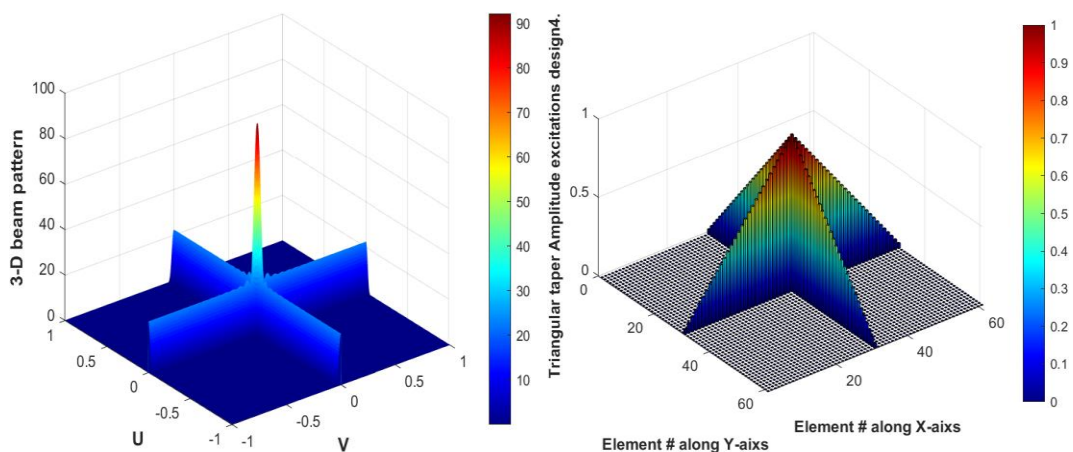
Figure 4. 28. Three-dimension patterns of the proposed cross array with size 121 elements (left), and normalized amplitude excitations (right) (design 4).

The Directivity of Triangular taper array design4 is (18.7 dB), the Peak SLL (-22.1dB), FNBW (6.26º), and HPBW (2.44º).

As can be seen from the results, the SLL is significantly reduced compared to previous designs, as well as obtaining a narrow HPBW.

4.4.3.5.Crossed Array optimized by GA (Design 5).

The amplitude element excitations of the proposed cross array can be reduced sidelobe level numerically through optimized using a GA (design 5). the element weightings w_n is obtained as in the first example.

Figure 4.29, show the comparison of radiation patterns of the uniform planar array, crossed array with uniform excitations (design 1), and optimized using a GA (design 5).
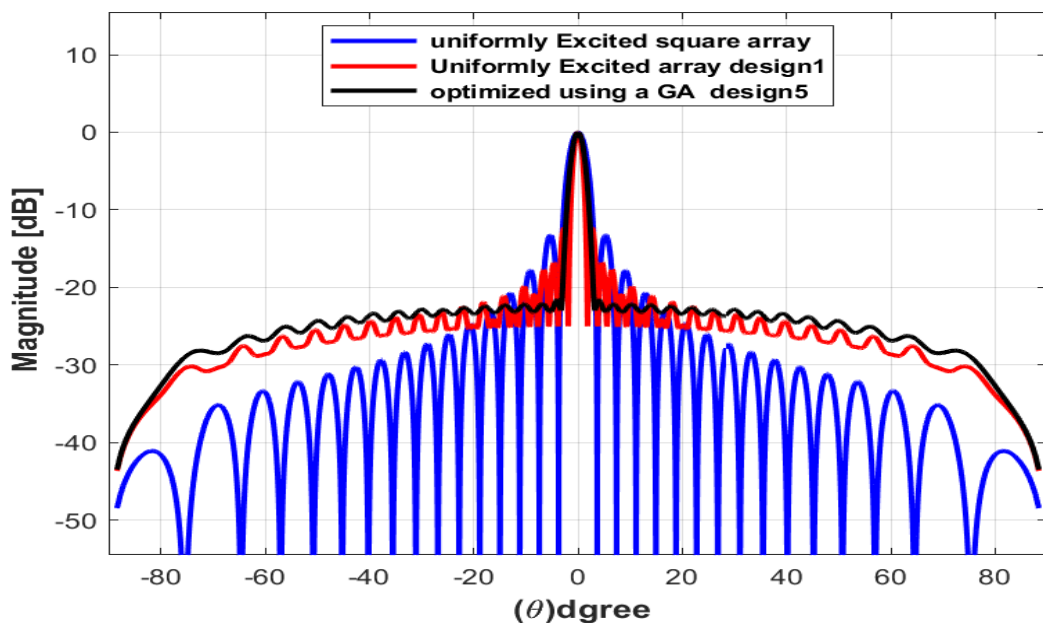
Figure 4. 29 radiation patterns of the uniform planar array that size 961 elements comparison with the proposed cross array that size 121 elements (design 1) and (design 5).

Figure 4.30, show the corresponding amplitude excitations, and the radiation patterns in three-dimension for the proposed cross array (design5).
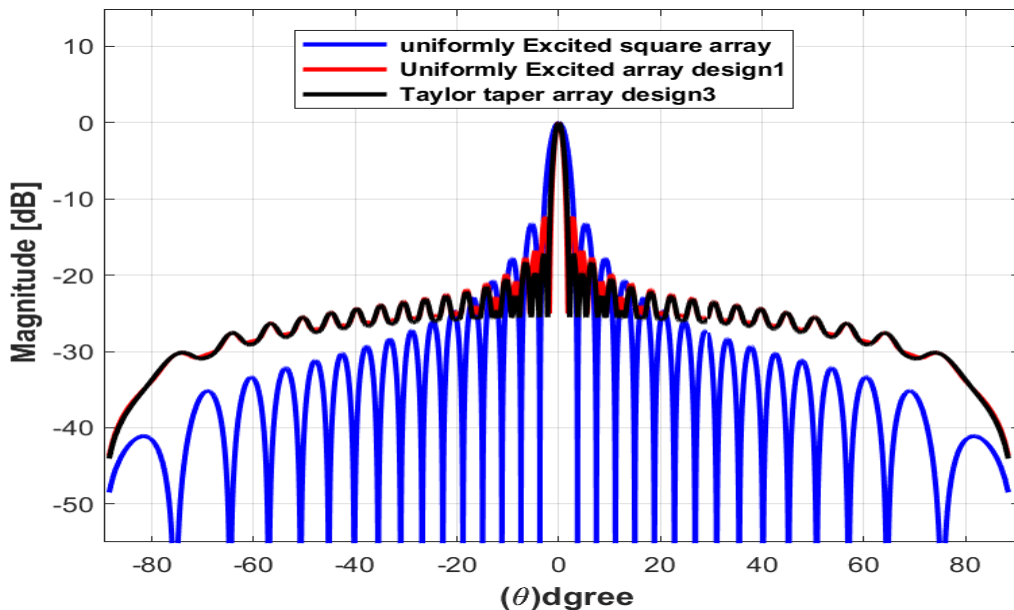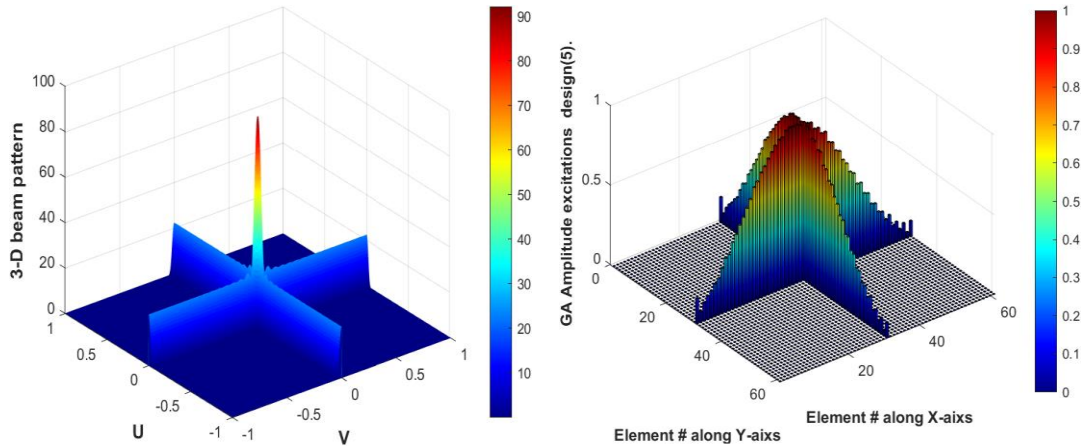

Figure 4. 30. Three-dimension patterns of the proposed cross array with size 121 elements (left), and normalized amplitude excitations (right) (design 5).

The Directivity of optimized using a GA array design 5 is (17.9 dB), the Peak SLL (-22.5 dB), FNBW (6.4º), and HPBW (2.4º).

As can be seen from the results, the SLL is significantly reduced compared to previous designs, as well as obtaining a narrow HPBW.

4.5. Comparison Results of Example 2

Figure 4.31 and table 4.2 show the comparison results of these five designs.
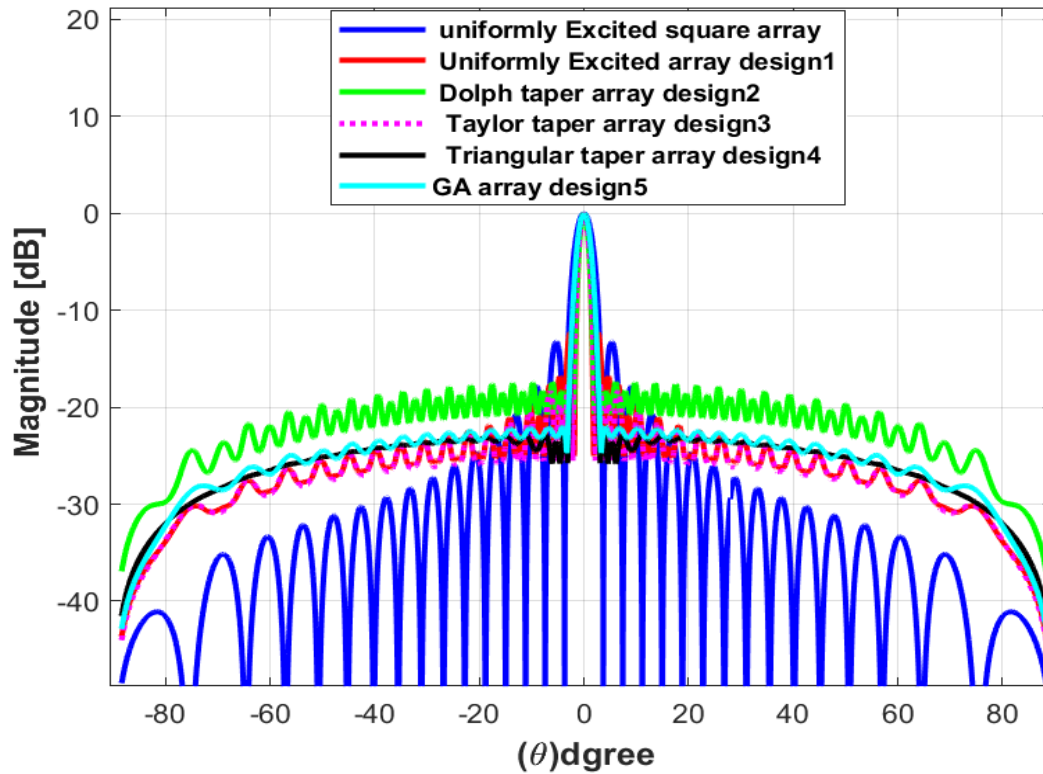
Figure 4. 31. Radiation patterns of the tested arrays for square array with size (2N+1) ×(2N+1) =31 ×31=961 elements and crossed array with size 4(2N) +1=121 elements.

Table (4.2). Performance measures of the proposed designs with 121 elements and the conventional square array with 961 elements				
The Method	**Directivity [dB]**	**Peak SLL [dB]**	**FNBW [Deg.]**	**HPBW [Deg.]**
uniformly Excited square array	30.9	-13.2	7.6	3.28
Uniformly Excited array design1	18.1	-12.3	3.58	1.6
Dolph taper array design2	18.4	-17.5	4.02	1.8
Taylor taper array design3	17.7	-17.1	4.46	1.84
Triangular taper array design4	18.7	-22.1	6.26	2.44
GA array design5	17.9	-22.5	6.4	2.4

From Figure 4.31 and Table 4.2, it can be seen that the results of the method that use the GA are the best one among all other methods. The reason is that the GA can be scanned freely beamforming in both azimuth and elevation direction, as well as controlling the parameters of the radiation pattern and generating nulls by setting some constrained for controlling GA.

CHAPTER FIVE

CONCLUSIONS AND FUTURE WORK

5.1.CONCLUSIONS

Antenna arrays give flexible and versatile solutions to the synthesis of the required radiation patterns. Generally, the array radiation pattern can be designed by five major parameters which are; the general array shape (i.e., structural layout of the array elements such as linear and planar configurations), the elements spacing's, the element excitation amplitude, the element excitation phase, and finally the patterns of the array elements. These five design factors have been utilized by many designers to synthesis array patterns in either analytical or numerical techniques. These synthesis techniques have been well investigated in the literature. This thesis provides a study about the most powerful methods that may be used to optimize and improve the array radiation pattern.

The analytical methods that depend on the deterministic equations are generally simpler than the numerical optimization methods. However, the optimization methods have been proven to be powerful tools in designing antenna arrays with better performance and optimum results. The superiority of the global optimization methods becomes more profound when dealing with large arrays that consist of hundreds number of elements which is the practical case in nowadays applications. Thus, in this thesis, the global optimization methods were considered for optimizing and synthesizing the planar arrays.

99

In the literature, most of the array pattern optimization methods consider all the array elements as design variables. Thus, these methods encounter many disadvantages such as slow convergence time, and high complexity in their circuitry systems.

The optimized methods presented in chapter three offers much easier solutions as only limited boundary square rings are needed to optimize their element excitation amplitudes and phases. Such modifications reduce the cost and complexity of the optimization process and achieve the desired radiation patterns by modifying the elementary excitations of only the outer square rings.

An important and new approach to simplify the fully filled planar arrays is the two perpendicular crossed linear arrays. The element excitation amplitudes of the crossed array can be optimized in such a way that its radiation performance becomes the same as that of the fully filled conventional planar array, of course, such similar performance has been obtained with a far less number of array elements.

Finally, to count for some real environment parameters such as element type, mutual coupling between array elements, and the scattering, the CST full microwave simulator modelling has been used to verify some designed array performance. It is found there is a good agreement between the MATLAB and the CST results for all considered scenarios. This fully confirms the capability and effectiveness of the investigated methods to be used with real-life applications of the antenna arrays.

The concluding remarks about these two proposed methods are explained in the following sub-sections.

5.1.1. PLANAR ARRAY OPTIMIZATION

It has been shown from the results that the same radiation patterns with particular nulls and peak sidelobe level can be obtained by the fully and partially optimized planar arrays. The number of the optimized elements in the partially planar array is much lower than that of the fully planar array. This gives the superiority of the proposed partially planar array, especially when using phase-only control. The complexity in terms of the number of optimized elements of the total number of the array elements is reduced from 100% for the fully optimized array to only 51% for the proposed array. Other advantages may include the cost and the convergence time of the optimizer. Moreover, the directivity of the proposed partially array was found to be slightly lower than that of the fully planar array. Also, when investigating the different design scenarios with the CST Studio Suite, results were converging significantly.

5.1.2. CROSS ARRAAY

It has been shown from the presented results that the designed cross array with a total number of elements equal to $4(2N) + 1$ and adjusted amplitude excitations can be an alternative to the conventional square planar array with a total number of elements equal to $(2N + 1) \times (2N + 1)$. For a small size array, for example1 N=2 (the total number of elements is 17), the dilution factor was found to be 68%. This factor has been significantly reduced to large array size, for example2 at N=15, to only 12.59 %. Thus, the number of the elements in the crossed arrays has been greatly reduced compared to that of the conventional planar array. This reduction has come at the cost of

relatively lower directivity. Nevertheless, the peak sidelobe level of the designed pattern of the crossed array is much lower than that of the conventional square planar array which is another key advantage of the proposed array.

5.2.FUTURE WORK

The described methods in this thesis can be further extended and investigated in future work. Some suggestions are as follows

1. The two designed arrays (i.e., a planar array with optimized outer square rings and the two crossed linear arrays) can be implemented in practice. In this case, one needs to provide appropriate RF components such as variable attenuators and phase shifters. These components need to be carefully selected to realize the configured element excitations taking into account the design errors and limitations.

2. Other array configurations such as circular arrays can be also investigated by applying the proposed optimization methods. Further, the conformal array can be also investigated.

3. In this thesis, the element excitation amplitudes and phases are only optimized for obtaining the minimum sidelobe level and controlled nulls. However, the array design parameters can be also optimized for including more performance features such as maximum directivity, minimum beam width and getting their optimum values.

4. The array elements can be also optimized to get a flat-top beam pattern or reconfiguration between sum and difference array patterns under some common radiation constraints.

REFERENCES

[1]   KHODIER, M.M.Christodoulou, C.G., "Linear Array Geometry Synthesis With Minimum Sidelobe Level and Null Control Using Particle Swarm Optimization." IEEE transactions on antennas and propagation,vol. 53, no. 8, pp. 2674–2679 August 2005, doi: 10.1109/tap.2005.851762.

[2]   Ó. Quevedo-Teruel ,and E. R. Iglesias, "Ant Colony Optimization in Thinned Array Synthesis With Minimum Sidelobe Level." IEEE antennas and wireless propagation letters,VOL. 5, pp. 349–352, 2006,   doi: 10.1109/LAWP.2006.880693.

[3]   C. Rocha-Alicano, D. Covarrubias-Rosales, C. Brizuela-Rodriguez, and M. Panduro-Mendoza, "Differential evolution algorithm applied to sidelobe level reduction on a planar array", AEU - Int. J. Electron. Commun., vol. 61, no. 5, pp. 286–290, 2007, doi:10.1016/j.aeue.2006.05.008.

[4]   L. Hadj Abderrahmane and B. Boussouar, "New optimisation algorithm for planar antenna array synthesis", AEU - International Journal of Electronics and Communications, vol. 66, no. 9. pp. 752–757, 2012, doi: 10.1016/j.aeue.2012.01.005.

[5]   Y.-X. Zhang, Y.-C. Jiao, and L. Zhang, "Antenna Array Directivity Maximization With Side Lobe Level Constraints Using Convex Optimization", IEEE Transactions on Antennas and Propagation, vol. 69, no. 4. pp. 2041-2052, 2021, doi: 10.1109/tap.2020.3026886.

[6]   E. Yoshimoto and M. V. T. Heckler, "Optimization of planar antenna arrays using the firefly algorithm", Journal of

Microwaves, Optoelectronics and Electromagnetic Applications, vol. 18, no. 1. pp. 126–140, 2019, doi: 10.1590/2179-10742019v18i11646.

[7]   JOHN_H._HOLLAND, Adaptation in Natural and Artificial Systems: An Introductory Analysis with Applications to Biology, Control, and Artificial Intelligence, Bradford, MIT Press, 1992.

[8]   DAVID E.GOLDBERG, Genetic Algorithms in Search, Optimization and Machine Learning, Hardcover,Addison-Wesley Puplishing Company, 1989.

[9]   D. E. B. Douglas Werner, Micah Gregory, Zhi Hao Jiang, Optimization Methods in Antenna Engineering, Singapore ,Springer Science+Business Media. vol. 1–4,pp.322-370, 2016,doi:10.1007/978-981-4560-44-3

[10]   R. L. Haupt, "Genetic algorithm design of antenna arrays", IEEE Aerospace Applications Conference Proceedings, vol. 1. pp. 103–109, 1996, doi: 10.1109/aero.1996.495875.

[11]   F. J. Ares-Pena, J. A. Rodriguez-Gonzalez, E. Villanueva-Lopez, and S. R. Rengarajan, "Genetic algorithms in the design and optimization of antenna array patterns", IEEE Transactions on Antennas and Propagation, vol. 47, no. 3. pp. 506–510, 1999, doi:10.1109/8.768786.

[12]   Sayidmarie, K. H. and Mohammed, J. R., "Design of a linear array with asymmetric low sidelobes ", Al-Raffidain Engineering Journal,College of Eng., University of Mosul, vol.12, No.1, pp.1-10, 2004.

[13]   Aboud H.A.,"Sidelobe Reduction using Multi-Element Auxiliary Antenna and Its Application" Ph.D.Thesis.Thesis, Mosul University, 2005.

[14] I. Yanhui Liu, Zaiping Nie, Senior, and Qing Huo Liu, "Reducing the Number of Elements in a Linear Antenna Array by the Matrix Pencil Method.", IEEE Transactions on antennas and propagation,vol. 56, no. 9.pp.2955-2962 2008.

[15] H. Wang and Y. Su, "Narrowband MIMO radar imaging with two orthogonal linear T/R arrays" International Conference on Signal Processing Proceedings, ICSP. pp. 2513–2516, 2008, doi:10.1109/ICOSP.2008.4697660.

[16] Wenji Zhang, Lian Li, and Fang Li, "Reducing the Number of Elements in Linear and Planar Antenna Arrays With Sparseness Constrained Optimization.", IEEE transactions on antennas and propagation,vol. 59, no. 8,pp.3106-3111, august 2011,doi:10.1109/TAP.2011.2158943.

[17] K. H. Sayidmarie and J. R. Mohammed, "Performance of a wide angle and wide band nulling method for phased Arrays" ,Progress In Electromagnetics Research M, vol. 33. pp. 239–249, 2013, doi:10.2528/PIERM13100603.

[18] J. R. Mohammed and K. H. Sayidmarie, "Sidelobe cancellation for uniformly excited planar array antennas by controlling the side elements", IEEE Antennas and Wireless Propagation Letters, vol. 13. pp. 987–990, 2014, doi: 10.1109/LAWP.2014.2325025.

[19] Y. Lu and Y. Tang, "A study of cross array with MIMO DBF", IEEE Antennas and Propagation Society International Symposium (APSURSI). pp. 482–483, 2014, doi: 10.1109/APS.2014.6904572.

[20] J. R. Mohammed, "Optimal null steering method in uniformly excited equally spaced linear arrays by optimising two edge

elements", Electron. Lett., vol. 53, no. 13, pp. 835–837, 2017, doi:10.1049/el.2017.1405.

[21] M. J. Martínez Silva, M. S. Ruiz Palacios, "Radiation Pattern Analysis of Mills Cross Array of Patch Antennas for 5G Mobile Handset Applications", International Journal For Research In Electronics &Electrical Engineering,vol. 3 no.12, pp.1–6, 2017 .

[22] J. R. Mohammed, "Element Selection for Optimized Multiwide Nulls in Almost Uniformly Excited Arrays" ,IEEE Antennas and Wireless Propagation Letters, vol. 17, no. 4. pp. 629–632, 2018, doi:10.1109/LAWP.2018.2807371.

[23] J. R. Mohammed, "Phased Sub-arrays Pattern Synthesis Method with Deep Sidelobe Reduction and Narrow Beam Width.",IETE Journal of Research, pp. 1–7, 2020,doi:org/10.1080/03772063.2020.1853616.

[24] J. R. Mohammed, "Simplified rectangular planar array with circular boundary for side lobe suppression", Progress In Electromagnetics Research M, vol. 97. pp. 57–68, 2020, doi: 10.2528/PIERM20062906.

[25] Ahmed J. Abdulkader,Jafar R. Mohammed,and Raad H. Thaher"Phase-Only Nulling with Limited Number of Controllable Side Elements." ,Progress In Electromagnetics ResearchC,Vol. 99, pp. 167–178, 2020,doi:10.2528/PIERC20010203.

[26] J. R. Mohammed and K. H. Sayidmarie, "Planar array with optimized perimeter elements", PervasiveHealth: Pervasive Computing Technologies for Healthcare, vol. 2. pp. 1520–1529, 2020, doi:10.4108/eai.28-6-2020.2297890.

[27] Boxuan Gu,Rongxin Jiang,Xuesong Liu , and Yaowu Chen,

"Optimization of Sparse Cross Array Synthesis via Perturbed Convex Optimization."MDPI journals,vol. 20. pp. 1–17, 2020,doi:10.3390/s20174929.

[28] C. A. Balanis, Antenna Theory Analysis And Design, Fourth Edi. Hoboken, New Jersey: John Wiley & Sons, Inc., 2016.

[29] A. . Harish and M. Sachidananda, Antennas and Wave Propagation, 13th ed. Delhi: Oxford University Press, 2007.

[30] D. D. Helmut E. Schrank , Gary E. Evans, Radar Hanbook, Second Edi., San Francisco: McGraw-Hill, 1990.

[31] R. J. Mailloux, Phased Array Antenna Handbook Third Edition, boston london:Artech House Antennas and Electromagnetics Analysis Library. 2018.

[32] R. Thompson, J. Moran, and G. Swenson, Interferometry and Synthesis in Radio Astronomy 3rd ed, Cham, Switzerland:Astronomy and Astrophysics Library. 2017, doi: 10.1007/978-3-319-44431-4.

[33] E. Garcia-Marin, J. L. Masa-Campos, and P. Sanchez-Olivares, "Planar array topologies for 5g communications in Ku Band," IEEE Antennas and Propagation Magazine, vol. 61, no. 2. pp. 112–113, 2019, doi: 10.1109/MAP.2019.2895633.

[34] J. Bracewell, R. N. & Roberts, "Aerial Smoothing In Radio Astronomy", Australian Journal of Physics, vol. 7. pp. 615–640, 1954, doi: 10.1071/PH540615.

[35] M. J. M. Silva, M. S. R. Palacios, U. De Guadalajara, B. Marcelino, and G. Barragán, "Radiation Pattern Analysis of

Mills Cross Array of Patch Antennas for 5G Mobile Handset Applications" International Journal For Research In Electronics & Electrical Engineering, vol. 3, no. 12. pp. 1–6, 2017

[36] Holland, John H., Adaptationin NaturalandArtificial system, Cambridge, MA: MIT Press 1975.

[37]   D. Goldberg, Genetic algorithms in optimization, search and machine learning, Boston, MA United States:Addison-Wesley Longman Publishing Co. Inc., 1988.

[38] R. L. Haupt and D. H. Werner, Genetic Algorithms in Electromagnetics. Hoboken, New Jersey.: A John Wiley & Sons, Inc., 2007.

[39] R. L. Haupt and S. E. Haupt, Practical Genetic Algorithms Second Edition, A JOHN WILEY & SONS, INC. ,2004.

[40] DavidA.Coley, An introduction to genetic algorithms for Scientists and Engineers ,World Scientific Publishing Co. 1999.

[41] R. L. H. S. E. Haupt, Practical Genetic Algorithms, Hoboken, New Jersey:A John Wiley & Sons, Inc.,2004.

[42] C. and J. E. R. R.REEVES, Genetic algorithms: principles and perspectives: a guide to GA theory, NEW YORK:Kluwer Academic Publishers, 2003.

[43] E. K. Burke and G. Kendall, Search methodologies: Introductory tutorials in optimization and decision support techniques, New York:Springer is part of Springer Science&Business Media, 2014.

[44] K. A. De Jong and W. M. Spears, "A formal analysis of the role

of multi-point crossover in genetic algorithms", Annals of Mathematics and Artificial Intelligence, vol. 5, no. 1, pp. 1–26, 1992, doi: 10.1007/BF01530777.

[45] A. Hassanat, K. Almohammadi, E. Alkafaween, E. Abunawas, A. Hammouri, and V. B. S. Prasath, "Choosing mutation and crossover ratios for genetic algorithms-a review with a new dynamic approach," Information (Switzerland)., vol. 10, no. 12, p. 390, Dec. 2019, doi: 10.3390/info10120390.

[46] M. Lynch, "Evolution of the mutation rate," Trends in Genetics, vol. 26, no. 8. pp. 345–352, 2010, doi: 10.1016/j.tig.2010.05.003.

البحوث المنشورة

[1] Abdulrazaq Abdulhaq Khmees and Jafar Ramadhan Mohammed, "**Obtaining Performance Similar to Rectangular Planar Antenna Using Crossed Arrays with Smaller Number of Elements**", IOP Conference Series: Materials Science and Engineering, Volume 1152, 1st International Ninevah Conference on Engineering and Technology (INCET 2021) 5th - 6th April 2021, Ninevah, Iraq.

[2] Jafar Ramadhan Mohammed and AbdulRazaq Abdulhaq Khmees, "**Planar Arrays with Adjustable Outer Square Rings**", Submitted to IETE Journal of Research (Second Round of Review).

[3] Jafar Ramadhan Mohammed and AbdulRazaq Abdulhaq Khmees, "**An Array with Crossed-Dipoles Elements for Controlling Side Lobes Pattern**", Submitted to JJEE An international journal (Second Round of Review).

الخلاصة

تقدم هذه الرسالة دراسة في طرق تركيب مصفوفة الهوائيات المستوية في ظل بعض القيود المفروضة على مخططات الاشعاع. من أجل الحصول على الأداء الأمثل من حيث الاتجاهية، ومستويات الفصوص الجانبية الدنيا، والتحكم في مواقع الاصفار وتبسيط تعقيد المصفوفة، يتم استخدام خوارزمية التحسين لتحسين معاملات تصميم المصفوفة. تم استخدام الخوارزمية الجينية وهي من أقوى طرق التحسين وأكثرها فاعلية لتحسين المصفوفات المدروسة وبالتالي الحصول على أنماط الإشعاع المطلوبة.

في هذه الدراسة البحثية، تم الأخذ في الاعتبار البعض من اشكال المصفوفات المستوية مثل الشكل المستطيل ثنائي الأبعاد ومصفوفتين خطيتين متعامدين على شكل المصفوفة المتقاطعة. بالنسبة للمصفوفات المستطيلة الشكل، تم تبسيط تعقيداتها من خلال اقتراح استراتيجية ذكية لتقسيم عناصر المصفوفة إلى مجموعتين منفصلتين. عناصر المصفوفة في المجموعة الأولى قابلة للتعديل بينما يُفترض أن تكون العناصر الأخرى ثابتة. بعبارة أخرى، تنقسم العناصر المستوية إلى مصفوفتين متجاورتين متماثلتين حول مركز المصفوفة. يتم اختيار إثارة العناصر من حيث السعات و / أو مراحل المصفوفة الخارجية الفرعية لتكون قابلة للتكيف أثناء عملية التحسين لتشكيل القيود المطلوبة على نمط المصفوفة، في حين أن إثارة عناصر المصفوفة الفرعية الداخلية التي لها تأثير أقل على نمط الإشعاع تكون ثابتة وخارجة من عملية التحسين. بهذه الطريقة، يمكن الحصول على جميع القيود المطلوبة من خلال تركيز عملية التحسين على العناصر الأكثر نشاطاً فقط والتي تكون أقل من العدد الإجمالي للعناصر للحصول على أداء مشابه جدًا لأداء المصفوفة المستوية التقليدية المحسنة بالكامل. تتمتع المصفوفة المقترحة بالعديد من المزايا مقارنة بالمصفوفات التقليدية على النحو التالي: تم تقليل عدد العناصر المتغيرة بشكل كبير؛ وبالتالي، تم تقليل سرعة التقارب للتحسين بشكل كبير. تم الحصول على جميع الميزات المطلوبة من خلال تكوين مصفوفة بسيطة دون الحاجة إلى مصفوفات معقدة. أيضا، تم تخفيض تكلفة التصنيع بشكل كبير.

من ناحية أخرى، يمكن الحصول على الأداء الجيد للمصفوفة المربعة الكبيرة التقليدية من خلال تصميم مصفوفة مكافئة تتكون من صفيفين خطيين متقاطعين مع عدد أقل بكثير من عناصر المصفوفة. تم الحصول على الأداء الجيد للمصفوفات المتقاطعة من خلال تصميم إثارة عناصر

المصفوفة وفقًا للطرق الحتمية المعروفة أو طرق التحسين العالمية. بشكل عام، وجد أن طريقة التحسين المستخدمة قادرة على توفير نمط مصفوفة يتطابق بشكل أفضل مع نمط المصفوفة المربعة الكبيرة التقليدية مع عدد أقل بكثير من عناصر المصفوفة.

<div dir="rtl">

<u>**إقرار المشرف**</u>

اشهد بان الرسالة الموسومة ب " **دراسة تحسين نمط المصفوفة المستوية** " تمت تحت اشرافي وهي جزء من متطلبات نيل شهادة الماجستير في هندسة الاتصالات.

التوقيع:
المشرف: أ.د. **جعفر رمضان محمد**
التاريخ: /   / 2021

<u>**إقرار المقيم اللغوي**</u>

اشهد باني قمت بمراجعة الرسالة الموسومة ب " **دراسة تحسين نمط المصفوفة المستوية** " من الناحية اللغوية وتصحيح ما ورد فيها من أخطاء لغوية وتعبيرية وبذلك أصبحت الرسالة مؤهلة للمناقشة بقدر تعلق الامر بسلامة الأسلوب وصحة التعبير.

التوقيع:
المقوم اللغوي:
التاريخ: /   / 2021

<u>**إقرار رئيس لجنة الدراسات العليا**</u>

بناء على التوصيات المقدمة من قبل المشرف والمقوم اللغوي أرشح هذه الرسالة للمناقشة.
التوقيع:
الاسم:
التاريخ: /   / 2021

<u>**إقرار رئيس القسم**</u>

بناء على التوصيات المقدمة من قبل المشرف والمقوم اللغوي ورئيس لجنة الدراسات العليا أرشح هذه الرسالة للمناقشة.
التوقيع:
الاسم:
التاريخ: /   / 2021

</div>

دراسة تحسين نمط المصفوفة المستوية

رسالة تقدم بها

عبدالرزاق عبدالحق خميس الصميدعي

إلى
مجلس كلية هندسة الالكترونيات
جامعة نينوى
كجزء من متطلبات نيل شهادة الماجستير
في
هندسة الاتصالات

بإشراف
أ.د. جعفر رمضان محمد

جامعة نينوى

كلية هندسة الالكترونيات

قسم هندسة الاتصالات

دراسة تحسين نمط المصفوفة المستوية

عبد الرزاق عبد الحق خميس الصميدعي

رسالة ماجستير علوم في هندسة الاتصالات

بإشراف
أ.د. جعفر رمضان محمد

2021 م   1442 هـ